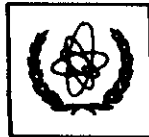




UNITED NATIONS EDUCATIONAL, SCIENTIFIC AND CULTURAL ORGANIZATION
INTERNATIONAL ATOMIC ENERGY AGENCY
INTERNATIONAL CENTRE FOR THEORETICAL PHYSICS
I.C.T.P., P.O. BOX 586, 34100 TRIESTE, ITALY, CABLE: CENTRATOM TRIESTE



SMR.996 - 29

SUMMER SCHOOL IN HIGH ENERGY PHYSICS AND COSMOLOGY

2 June - 4 July 1997

DARK MATTER IN THE UNIVERSE

M. KAMIONKOWSKI
Physics Department
Columbia University
New York, NY 10027
USA

Please note: These are preliminary notes intended for internal distribution only.

Marc Kamionkowski
(Columbia University)

I. Cosmology

- A. Evidence for Dark Matter
- B. Evidence for Nonbaryonic Dark Matter
- C. Local Halo Density

II. Dark-Matter Candidates

- A. MACHOS
- B. Light γ 's
- C. Axions: Properties + Detection
- D. Weakly-Interacting Massive Particles (WIMPs)
 - 1. Properties
 - 2. SUSY candidates
 - 3. Detection

III. Cosmic Microwave Background

- A. Determination of $\Omega_0, \Omega_b, \dots$
- B. Tests of Inflation
 - 1. Anisotropies
 - 2. Polarization

For More Information:

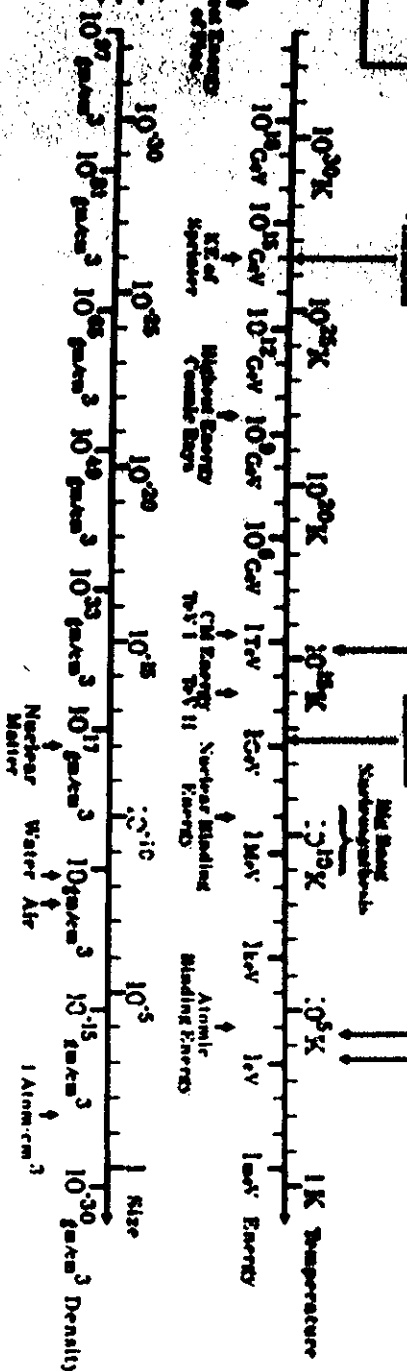
- ① Evidence for Dark Matter, WIMPs, 545^y DM;
G. Jungman, M. Kamionkowski, & K. Griest,
Phys. Repts. 267, 195 (1995).
- ② Axions:
M. S. Turner, *Phys. Repts.* 197, 67 (1990).
G. Raffelt, *Phys. Repts.* 198, 1 (1990).
G. Raffelt's Book (U. Chicago Press).
- ③ MACHOs
B. Paczynski,
- ④ Thermodynamics, Early-Universe, Light v/s:
Kolb + Turner, Early Universe
- ⑤ Cosmic Microwave Background:
Jungman, MK, Kosowsky, + Spergel,
Phys. Rev. D 54, 1332 (1996)
MK, Kosowsky, + Stebbins, *astro-ph/9611125*
Phys. Rev. D (in press)

QUANTUM
GAS/LIQUID
• Radiation
• Superconductivity
• Geophysics

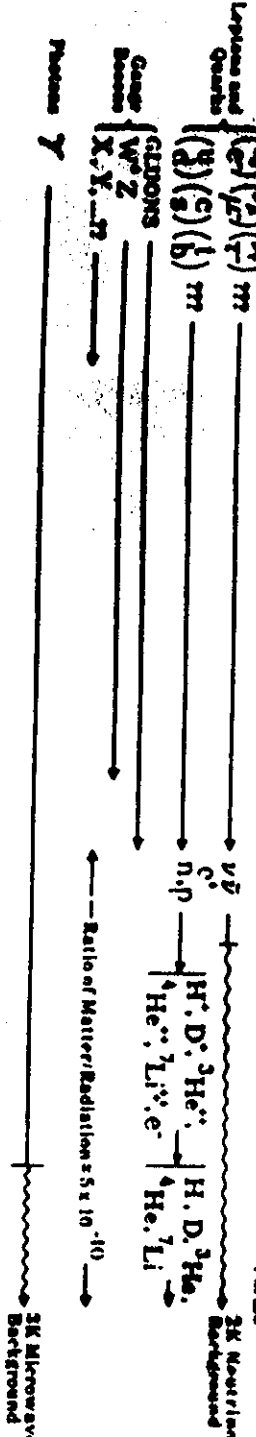
END OF
GRAND
UNIFICATION
• Order of
Matter-Accelerator
Asymmetry
• Inflation

ELECTRONIC
UNIFICATION
• Formation
of Matter
• Structure
of Atoms
• Structure
of Nucleus

MATTER
ELIMINATION
• Formation
of Structure
of Atoms
• Structure
of Nucleus
• Structure
of Matter
• Structure
of Radiation



CONSTITUENTS



Photon Y

3

PHYSICS REPORTS

11.1. Cosmic sources	195	13. Conclusions	319
11.2. Searches and limits of the MSSM	322	13.1. Summary of calculations	322
11.2.1. Overview	322	13.2. Central results	322
11.2.2. SUSY particle species	323	13.3. Concluded remarks	323
11.3. Dark density	325	Appendix A. Construction of the MSSM	342
11.4. Interacting scalar actions	326	A.1. Introduction	342
11.5. Decay widths	327	A.2. Superfield formalism	342
11.6. Interaction terms	328	A.3. Minimal supersymmetric standard model:	342
11.7. Comparison of direct and indirect rates	333	general discussion	343
11.8. Summary and related models	333	A.4. Minimal supersymmetric standard model:	343
12. Other possible dark-matter candidates	334	spacetime and interactions	347
12.1. The field and all of heavy-susy dark	334	A.5. SUSY-GUT and supergravity models	350
12.2. Summary	336	A.6. Parameterizations	361
12.3. Other supersymmetric dark-matter candidates	336	Appendix B. User's guide for Muon-drift	363
	336	References	364

Abstract

There is almost universal agreement among astronomers that most of the mass in the Universe and most of the mass in the Galactic halo is dark. Many lines of reasoning suggest that the dark matter consists of some new, as yet undiscovered, very light supersymmetric particle (WIMP). There is now a vast experimental effort being undertaken to detect WIMPs in the halo. The most promising techniques involve direct detection in low-background laboratory detectors and indirect detection through observation of energetic annihilation from annihilation of WIMP candidates, perhaps the best motivated and certainly the most theoretically developed of the search. Of the many WIMP candidates, perhaps the best understood is the neutralino dark matter. We review the minimal supersymmetric extension of the standard model and discuss prospects for detection of neutralino dark matter. We review in detail how to calculate the cosmological abundance of the neutralino and the cross rates for both direct- and indirect-detection schemes, and we discuss astrophysical and laboratory constraints on supersymmetric models. We review and classify all constraints from particle physics, nuclear physics, and astrophysics other than air catch-up in the calculations. We briefly review other related dark-matter candidates and detection techniques.

Susy symmetric dark matterGordon Jungman^a, Robert K. Schaefer^b, Kim Griest^c

^a Department of Physics, University of California, Berkeley, CA 94720, USA
^b Department of Physics, University of Michigan, Ann Arbor, MI 48109, USA
^c Department of Physics, University of California, San Diego, CA 92093, USA. E-mail address:
 jungman@hep.ucsd.edu

1. Introduction	221	14. Summary and scalar fields	226
2. Dark matter in the Universe	226	15. Other dark states	226
3. History of dark	226	16. Summary and conclusions	226
4. Theoretical arguments	226	17. Summary of cross sections	226
5. Direct detection of dark matter in the laboratory	227	18. Theoretical ingredients	226
6. Why	227	19. Astrophoton (photon) interaction	226
7. Overview of detection constraints	226	20. Solar interaction	226
8. Cosmological abundance of a WIMP	228	21. General axial-vector, vector, and scalar	226
9. SUSY and other theories	228	22. Comparison of spin and scalar cross	226
10. Summary and conclusions	228	23. Direct detection of neutrinos	226
11. Acknowledgments	229	11. Theory	226
12. References	229	12. Detection	226
13. Appendix: SUSY theory	229	13. Reconstruction techniques	226
14. Summary and conclusions	229	14. Experimental methods for WIMP annihilations	226
15. Summary and conclusions	229	15. In the Sun and other hosts	227
16. SUSY-GUT and supergravity models	229	16. Galactic	227
17. Laboratories	229	17. Direct and indirect detection	226
18. Summary	229	18. Backgrounds	226
19. Summary and conclusions	229	19. Atmospheric neutrinos	226
20. Summary	229	20. Neutrino masses	226
21. Atmospheric neutrinos	229	21. Atmospheric neutrino fluxes and fluxes	226
22. Summary	229	22. Current status of atmospheric neutrino fluxes	226
23. Summary	229	23. Summary of atmospheric neutrino fluxes	226
24. Summary	229	24. Summary of atmospheric neutrino fluxes	226
25. Summary	229	25. Summary of atmospheric neutrino fluxes	226
26. Summary	229	26. Summary of atmospheric neutrino fluxes	226
27. Summary	229	27. Summary of atmospheric neutrino fluxes	226
28. Summary	229	28. Summary of atmospheric neutrino fluxes	226
29. Summary	229	29. Summary of atmospheric neutrino fluxes	226
30. Summary	229	30. Summary of atmospheric neutrino fluxes	226
31. Summary	229	31. Atmospheric neutrino fluxes and fluxes	226
32. Summary	229	32. Current status of atmospheric neutrino fluxes	226
33. Summary	229	33. Summary of atmospheric neutrino fluxes	226
34. Summary	229	34. Summary of atmospheric neutrino fluxes	226
35. Summary	229	35. Summary of atmospheric neutrino fluxes	226
36. Summary	229	36. Summary of atmospheric neutrino fluxes	226
37. Summary	229	37. Summary of atmospheric neutrino fluxes	226
38. Summary	229	38. Summary of atmospheric neutrino fluxes	226
39. Summary	229	39. Summary of atmospheric neutrino fluxes	226
40. Summary	229	40. Summary of atmospheric neutrino fluxes	226
41. Summary	229	41. Summary of atmospheric neutrino fluxes	226
42. Summary	229	42. Summary of atmospheric neutrino fluxes	226
43. Summary	229	43. Summary of atmospheric neutrino fluxes	226
44. Summary	229	44. Summary of atmospheric neutrino fluxes	226
45. Summary	229	45. Summary of atmospheric neutrino fluxes	226
46. Summary	229	46. Summary of atmospheric neutrino fluxes	226
47. Summary	229	47. Summary of atmospheric neutrino fluxes	226
48. Summary	229	48. Summary of atmospheric neutrino fluxes	226
49. Summary	229	49. Summary of atmospheric neutrino fluxes	226
50. Summary	229	50. Summary of atmospheric neutrino fluxes	226
51. Summary	229	51. Summary of atmospheric neutrino fluxes	226
52. Summary	229	52. Summary of atmospheric neutrino fluxes	226
53. Summary	229	53. Summary of atmospheric neutrino fluxes	226
54. Summary	229	54. Summary of atmospheric neutrino fluxes	226
55. Summary	229	55. Summary of atmospheric neutrino fluxes	226
56. Summary	229	56. Summary of atmospheric neutrino fluxes	226
57. Summary	229	57. Summary of atmospheric neutrino fluxes	226
58. Summary	229	58. Summary of atmospheric neutrino fluxes	226
59. Summary	229	59. Summary of atmospheric neutrino fluxes	226
60. Summary	229	60. Summary of atmospheric neutrino fluxes	226
61. Summary	229	61. Summary of atmospheric neutrino fluxes	226
62. Summary	229	62. Summary of atmospheric neutrino fluxes	226

Received 1995-06-15; accepted 1995-12-15

What IS the Dark Matter??

BBN: $\Omega_b < 0.1$

Nonrelativistic matter density: $\Omega_0 > 0.1$

- Dynamics/LSS ($\Omega_0 > 0.3$)
- Quasar-Lensing Statistics
- Dicke Coincidence: $\Omega_0 = 1$
- Horizon Problem \Rightarrow Inflation (more than meets the eye)

\implies Nonbaryonic Dark Matter

also, Clusters: $\Omega_0 \gg \Omega_b$

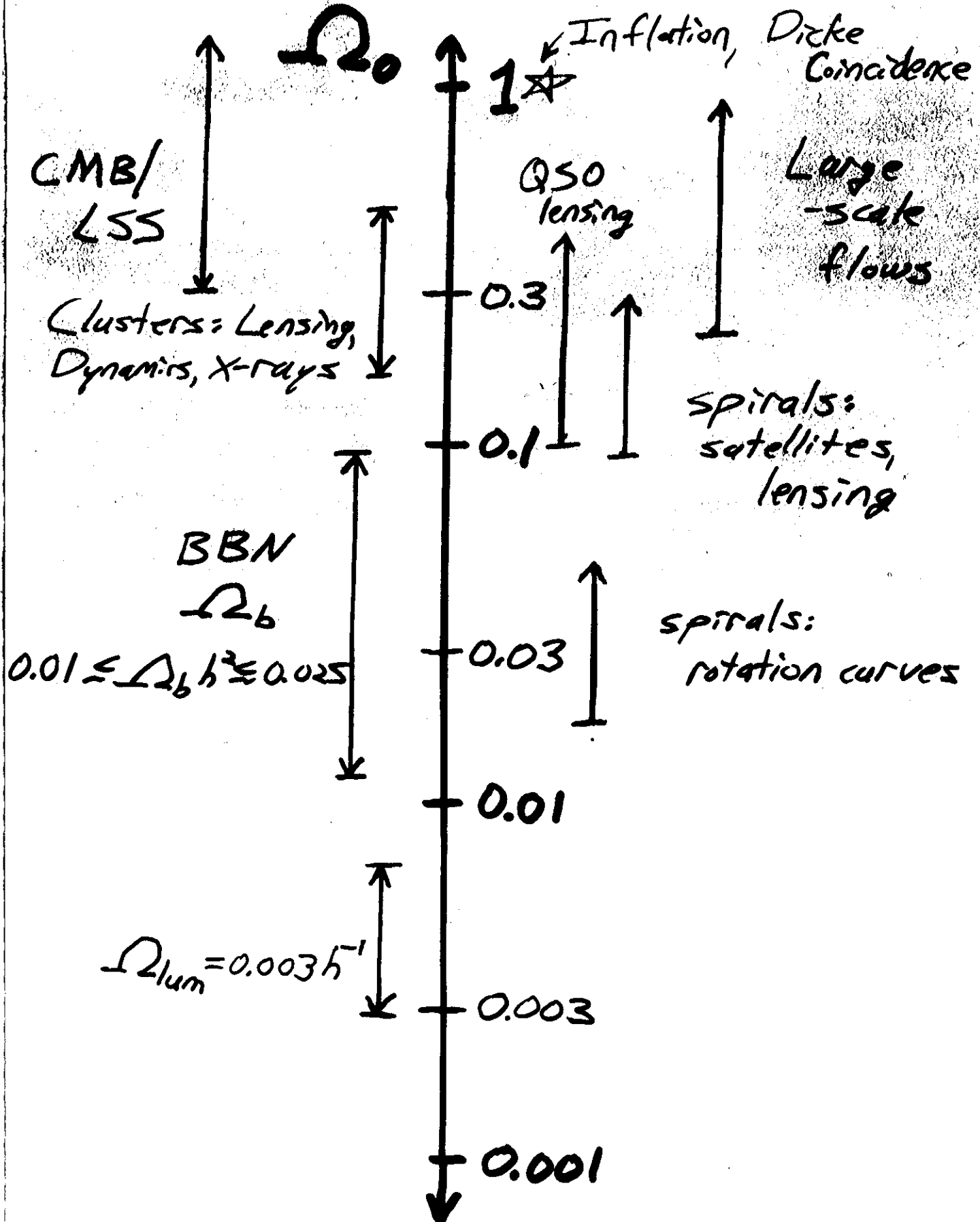
Massive Neutrinos??

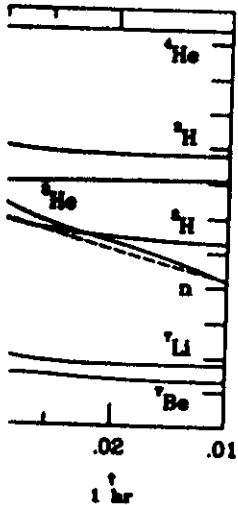
- Structure formation difficult
- Tremaine-Gunn (or Pauli principle): Can't pack so many light neutrinos into halo.

MACHOS??

- Why would halo baryons be dark??
- What if $\Omega_{halo} > \Omega_b$??
- μL in LMC: verdict not in

\implies DM = Something Else





ynthesis. The dashed line is the n of ${}^4\text{He}$, and the number abun-

to: $T_F \propto g_*^{1/6}$, at a higher the dependence of T_F upon of additional light particle

), $X_A \propto \eta^{4-1}$. For a larger I build up slightly earlier, rlier, when the neutron-to-and the time ${}^4\text{He}$ synthesis-proton ratio is only slowly sensitivity of ${}^4\text{He}$ production amount of D and ${}^3\text{He}$ left (using η). This sensitivity D and ${}^3\text{He}$ decreasing as of $\eta \approx 3 \times 10^{-10}$ results one which dominates at

ss fraction of ${}^4\text{He}$ is $Y_P = 0.014[\tau_{1/2}(n) - 10.6 \text{ min}]$.

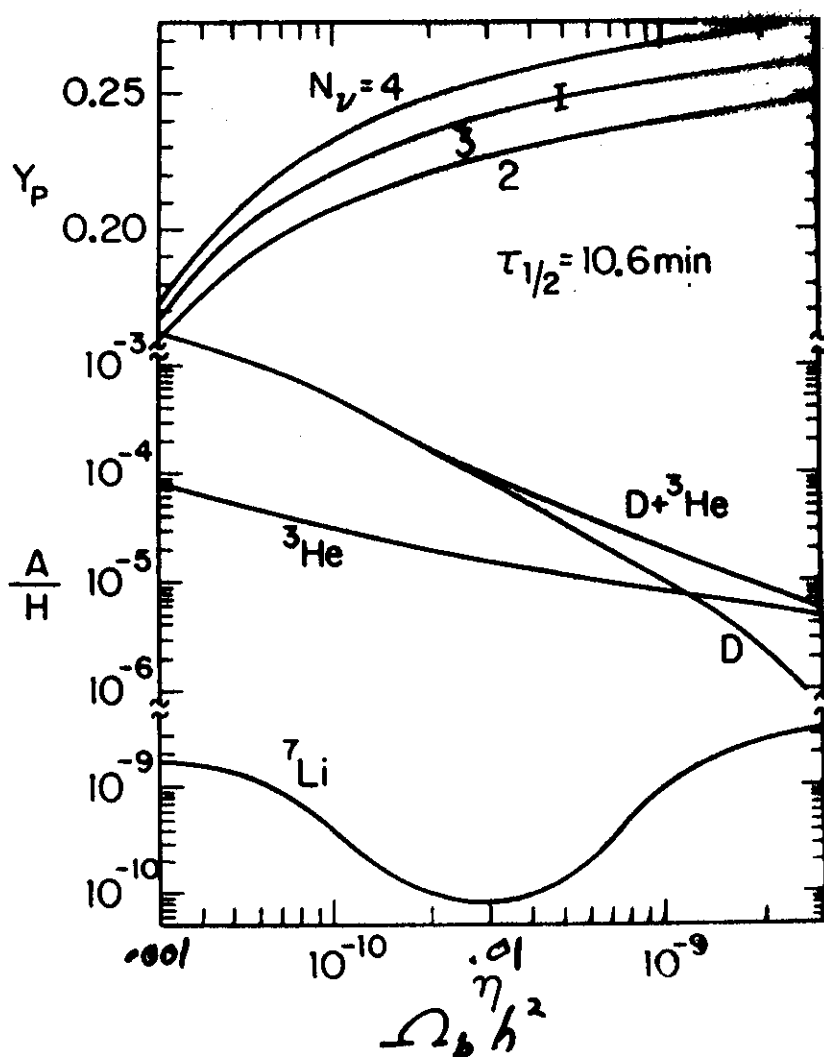


Fig. 4.4: The predicted primordial abundances of the light elements as a function of η . The error bar indicates the change in Y_P for $\Delta\tau_{1/2} = \pm 0.2$ min.

① Dark Matter is Abundant:

$$\Omega_0 \gg \Omega_{\text{lum}}$$

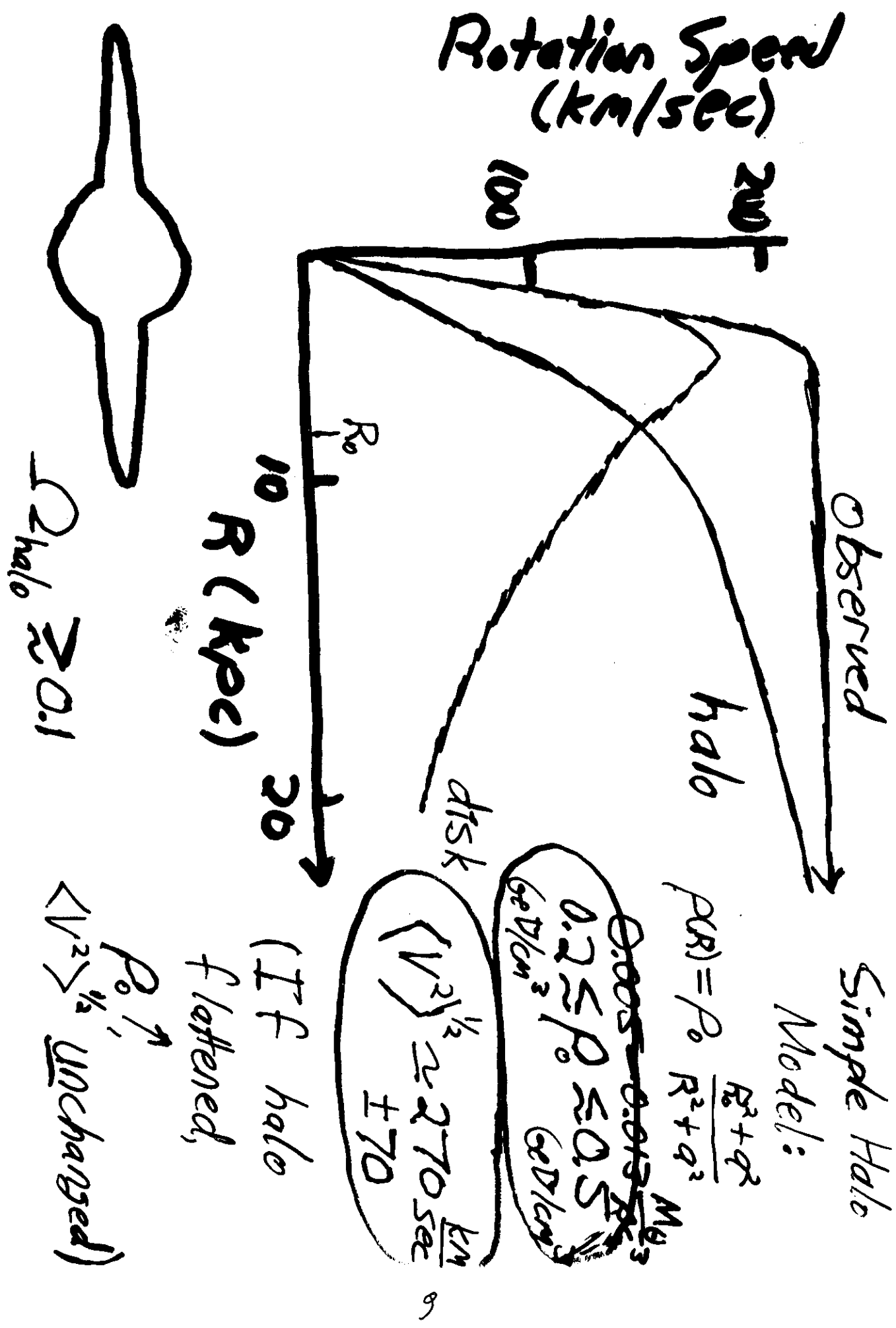
② There is Nonbaryonic
Dark Matter:

$$\Omega_0 > \Omega_b$$

$$(\text{Clusters: } \Omega_0 \gtrsim 3\Omega_b)$$

③ Not Enough Baryonic Matter
to Make Up All of Halo
(probably).

$\Rightarrow \exists$ nonbaryonic matter
in Galactic halo



Local Halo Dark-Matter Density:

$$\text{Halo: } \rho_h(r) = \frac{\rho_0 (a^2 + r_0^2)}{a^2 + r^2} \quad \begin{array}{l} \text{local halo density} \\ \text{at } \sim 8.5 \text{ kpc} \\ (\text{Galactocentric radius}) \\ \text{scale factor} \end{array}$$

(cored)
isothermal sphere

$$\text{DM velocity distribution: } f(\bar{v}) = \frac{e^{-\bar{v}^2/v_0^2}}{\pi^{1/2} v_0^3}$$

Circular speed: (from halo)

$$V_h^2(r) = 4\pi G \rho_0 (r_0^2 + a^2) \left[1 - \frac{a}{r} \arctan \frac{r}{a} \right]$$

$$\frac{a}{r_0} \arctan \frac{r_0}{a} = 1 - \frac{V_h^2(r_0)}{V_0^2} \quad \begin{array}{l} \text{fixes } a/r_0 \\ \text{given } V_h(r_0)/V_0 \end{array}$$

$$V_0 = 220 \text{ km/sec} = V_h(\infty) \quad (\text{since disk is finite})$$

$$\Rightarrow \rho_0 = \frac{V_0^2}{4\pi G r_0^2 [1 + (a/r_0)^2]}$$

$$= 0.47 \frac{G M}{cm^3} \left(\frac{V_0}{220 \text{ km/sec}} \right)^2 \left(\frac{r_0}{8.5 \text{ kpc}} \right)^{-2} \left[1 + \left(\frac{a}{r_0} \right)^2 \right]^{-1}$$

$$\text{Also, } V_0 = V_\infty \quad \bar{v} = \langle v^2 \rangle^{1/2} = \sqrt{\frac{3}{2}} V_0 \approx 270 \frac{\text{km}}{\text{s}}$$

What is $V_h(r_0)$?

$$V_{tot}^2(r) = V_h^2(r) + V_g^2(r) \quad \text{disk contribution}$$

$$\begin{array}{l} \text{total rot} \\ \uparrow \quad \text{speed} \end{array} \quad \text{Disk contribution: } V_d^2(r_0) \approx \left(37 \frac{\text{km}}{\text{s}}\right)^2 \left(\frac{\Sigma}{50 M_\odot \text{pc}^2}\right)$$

$$\Sigma = 37-65 \text{ } M_\odot/\text{pc}^2$$

$$\Rightarrow 118 \text{ km/s} < V_d(r_0) < 155 \text{ km/s.}$$

$$150 \text{ km/s} < V_h(r_0) < 185 \text{ km/s} \quad (\text{for } V_0 = 220)$$

$$\Rightarrow 0.06 \leq \frac{g}{r_0} \leq 0.9$$

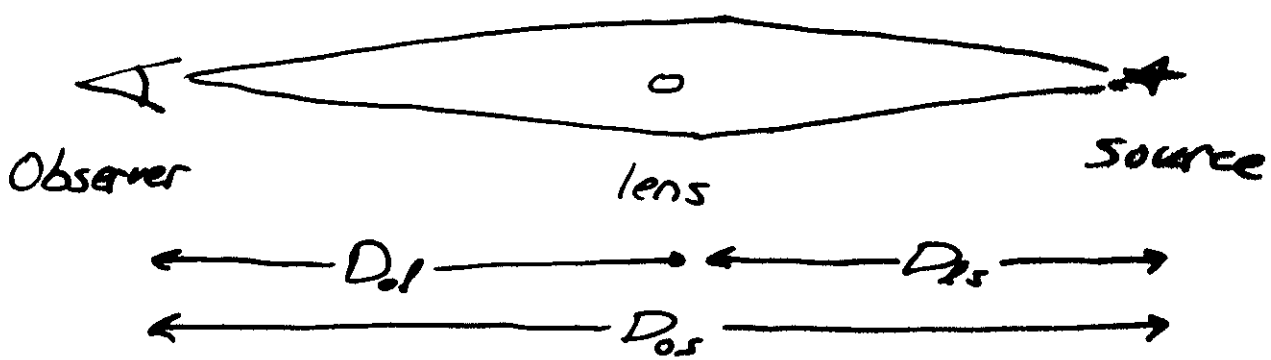
$$\Rightarrow \rho_0 = 0.26 - 0.47 \text{ GeV/cm}^3$$

$$(\text{for } \Sigma = 50, \frac{g}{r_0} = 0.6, \rho_0 = 0.35 \text{ GeV/cm}^3)$$

If halo flattened $\rho_0 \uparrow$

$$\Rightarrow 0.1 \frac{\text{GeV}}{\text{cm}^3} \lesssim \rho_0 \lesssim 0.7 \frac{\text{GeV}}{\text{cm}^3}$$

Gravitational Microlensing and MACHOs in the Halo?

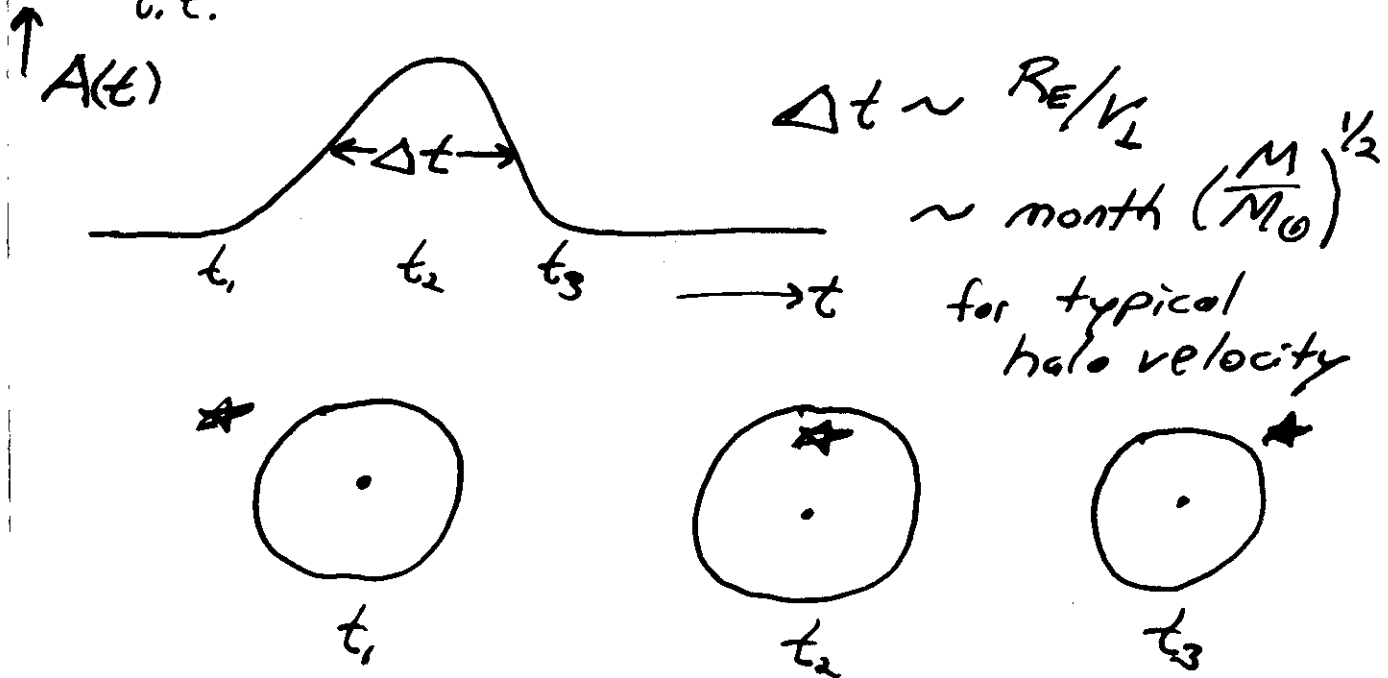


If lens lies within

$$R_E = \left[\frac{4GM_\odot}{c^2} \frac{D_{ol}D_{ls}}{D_{os}} \right]^{1/2}$$

of observer-source line of sight, then
the source is amplified by $A > 1.2$

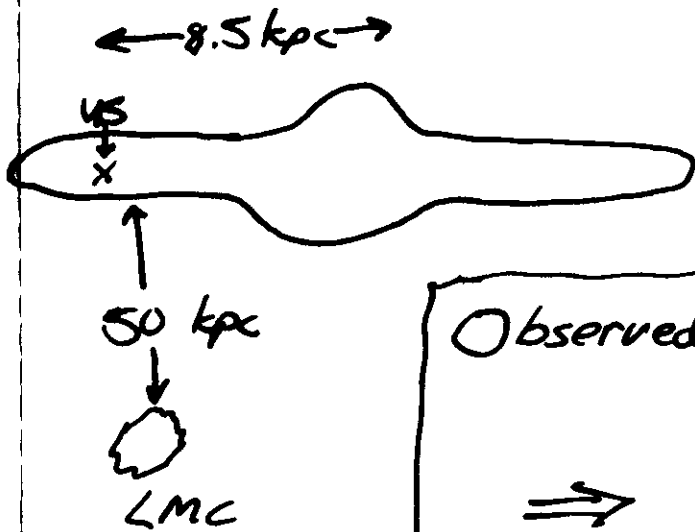
i.e.



If n = number density of lenses,

$$\text{"optical depth"} \quad \tilde{\tau} \sim \pi R_E^2 D_{\text{as}} n$$

is probability any given source is being lensed at any given time.



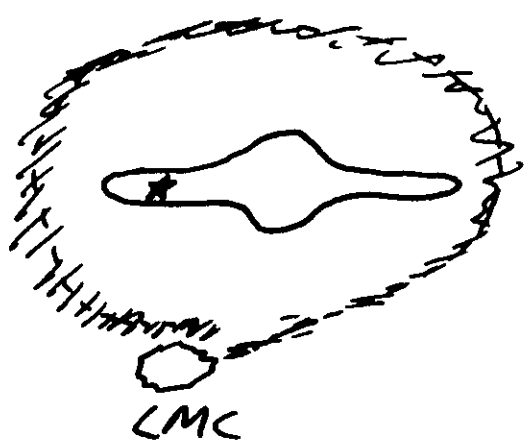
Expect $\tilde{\tau} \sim 10^{-6}$
for all-MACHO halo

Observed: 6-8 events toward
LMC in 2 yrs data
 \Rightarrow 30-50% (\pm a lot)
of halo in MACHOs
 $\langle M_s \rangle \sim 0.4 M_\odot$
 \Rightarrow White Dwarfs?

However: — $\tilde{\tau}_{\text{Bulge}}^{\text{obs}} \sim 2-3 \tilde{\tau}_{\text{Bulge}}^{\text{upred}}$

- Why WD's in halo but absolutely no low-mass stars or stellar remnants?
- new Variable stars? LMC lensing LMC?
warp in our disk?

Another possible explanation:



Could be that LMC
tail provides small
stellar population just in
front of LMC (Zhao 1986)

Recent: Zaritsky et al. Find anomalous
stellar population toward LMC which
can be accounted for by an LMC
tail at 40 kpc.

Are there MACHOs in the halo?

Verdict is still out.

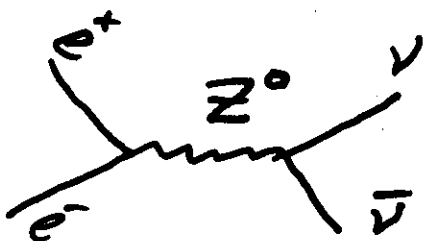
Observations might be explained by
conventional astrophysics; no halo.
New observations will clarify.

Cosmological Abundance of Light ν

($m_\nu \lesssim M_{\text{Pl}}$)

Early Universe:

$$\nu\bar{\nu} \leftrightarrow e^+e^-$$



$$n_\nu \sim T^3 \quad \sigma(\nu\bar{\nu} \rightarrow e^+e^-) \simeq G_F^2 T^2$$

$$(\text{for } T \gg m_\nu) \quad \Gamma(\nu\bar{\nu} \leftrightarrow e^+e^-) \simeq n \sigma v$$

$$\simeq G_F^2 T^5 \left(\frac{\nu\bar{\nu}}{\text{annihilation rate}} \right)$$

$$\text{Expansion Rate: } H \sim T^2/m_{\text{pl}}$$

$$\Gamma > H \quad \text{for } T \gtrsim M_{\text{Pl}} \quad \nu\bar{\nu} \leftrightarrow e^+e^-$$

$$\Gamma \leq H \quad \text{for } T \lesssim M_{\text{Pl}} \quad \nu\bar{\nu} \leftrightarrow e^+e^-$$

\therefore After $T \simeq M_{\text{Pl}}$, $\nu\bar{\nu}$ annihilation "freezes out", and number of neutrinos per comoving volume remains constant

$$n_\nu a^3 = \text{const} \Rightarrow (n_\nu a^3)_{\text{today}} = (n_\nu a^3)_{T=M_{\text{Pl}}}$$

$$(\text{Entropy}/\text{comoving Volume}) = \text{const}$$

Entropy density: $S \propto g_* T^3$

$$g_* = \sum_{\text{bosons}} g_i + \frac{7}{8} \sum_{\text{fermions}} g_i$$

Effective
of
relativistic
degrees of
freedom

$$T \approx 1 \text{ MeV}, \quad g_* = \frac{11}{2} \quad (g_s=2, \quad g_{e\bar{e}}=4)$$

$$T \approx 2.7 \text{ K} \quad g_* = 2 \quad (g_s=2)$$

(today)

$$\text{Since } g_* T^3 a^3 = \text{const}, \quad \left(\frac{T_\nu}{T_8} \right)_{\text{today}} = \left(\frac{4}{11} \right)^{1/3}$$

$$\text{i.e., } n_\nu = \frac{3}{4} \left(\frac{4}{11} \right) n_\nu \quad \text{today}$$

(Fermi vs. Base) ——————
 $\Omega_\nu = \frac{\rho_\nu}{\rho_c} = \frac{m_\nu n_\nu}{\rho_c} \quad n_\nu = 411 \text{ cm}^{-3}$
 $\rho_c = 10^4 h^2 \text{ eV/cm}^3$

$$\Rightarrow \Omega_\nu h^2 = \frac{m_\nu}{90 \text{ eV}} \quad \begin{matrix} \text{for} \\ \text{two-component} \\ \text{neutrino} \end{matrix}$$

$$\text{e.g., if } h=0.5, \quad m_\nu = 5 \text{ eV} \Rightarrow \Omega_\nu = 0.2$$

$$m_\nu \approx 25 \text{ eV} \Rightarrow \Omega_\nu \approx 1$$

Gunn-Tremaine Bound:

(Can't pack too many light fermions
into galactic halo)

Heisenberg: $\Delta x \Delta p \gtrsim 1$

$$\nu \text{ number density} = n_\nu = \frac{\rho_{\text{halo}}}{m_\nu}$$

typical ν momentum: $\Delta p \simeq m_\nu \bar{v}$

$$\text{for } \rho_{\text{halo}} = 0.3 \text{ GeV/cm}^3$$

$$\bar{v} \simeq 300 \text{ km/sec}$$

$$m_\nu \gtrsim 10 eV \left(\frac{\rho}{0.3 \text{ GeV/cm}^3} \right)^{1/4} \left(\frac{v}{300 \text{ km/s}} \right)^{-3/4}$$

Dwarf galaxies: $\bar{v} \downarrow \Rightarrow m_\nu \uparrow$

QM: Light ν unlikely halo DM

Axions: Particle DM Candidate

Electromagnetism: $H_{\text{em}} \sim \vec{E}^2 + \vec{B}^2$

Strong Interactions (Quantum Chromodynamics):

$$H_{\text{QCD}} \sim \vec{E}_s^2 + \vec{B}_s^2 + a \vec{E}_s \cdot \vec{B}_s$$

Neutron Electric Dipole Moment:

$$d_n \approx 10^{-25} \text{ e-cm} \Rightarrow \text{coupling } a \approx 10^{-10} !$$

Strong-CP Problem: Why a so small?

Peccei-Quinn Solution:

Make a dynamical variable,

$$\text{Potential } V(a) \propto a^2$$

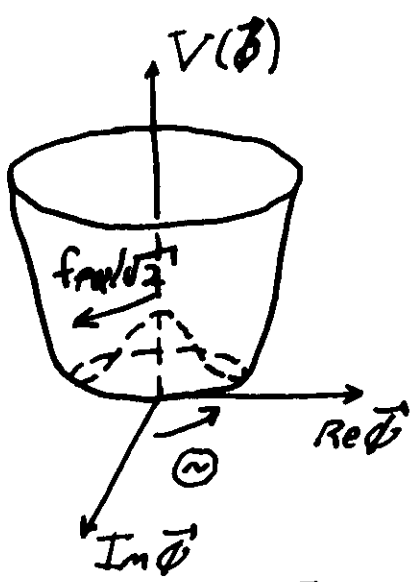
$\Rightarrow V$ minimized at $a=0$.

i.e., a is a scalar field;

its quanta are axions

(Wilczek, Weinberg)

A priori, $10^{-3?} \leq m_a \leq 10^{19} \text{ GeV}$



Cosmological Production of Axions

$$V(\vec{\phi}) = \lambda \left((\vec{\phi})^2 - f_{PQ}^2 / 2 \right)^2$$

$$\langle |\vec{\phi}| \rangle = f_{PQ} / \sqrt{2}$$

$$NG \text{ field: } a = f_{PQ} \odot$$

$$T \gg \Lambda_{QCD} \Rightarrow m_a = 0$$

$$T \ll \Lambda_{QCD}, \quad V(a) = m_a^2 f_{PQ}^2 \left(1 - \cos \left[\frac{a}{f_{PQ}} \right] \right)$$

$$\simeq \frac{1}{2} m_a^2 a^2 + \dots$$

$$m_a \simeq \frac{1}{2} \frac{f_\pi m_e}{f_{PQ}} \simeq 0.62 \text{ eV} \frac{10^7 \text{ GeV}}{f_{PQ}}$$

i.e. at $T \sim \Lambda_{QCD}$, instanton effects tip the Mexican hat.

then, \odot oscillates: $\ddot{\phi} + 3H\dot{\phi} + m_a^2 \phi = 0$

$$\text{solt: } \rho_a = \frac{1}{2} f_{PQ}^2 [\langle \dot{\phi}^2 \rangle + m_a^2 \langle \phi^2 \rangle] \\ \propto a^{-3}$$

\therefore axions form cold nonrelativistic condensate

Estimate of cosmological axion mass density:

$$\frac{\rho_a}{5} \approx \frac{m_a^2 f_{\text{ax}}^2 \langle \dot{\phi}^2 \rangle / 2}{2\pi^2 g_* T_{\text{QCD}}^3 / 45} = \text{const}$$

$$T_{\text{QCD}} \approx \text{GeV} \quad g_* \approx 60 \quad m_a f_{\text{ax}} \approx m_\pi f_\pi / 2$$

$$\Rightarrow \frac{\rho_a}{5} \approx 500 \text{ eV}$$

$$\Omega_a = \frac{\rho_a}{\rho_c} = \frac{(\rho_a/5) S_{\text{today}}}{\rho_c} \left[\frac{2970 \text{ cm}^{-3}}{10^4 h^2 \text{ eV/cm}^3} \right]$$

$$\Rightarrow \Omega_a h^2 \approx 100$$

More precisely:

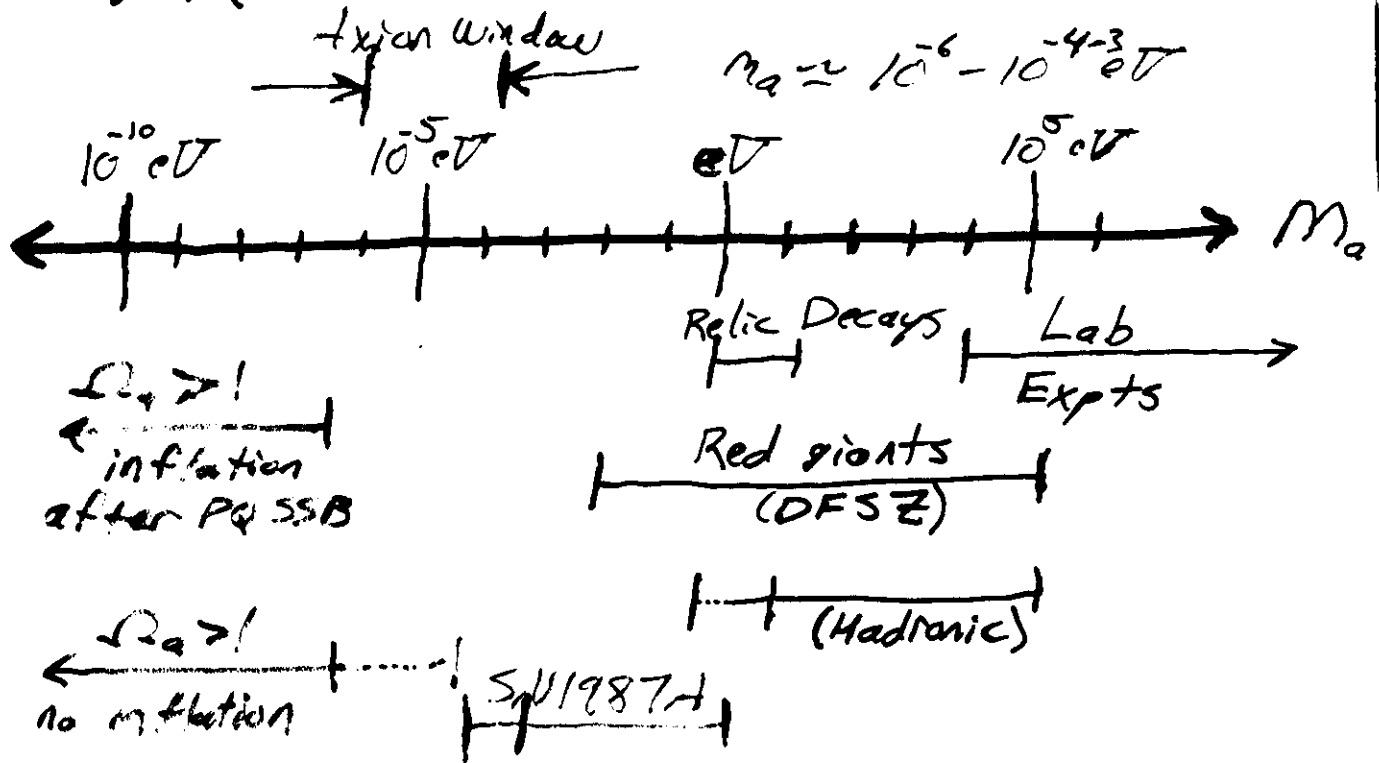
$$\Omega_a h^2 = 0.1 \times 10^{+0.4} \Theta_i^2 \left(\frac{m_a}{10^5 \text{ eV}} \right)^{-1}$$

or

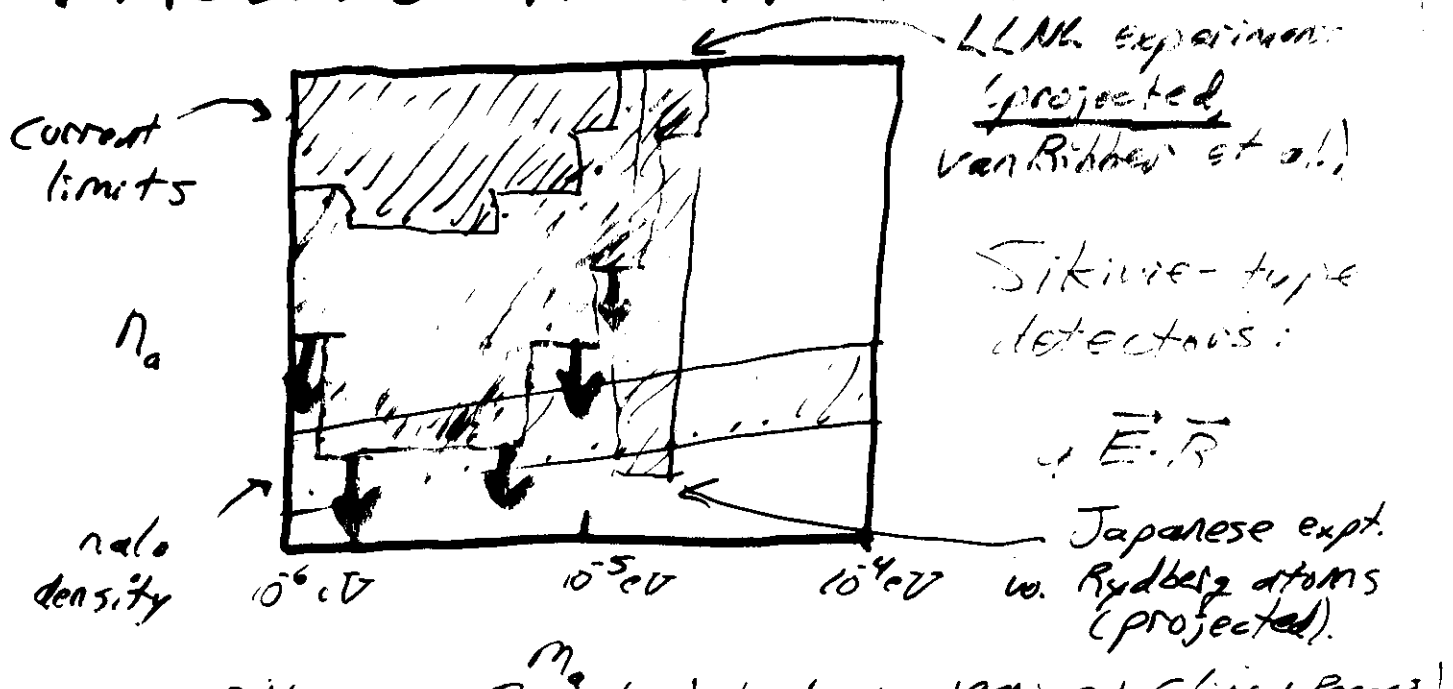
$$= 0.85 \times 10^{+0.4} \left(\frac{m_a}{10^5 \text{ eV}} \right)^{-1}$$

$$\text{if } \langle \dot{\phi}^2 \rangle = \pi^2 / 3$$

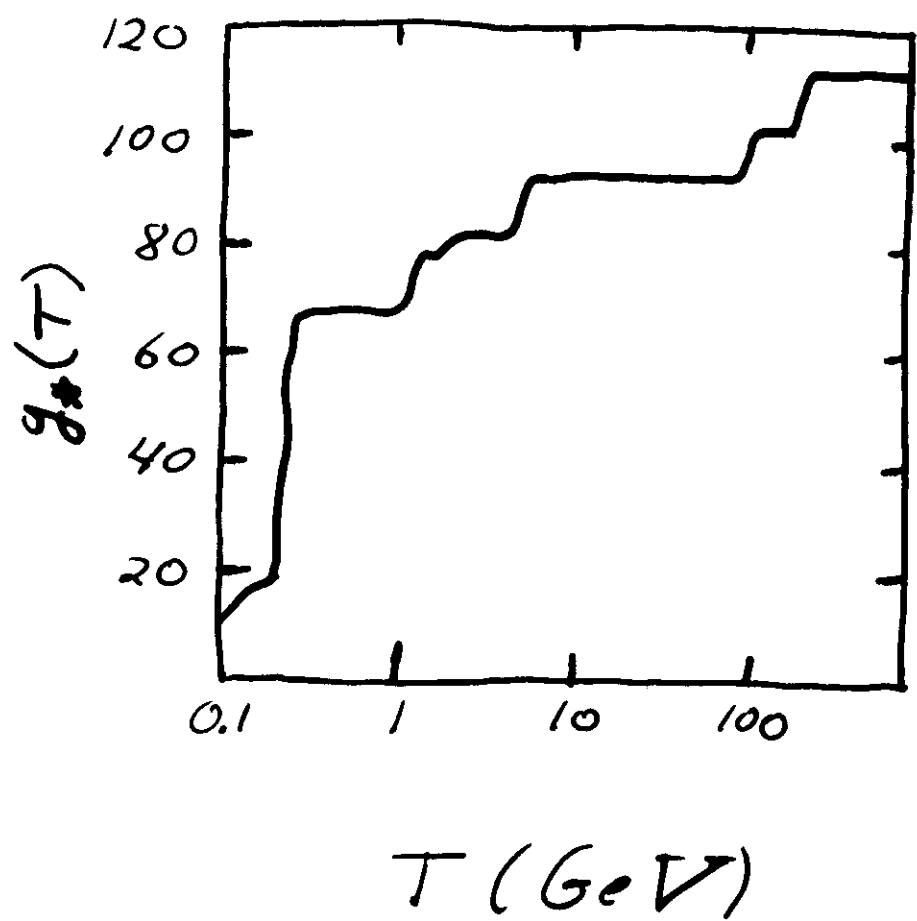
Axion Mass Constraints



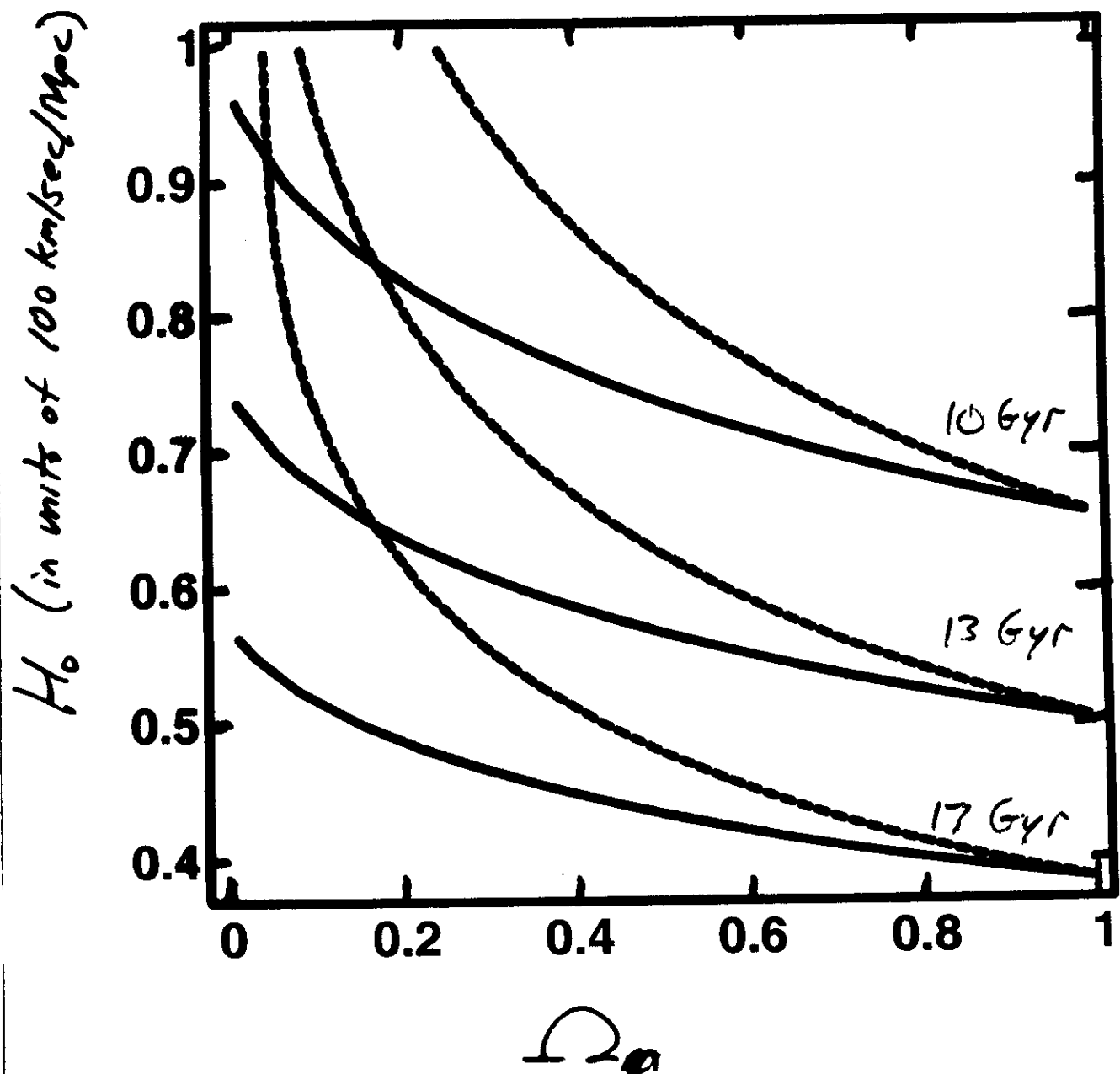
PROBING THE AXION WINDOW:



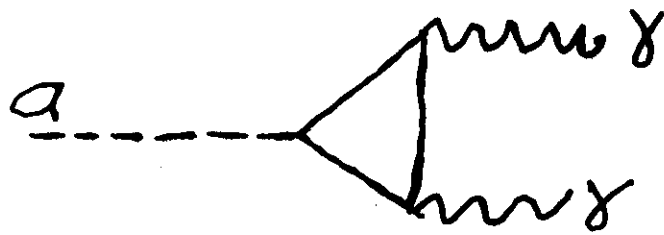
see van Bibber et al., Particle Astrophysics, 1990 ed. Cline + Parker!



— Open
 - - - Flat Λ ($\Omega_m + \Lambda = 1$)



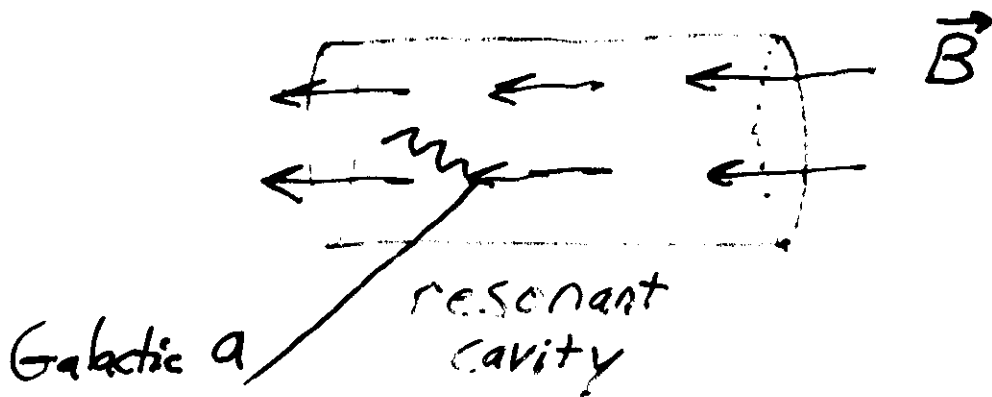
Axion Detection:



$$\tilde{\tau}_{a \rightarrow \gamma\gamma} \sim 10^{50} \text{ sec} \left(\frac{m_a}{10^{-5} \text{ eV}} \right)^{-5} \gg t_u$$

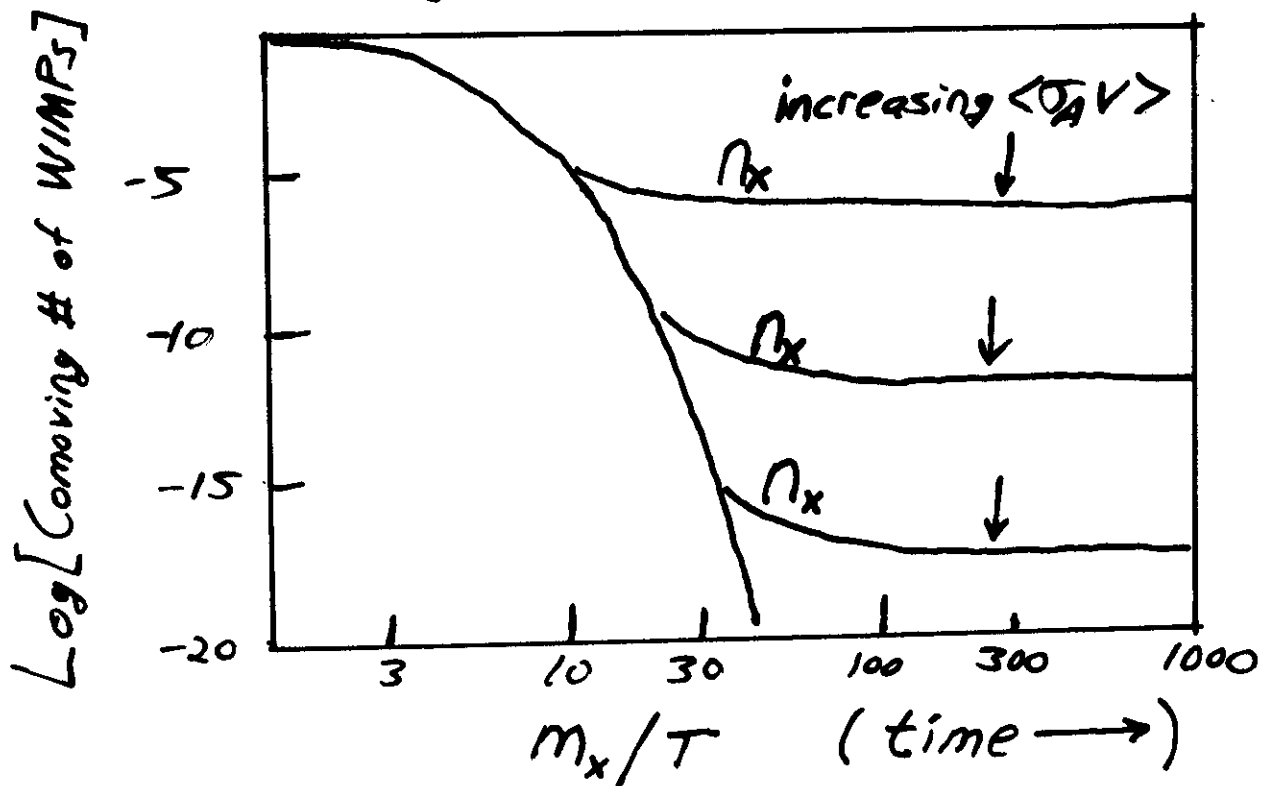
!

$$L_{\text{int}} \propto a \vec{E} \cdot \vec{B}$$



Convert Galactic axions to fundamental-mode excitations of resonant cavity in strong \vec{B} field.
(Sikivie)

Cosmological Abundance of WIMPs:



Thermal Equil. from $(XX \leftrightarrow g\bar{g}, l\bar{l}, W^+W^- \dots)$

$$\text{Rate } \Gamma(XX \rightarrow \text{stuff}) = \rho_x \langle \sigma_A v \rangle$$

$$\text{Expansion Rate: } H \sim \sqrt{G\rho} \sim T^2/m_{pl}$$

$$\text{Early: } T \gg m_x \quad \rho_x \sim T^3 \sim \rho_g \quad \Gamma \gg H$$

$$\text{Late: } T \ll m_x \quad \rho_x^{eq} \sim e^{-m_x T} \quad \Gamma \ll H$$

\Rightarrow Free ~~re~~cool at $\Gamma \approx H$

$$\text{Also } \Omega_x \propto \langle \sigma_A v \rangle^{-1}$$

Relic Abundance of WIMP:

Equilibrium # density: $\eta_x^{eq} = \frac{g}{(2\pi)^3} \int f(\vec{p}) d^3 \vec{p}$

$$f(\vec{p}) = \frac{1}{e^{-E/kT} + 1}$$

$T \gg m_\chi$: $\eta_x^{eq} \propto T^3 \sim \rho$

$T \ll m_\chi$: $\eta_x^{eq} \simeq g \left(\frac{m_\chi T}{2\pi} \right)^{\frac{3}{2}} e^{-m_\chi/T}$

$T \gg m_\chi$: $\chi \bar{\chi} \leftrightarrow l \bar{l} \leftarrow \begin{matrix} \text{maintains} \\ \text{equil. # density} \end{matrix}$

$$\ell = \{ \nu, e, \mu, \tilde{\mu}, \tau, \tilde{\tau}, d, \tilde{s}, b, \tilde{t}, W^\pm, Z^0, H^0, \dots \}$$

Interconversion rate: $\Gamma = \langle \sigma_A v \rangle \eta_x$

More generally, η_x satisfies Boltzmann eq:

$$\frac{d\eta_x}{dt} + 3H\eta_x = -\langle \sigma_A v \rangle [\eta_x^2 - (\eta_x^{eq})^2]$$

$$H(T) = 1.66 g_*^{1/2} T^2 / m_p$$

$$T \gtrsim m_\chi, \quad H \propto T^2, \quad \eta_x \propto T^3, \quad H \ll \langle \sigma_A v \rangle \eta_x$$

$$T \lesssim m_\chi, \quad \eta_x^{eq} \propto e^{-m_\chi T}, \quad \eta_x \ll \langle \sigma_A v \rangle \ll H$$

$\Rightarrow \eta_x$ "freezes out" at temperature T_f

when $\Gamma(T_f) \simeq H(T_f) \quad T_f \sim m_\chi / 30$

After freezeout, $\frac{\gamma_x}{S} \approx \text{const}$, $S = 0.4 g_* T^3$

Using $T' = \langle \bar{\nu}_x v \rangle \gamma_x = H$ at freezeout,

$$\left(-\frac{\gamma_x}{S} \right)_0 = \left(\frac{\gamma_x}{S} \right)_f \approx \frac{100}{m_\pi m_{pe} g_*^{1/2} \langle \bar{\nu}_x v \rangle}$$

$$= \frac{10^{-8}}{\left[\left(\frac{m_\pi}{(GeV)} \right) \left(\frac{\langle \bar{\nu}_x v \rangle}{10^{-27} \text{cm}^3/\text{sec}} \right) \right]}$$

$$S_0 \approx 4000 \text{ cm}^{-3}, \rho_0 \approx 10^{-5} \text{ g/cm}^3$$

$$\Rightarrow Q_x h^2 = \frac{m_\pi \gamma_x}{\rho_0} \approx \frac{3 \times 10^{-27} \text{ cm}^3/\text{sec}}{\langle \bar{\nu}_x v \rangle}$$

More accurately:

$$\bar{\nu}_x v = a + b v^2 + \dots$$

$$Q_x h^2 = 2.82 \times 10^8 \text{ fm} (m/\text{GeV})$$

$$Y_0^{-1} = 0.264 g_*^{1/2} m_{pe} m_\pi \left\{ \frac{a}{X_f} + 3 \frac{(b - \frac{1}{2} a)}{X_f^2} \right\}$$

$$X_f = \ln \left[0.0764 m_{pe} \left(a + \frac{6b}{X_f} \right) c (2+c) m_\pi / (g_* X_f)^{1/2} \right]$$

$$g_* = g(T_f) \quad c \approx \frac{1}{2}$$

Boltzmann Eqn:

$$\Rightarrow \Omega_X h^2 \simeq \left(\frac{\langle \sigma_A v \rangle}{3 \times 10^{-27} \text{ cm}^3 \text{ sec}^{-1}} \right)^{-1}$$

Suppose X = new particle with
electroweak interactions

$$\Rightarrow \sigma \sim \frac{\alpha^2}{(100 \text{ GeV})^2} \quad \begin{array}{l} \text{fine-structure} \\ \text{constant} \end{array} \quad \begin{array}{l} \text{typical} \\ \text{EW mass} \end{array}$$

\therefore If $\sigma_A v \sim$ electroweak scale

$$\Rightarrow \Omega_X \sim 1 !!$$

(i.e. If \exists another stable EW particle,
it should be the dark matter.)

E.g. $X = \text{Heavy } v \quad (m_v \lesssim \text{TeV}; m_v \gtrsim \text{GeV})$

More plausible: Lightest Supersymmetric
Particle.

(Relevant) Aside:

Model-Independent Bound
to WIMP Mass:

(Kamionkowski + Griest, PRL 64 1991)

$$\Omega_x h^2 \simeq \frac{3 \times 10^{-27} \text{ cm}^3/\text{sec}}{\langle \sigma v \rangle}$$

$$t_u \gtrsim 10 \text{ Gyr} \Rightarrow \Omega_x h^2 \lesssim 1$$

Unitarity (i.e., probability ≤ 1):

$$\langle \sigma v \rangle \leq \frac{3 \times 10^{-22} \text{ cm}^3/\text{sec}}{(m_x / \text{TeV})^2}$$

$$\Rightarrow \langle \sigma v \rangle \gtrsim 3 \times 10^{-27} \text{ cm}^3/\text{sec}$$

$$\Rightarrow \boxed{m_x \lesssim 300 \text{ TeV}}$$

= for strong interaction

for weak interaction σ reduced by α^2 ,
so expect $m_x \lesssim 3 \text{ TeV}$ for WIMP

Supersymmetry:

New symmetry between fermions/bosons
(like isospin for proton/neutron).

For every fermion, \exists bosonic partner + vice versa.
(e.g. electron \leftrightarrow selection, quark \leftrightarrow squark)

Why?

- (1) Explaining Mass Hierarchy ($EW \xleftrightarrow{10^{-16} GeV} IC^{15-19}$ GUT/Planck)
- (2) Gravity
- (3) Strings
- (4) Aesthetics
- (5) Fine-constant Unification
- (6) ...

Cosmology:

New symmetry \Rightarrow Lightest SUSY
(R-parity)
and weakly interacting $\Rightarrow \underline{\Omega_{LSP} \sim 1}$

Undetermined SUSY Parameters:

M (gaugino mass)

$\mu_{\tilde{\chi}}$ (higgsino mass)

$\tan \beta$ ($\langle \cos \theta / \sin \theta \rangle$)
- m_t/m_b

$M_{\tilde{g}}$ (squark masses)

$> M_{\tilde{\chi}}$

M_{H^0} (mass of
lightest Higgs)
 $< M_{\tilde{\chi}}$

$M_{\tilde{t}}$ (top quark mass)

~~Bottom quark mass~~

63 parameters in minimal SUSY SM or
predicted by, e.g., GUTs, SUGRA, string

Determine

Mass and

Composition of $\tilde{\chi}$

Qualitative

Relative

Inertial +

$M_{\tilde{\chi}} =$ Determined

Most models: LSP is neutralino: (Ellis et al 1984)

$$\tilde{\chi} = \alpha_1 \tilde{\gamma} + \alpha_2 \tilde{Z} + \alpha_3 \tilde{H}_1 + \alpha_4 \tilde{H}_2$$

(e.g. photino, higgsino, Z-ino, gaugino, B-ino, W_S -ino)

Spin $\frac{1}{2}$ Majorana (its own antiparticle)

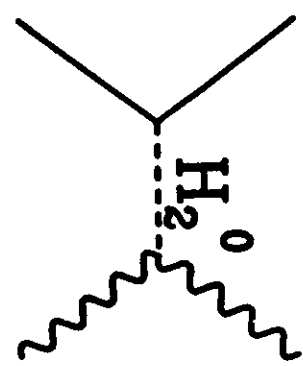
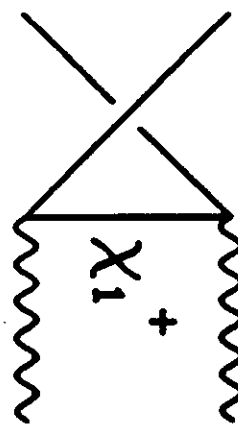
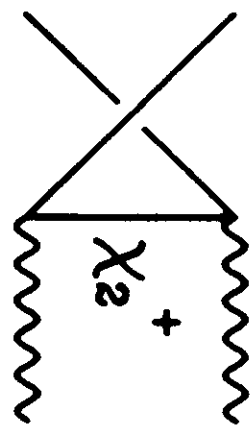
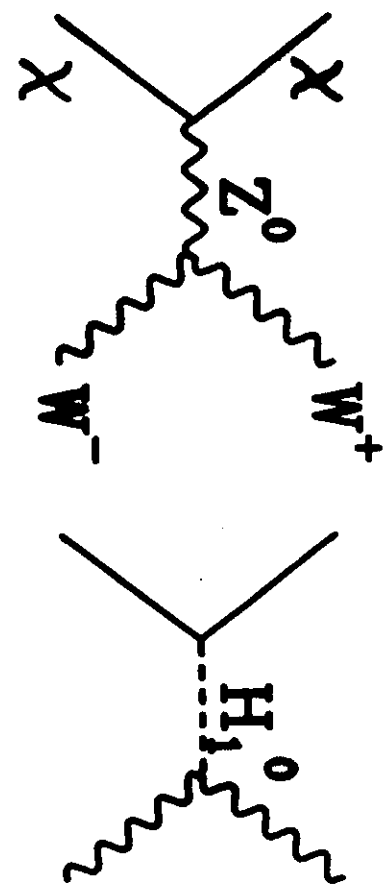
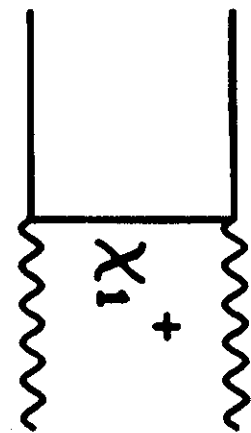
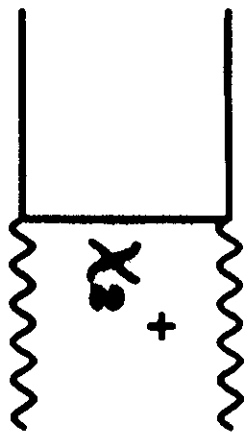
$$10 \text{ GeV} \lesssim M_\chi \lesssim \text{few TeV}$$

To get relic abundance, need annihilation cross section for:

$$\tilde{\chi}\tilde{\chi} \rightarrow \left\{ gg, \ell\bar{\ell}, W^+W^-, Z^0Z^0, \text{ Higgs bosons, etc.} \right\}$$

Griest, MK, Turner (1990): Monte Carlo survey of SUSY parameter space
⇒ $\Omega_\chi \sim 1$ in most models!
(also in Jungman, MK, + Griest 1996)

1. 2



V. CONCLUSIONS

In this paper, we have studied in some detail the possibility of a "heavy" neutralino ($m_{\tilde{\chi}} > m_W$), mapping out completely the cosmologically allowed regions of parameter space. The main difference between a heavy and a light ($m_{\tilde{\chi}} < m_W$) neutralino is that additional annihilation channels open up (various pairs of Higgs and gauge bosons). We have calculated the annihilation cross sections into these new channels for a general neutralino state. In large regions of the parameter space for the minimal supersymmetric extension of the standard model ($\mu, M, \tan\beta, m_{H_1^0}, m_f$, and m_i) the new channels make a substantial contribution to the annihilation cross section, and for a neutralino that is Higgsino-like, the gauge-boson final states ($W^+ W^-$, $Z Z$) often dominate all the other channels by a factor of 10. On the other hand, for a heavy neutralino that is gaugino-like, the new final states are typically subdominant. The new channels contribute and cannot be ignored for neutralinos that are mixed states.

Using our results for the new annihilation channels along with previous results for the fermion final states, we have calculated the total annihilation cross section for heavy neutralinos and, from this, the relic cosmological abundance of heavy neutralinos. We find that for a large portion of the parameter space, a heavy neutralino of mass between m_W and 3200 GeV can have a cosmologically interesting relic abundance, i.e., $0.023 \leq \Omega_{\tilde{\chi}} h^2 \leq 1$. Thus, we conclude that a heavy neutralino is a well motivated and viable dark-matter candidate. Based upon the cosmological constraint $\Omega_{\tilde{\chi}} h^2 \leq 1$, we have mapped out the regions of parameter space that are cosmologically forbidden. In particular, for $m_{\tilde{\chi}} < 180$ GeV, one can completely rule out a neutralino that is heavier than about 3200 GeV. For a neutralino that is Higgsino-like, the bound is about 3000 GeV, while if the neutralino is gaugino-like, the bound is about 550 GeV. (If a top quark of mass less than 120 GeV is discovered, the general bound drops to 2600 GeV.) As noted in the Introduction, Olive and Srochnicki⁶ have recently considered the case of a heavy neutralino that is either pure gaugino or pure Higgsino. In these limiting cases and for the values of $m_{\tilde{\chi}}$ and $\tan\beta$ they have considered, our results agree with theirs. Finally, it is interesting to note that the cosmological upper bound to the neutralino mass is comparable to that which follows by insisting that low-energy supersymmetry "solve" the hierarchy problem.

ACKNOWLEDGMENTS

M.P.K. would like to thank R. G. Sachs for encouragement during the early part of this work. This research was supported in part by the DOE (at Chicago), by NASA (Grant No. NGW-140) and the DOE at Fermilab, and by the NSF Office of Science and Technology Centers, under cooperative agreement AST-8809616 (at Berkeley). M.P.K. also acknowledges financial support through the NASA Graduate Student Research Program.

APPENDIX A: CROSS SECTION FOR $\tilde{\chi} \rightarrow W^+ W^-$

Let us review the masses and mixing parameters of the minimal supersymmetric standard model. The quantities M, M' , and μ are the masses that appear in the neutralino mass matrix Y , Eq. (C38) of Ref. 1, and Z_{ij} are the elements of the real orthogonal matrix that diagonalizes Y . The masses of the four neutralinos are the absolute values of the eigenvalues of Y , $m_{\tilde{\chi}_i}$; one should keep in mind the fact that the $m_{\tilde{\chi}_i}$ may be negative. The mass of the lightest neutralino is the n th eigenvalue of Y which we shall denote by $m_{\tilde{\chi}}$. The chargino masses $m_{\tilde{\chi}_i^\pm}$, given by Eq. (C18) in Ref. 1, are always positive. The quantities ϕ_- and ϕ_+ , determined from formulas given in Ref. 22, describe the mixing of the charginos. The squares of the Higgs-boson masses ($m_{H_1^0}^2$ and $m_{H_2^0}^2$), α , and β are given in Appendix A of Ref. 11. Finally, the quantities g and g' are, respectively, the U(1) and SU(2) gauge couplings. In this appendix only, some quantities are scaled by m_W in order to simplify some of the equations. Specifically,

$$\omega = \left[\frac{m_{\tilde{\chi}}}{m_W} \right]^2, \quad \kappa_i = \left[\frac{m_{\tilde{\chi}_i^\pm}}{m_W} \right]^2, \\ \zeta = \left[\frac{m_Z}{m_W} \right]^2, \quad s = \frac{(p_1 + p_2)^2}{m_W^2}, \quad (A1)$$

where $s m_W^2$ is the square of the center-of-mass energy, and p_1 and p_2 are the four-momenta of the incoming neutralinos. (In Appendix B, these same quantities will be rescaled by m_Z .)

Next we define the quantities

$$\begin{bmatrix} e_1 \\ e_2 \end{bmatrix} = 2 \left[\frac{Z_{n3}}{\sqrt{2}} \begin{bmatrix} \sin\phi_- \\ \cos\phi_- \end{bmatrix} + Z_{n2} \begin{bmatrix} \cos\phi_- \\ -\sin\phi_- \end{bmatrix} \right], \\ \begin{bmatrix} f_1 \\ f_2 \end{bmatrix} = 2 \left[\frac{-Z_{n4}}{\sqrt{2}} \begin{bmatrix} \sin\phi_+ \\ \epsilon \cos\phi_+ \end{bmatrix} + Z_{n2} \begin{bmatrix} \cos\phi_+ \\ -\epsilon \sin\phi_+ \end{bmatrix} \right], \quad (A2)$$

where $\epsilon = \det X / |\det X|$ and X is the matrix defined in Eq. (C9) of Ref. 1. From these we define

$$\begin{aligned} C_i^{(1)} &= e_i^2 f_i^2, \quad C_i^{(2)} = e_i^3 f_i + e_i f_i^3, \\ C_i^{(3)} &= e_i^4 + f_i^4, \quad C_i^{(4)} = e_i^2 - f_i^2, \quad C_i^{(5)} = e_i^2 + f_i^2, \\ D^{(1)} &= e_1^2 e_2^2 + f_1^2 f_2^2, \quad D^{(2)} = e_1^2 e_1 f_1 + f_1^2 e_1 f_1, \quad (A3) \\ D^{(3)} &= e_1^2 f_2^2 + e_2^2 f_1^2, \quad D^{(4)} = e_1^2 e_2 f_2 + f_1^2 e_2 f_2, \\ D^{(5)} &= 2e_1 e_2 f_1 f_2, \end{aligned}$$

where $i = 1, 2$.

The following dimensionless quantities are also useful:

$$\begin{aligned} \gamma &= \left[\left(1 - \frac{4\omega}{s} \right) \left(1 - \frac{\zeta}{s} \right) \right]^{1/2}, \\ L_i &= \frac{1}{\gamma s} \ln \left(\frac{(1+\gamma)s-2-2\omega+2x_i}{(1-\gamma)s-2-2\omega+2x_i} \right), \\ K_i &= \frac{1}{\gamma s} \left[\frac{1}{(1+\gamma)s-2-2\omega+2x_i} \right. \\ &\quad \left. - \frac{1}{(1-\gamma)s-2-2\omega+2x_i} \right], \end{aligned} \quad (\text{A4})$$

$$A = \frac{m_{\tilde{\chi}}}{m_W} \sin \alpha + 2[Q \sin(\beta - \alpha) - R \cos \alpha],$$

$$C = \frac{m_{\tilde{\chi}}}{m_W} \cos \alpha - 2[Q \cos(\beta - \alpha) + R \cos \alpha],$$

where

$$\begin{aligned} Q &= \frac{Z_{n3}}{g}(gZ_{n2} - g'Z_{n1}), \\ R &= \frac{1}{2m_W}(M^2 Z_{n2}^2 + M'^2 Z_{n1}^2 - 2\mu Z_{n3} Z_{n4}), \\ F &= Z_{n3}^2 - Z_{n1}^2. \end{aligned} \quad (\text{A5})$$

The total cross section, averaged over neutralino spin for the process $\tilde{\chi}\tilde{\chi} \rightarrow W^+W^-$ is given by

$$\begin{aligned} \sigma_{WW} &= \frac{1}{32\pi m_W^2} \left[\frac{s-4}{s-4\omega} \right]^{1/2} \\ &\times (X_{ZZ} + X_{HH} + X_{\tilde{\chi}\tilde{\chi}} + \\ &+ X_{\tilde{\chi}^+\tilde{\chi}^+} + X_{Z\tilde{\chi}^+} + X_{H\tilde{\chi}^+}). \end{aligned} \quad (\text{A6})$$

The quantities X_u arise from squaring the matrix element given by the Feynman diagrams in Fig. 2, summing over final state polarizations and averaging over initial neutralino spins. Specifically, X_{ZZ} comes from the square of the Z-exchange diagram, X_{HH} comes from the square of the Higgs-boson-exchange diagrams, $X_{\tilde{\chi}\tilde{\chi}}$ comes from the sum of the squares of the t - and u -channel exchange of the charginos, $X_{\tilde{\chi}^+\tilde{\chi}^+}$ comes from the interference be-

tween the t - and u -channel exchange of the charginos, and $X_{Z\tilde{\chi}^+}$ and $X_{H\tilde{\chi}^+}$ come from the interference of the chargino-exchange diagrams with the Z- and Higgs-boson-exchange diagrams. The interference between the Z- and Higgs-boson-exchange diagrams vanishes. The quantities X_u are given by

$$\begin{aligned} X_{ZZ} &= \frac{F^4 F^2}{24} \frac{(s-4)(s-4\omega)(\zeta^2 + 20s + 12)}{(s-\zeta)^2 + (\Gamma_Z/m_Z)^2}, \\ X_{HH} &= -\frac{F^4}{8 \sin^2 \beta} \left[2 + \left(\frac{s}{2} - 1 \right)^2 \right] (s-4\omega) A'^2, \\ X_{\tilde{\chi}\tilde{\chi}} &= \frac{F^4}{16} \sum_i \left[C_i^{(1)} G_i^{(1)} + \frac{m_{\tilde{\chi}_i^+}}{m_W} \frac{m_{\tilde{\chi}_i^+}}{m_W} C_i^{(2)} G_i^{(2)} \right. \\ &\quad \left. + C_i^{(3)} G_i^{(3)} \right], \\ X_{\tilde{\chi}^+\tilde{\chi}^+} &= \frac{F^4}{8} \left[D^{(1)} G^{(4)} \right. \\ &\quad \left. + \frac{m_{\tilde{\chi}}}{m_W} \left[\frac{m_{\tilde{\chi}_i^+}}{m_W} D^{(2)} + \frac{m_{\tilde{\chi}_i^+}}{m_W} D^{(4)} \right] G^{(5)} \right. \\ &\quad \left. - D^{(3)} G^{(6)} + \frac{m_{\tilde{\chi}_i^+}}{m_W} \frac{m_{\tilde{\chi}_i^+}}{m_W} D^{(5)} G^{(7)} \right], \end{aligned} \quad (\text{A7})$$

$$X_{Z\tilde{\chi}^+} = \frac{g^4 F}{8[(s-\zeta)^2 + (\Gamma_Z/m_Z)^2]^{1/2}} \sum_i C_i^{(5)} G_i^{(8)},$$

$$X_{H\tilde{\chi}^+} = -\frac{F^4 A'}{8 \sin \beta} \sum_i \left[\frac{m_{\tilde{\chi}}}{m_W} C_i^{(6)} G_i^{(9)} + 2 \frac{m_{\tilde{\chi}_i^+}}{m_W} e_i f_i G_i^{(10)} \right],$$

where Γ_Z is the Z width. Here

$$\begin{aligned} A' &= \frac{A \cos(\beta - \alpha)}{[(s - m_{H_1^0}^2/m_W^2)^2 + (\Gamma_{H_1^0}/m_W)^2]^{1/2}} \\ &+ \frac{C \sin(\beta - \alpha)}{[(s - m_{H_2^0}^2/m_W^2)^2 + (\Gamma_{H_2^0}/m_W)^2]^{1/2}}, \end{aligned} \quad (\text{A8})$$

where $\Gamma_{H_i^0}$ is the width of the H_i^0 , and the G are given by

$$G_i^{(1)} = 4\kappa_i K_i \{ -(\kappa_i - \omega - 2)^2 s + 4(\kappa_i - \omega - 1)^2 + 2\omega + 36 \} - \frac{1}{s} [2s^2 + s(40 - 6\omega - 36\kappa_i) + 24\omega - 12(\kappa_i - \omega)^2 + 120\kappa_i] - 4L_i \{ s^2(4\kappa_i - 2\kappa_i^2 - \kappa_i\omega) + s[8 - 9\kappa_i - 12\omega + 14\kappa_i^2 - 6\omega\kappa_i + 4\omega^2 - 3\kappa_i(\kappa_i - \omega)^2] + 6\kappa_i - 8\omega + 8\omega^2 - 13\kappa_i^2 + 6\omega\kappa_i + 8\kappa_i(\kappa_i - \omega)^2 - (\kappa_i - \omega)^4 \},$$

$$G_i^{(2)} = 24K_i \{ 2 - (\kappa_i + \omega)^2 - (\kappa_i - \omega)^2 \} + 16 - 4s + \frac{8L_i}{s - 2 - 2\omega + 2\kappa_i} \{ s^2(\kappa_i - 1) + s[(\kappa_i - \omega)^2 - 6\kappa_i + 2\omega + 4] - 7(\kappa_i - \omega)^2 + 5\kappa_i - 7\omega + 2 \},$$

$$G_i^{(3)} = 2K_i \{ (\kappa_i - \omega - 2)^2 s + \kappa_i [\kappa_i(\kappa_i - 4\omega - 2) + 6\omega^2 + 6\omega + 5] - 2(\omega + 2)(2\omega^2 - \omega + 2) \} + (\omega - 1)^2(\omega + 2)^2 + \frac{L_i}{s - 2 - 2\omega + 2\kappa_i} \{ s^2(3\kappa_i^2 + \omega^2 - 8\kappa_i + 4) + 2s[5\kappa_i^2 - (11\omega + 14)\kappa_i^2 + (7\omega^2 + 16\omega + 17)\kappa_i - \omega^3 - 10\omega^2 + 3\omega - 8] + 4[2(\kappa_i - \omega)^4 - 4(\kappa_i - \omega)^3 - \kappa_i(\kappa_i - \omega)^2 + 8\kappa_i^2 + 9\omega\kappa_i + 9\kappa_i - (\omega - 4)(\omega + 1)] \} - \frac{1}{s} [-2s^2 + (12\kappa_i - 16\omega - 40)s + 36(\kappa_i - \omega)^2 - 24\kappa_i + 88\omega + 48],$$

$$G_i^{(4)} = -\frac{L_2}{\kappa_1 - \kappa_2} \{ s(\kappa_2 - \omega - 2)^2 \kappa_2 + (\kappa_2 - \omega)^4 + 2(\omega - \kappa_2)^3 + 5\kappa_2^2 - 8\kappa_2 - (\omega + 2)(3\omega - 2) \} + (1 \leftrightarrow 2) + \frac{\omega L_2}{2 + 2\omega - \kappa_1 - \kappa_2 - s} \{ \kappa_2 s^2 + s[(\kappa_2 - \omega)^2 - 6\kappa_2 + 2\omega - 3] - 4(\kappa_2 - \omega)^2 + 8\kappa_2 + 2\omega + 2 \} + (1 \leftrightarrow 2) - \frac{1}{s} [-2s^2 + (6\kappa_1 + 6\kappa_2 - 16\omega - 40)s + 9(\kappa_1 + \kappa_2)^2 - (36\omega + 12)(\kappa_1 + \kappa_2) + 3(\kappa_1 - \kappa_2)^2 + 4(9\omega^2 + 22\omega + 12)],$$

$$G_i^{(5)} = 8 - 2s - \frac{6L_2}{\kappa_1 - \kappa_2} \{ -(\kappa_2 - \omega)^2 + 2 - \kappa_2 - \omega \} + (1 \leftrightarrow 2) + \frac{L_2}{s - 2 - 2\omega + \kappa_1 + \kappa_2} \{ s^2(2\kappa_2 - 2) + s[2(\kappa_2 - \omega)^2 - 6\kappa_2 - 2\omega + 11] - 2(\kappa_2 - \omega)^2 + 4\kappa_2 - 8\omega - 2 \} + (1 \leftrightarrow 2),$$

$$G_i^{(6)} = \frac{18\omega}{\kappa_1 - \kappa_2} (\kappa_2 L_2 - \kappa_1 L_1) + \frac{s^2}{6} - \frac{s}{12} [6(\kappa_1 + \kappa_2) + 8\omega - 40] - \{ \frac{1}{s} (\kappa_1 + \kappa_2) - \omega \}^2 + \kappa_1 + \kappa_2 - \frac{1}{s} (\kappa_1 - \kappa_2)^2 + \frac{1}{s} \omega + \frac{L_2}{2 + 2\omega - \kappa_1 - \kappa_2 - s} \{ s^2(4\kappa_2 - \kappa_2^2) + s[-2\kappa_2(\kappa_2 - \omega)^2 + 8\kappa_2^2 - 8\omega\kappa_2 - 9\kappa_2 + 4(\omega - 2)(\omega - 1)] - (\kappa_2 - \omega)^4 + 4\kappa_2(\kappa_2 - \omega)^2 - 5\kappa_2^2 + (2\omega + 2)\kappa_2 + 9\omega^2 - 8\omega \} + (1 \leftrightarrow 2),$$

$$G_i^{(7)} = \frac{L_2}{\kappa_1 - \kappa_2} \{ s(\kappa_2 - \omega - 2)^2 - 4(\kappa_2 - \omega)^2 + 8\kappa_2 - 28\omega - 4 \} + (1 \leftrightarrow 2) + \frac{L_2}{s - 2 - 2\omega + \kappa_1 + \kappa_2} \{ s^2(\omega - \kappa_2) + s[-(\kappa_2 - \omega)^2 + 6(\kappa_2 - \omega)] + 4(\kappa_2 - \omega)^2 - 8(\kappa_2 + \omega) + 4 \} + (1 \leftrightarrow 2) + 2s - 8,$$

$$G_i^{(8)} = L_i \{ \kappa_i s^2(4 + \omega - \kappa_i) + s[4\kappa_i^2 - 5(\kappa_i + 3\omega) - (\kappa_i - \omega)^3 - 10\omega\kappa_i + 6\omega^2 + 8] + 2(\kappa_i - \omega)^3 - 8\omega(\kappa_i - \omega) - 6r_i - 10\omega + 4 \} + \frac{1}{s} [-s^3 + s^2(3\kappa_i + \omega - 18) + s[6(\kappa_i - \omega)^2 - 12\kappa_i + 36\omega + 28] - 12(\kappa_i - \omega)^2 - 12\kappa_i + 44\omega + 24],$$

$$G_i^{(9)} = L_i \{ -\kappa_i s^2 + s[\kappa_i - 2 + 3\omega - (\kappa_i - \omega)^2] + 4 - 2(\kappa_i + \omega) - 2(\kappa_i - \omega)^2 \} + \frac{1}{s} [2s^2 + 4(\kappa_i - \omega - 1)s + 8(\kappa_i - \omega + 2)],$$

$$G_i^{(10)} = s(1 - s/2) + L_i \{ \frac{1}{s} (\kappa_i + \omega) s^2 - s(2 + \kappa_i + 3\omega) + 12\omega \}.$$

At zero velocity, the Higgs-boson- and Z-exchange diagrams vanish, and only the chargino-exchange diagrams remain. The rather lengthy expression for σ_{WW} times the relative velocity reduces to

$$\sigma_{WW} v (v \rightarrow 0) = \frac{g^4 (\omega - 1)^{3/2}}{128\pi |m_{\tilde{\chi}}| m_W} \left[\frac{e_1^2 + f_1^2}{1 - \omega - \kappa_1} + \frac{e_2^2 + f_2^2}{1 - \omega - \kappa_2} \right]. \quad (A10)$$

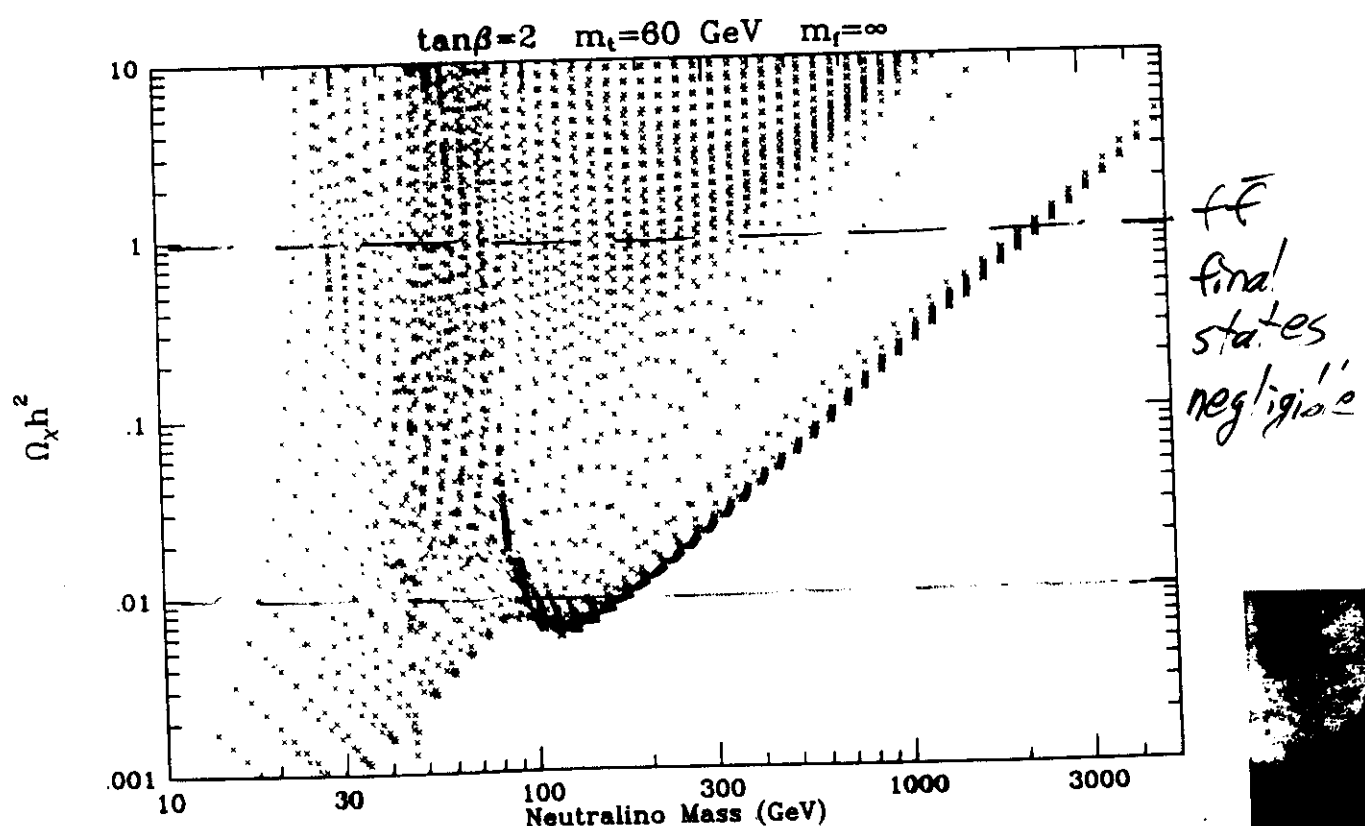
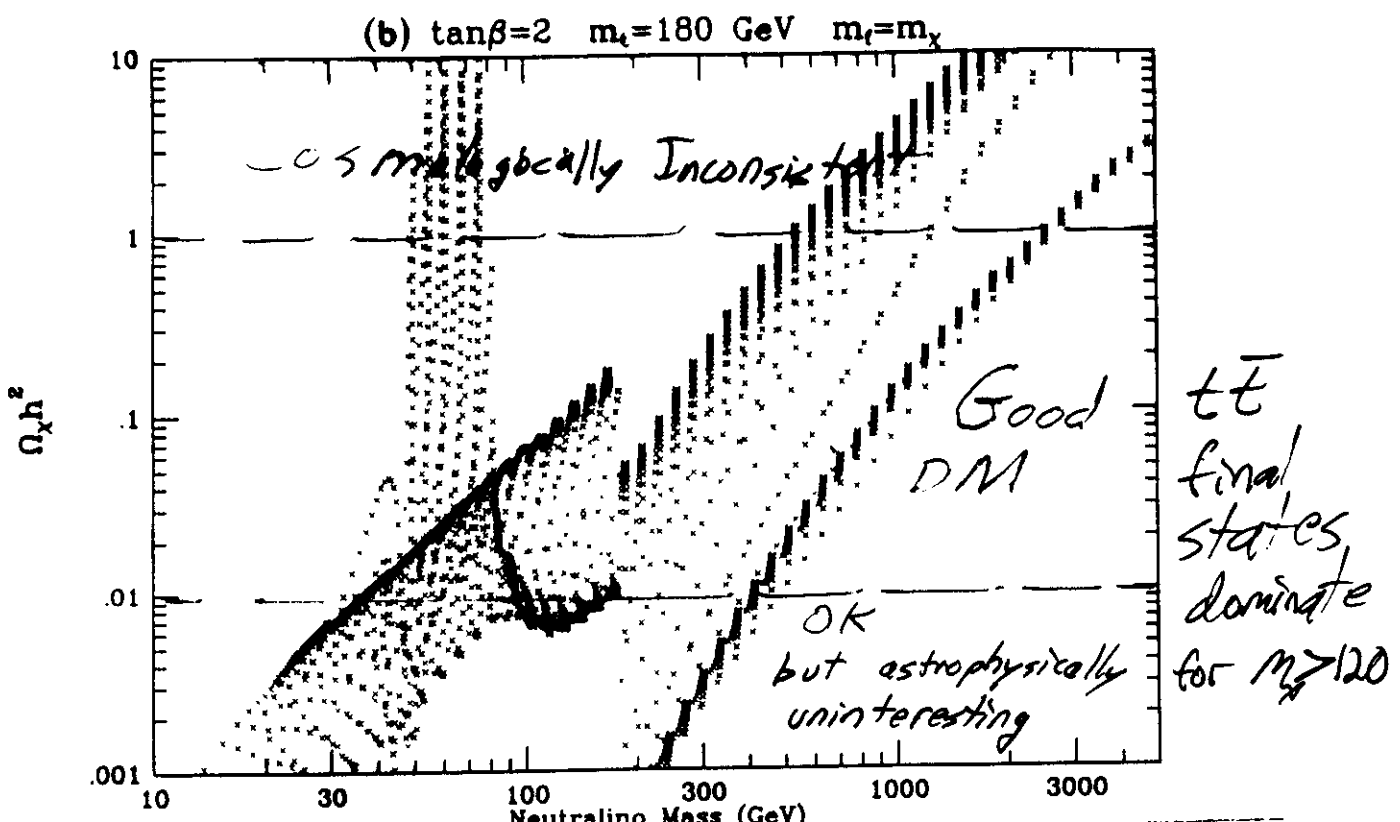
In the early Universe, this is at freeze-out and the v^2

terms are most certainly of importance. However, in the galactic halo, neutralino-neutralino relative velocities are of order $v^2 = v_{\text{halo}}^2 \approx 0$, and to a good approximation, the annihilation cross section times relative velocity should be given by $\sigma_{WW} v (v \rightarrow 0)$ (unless it vanishes).

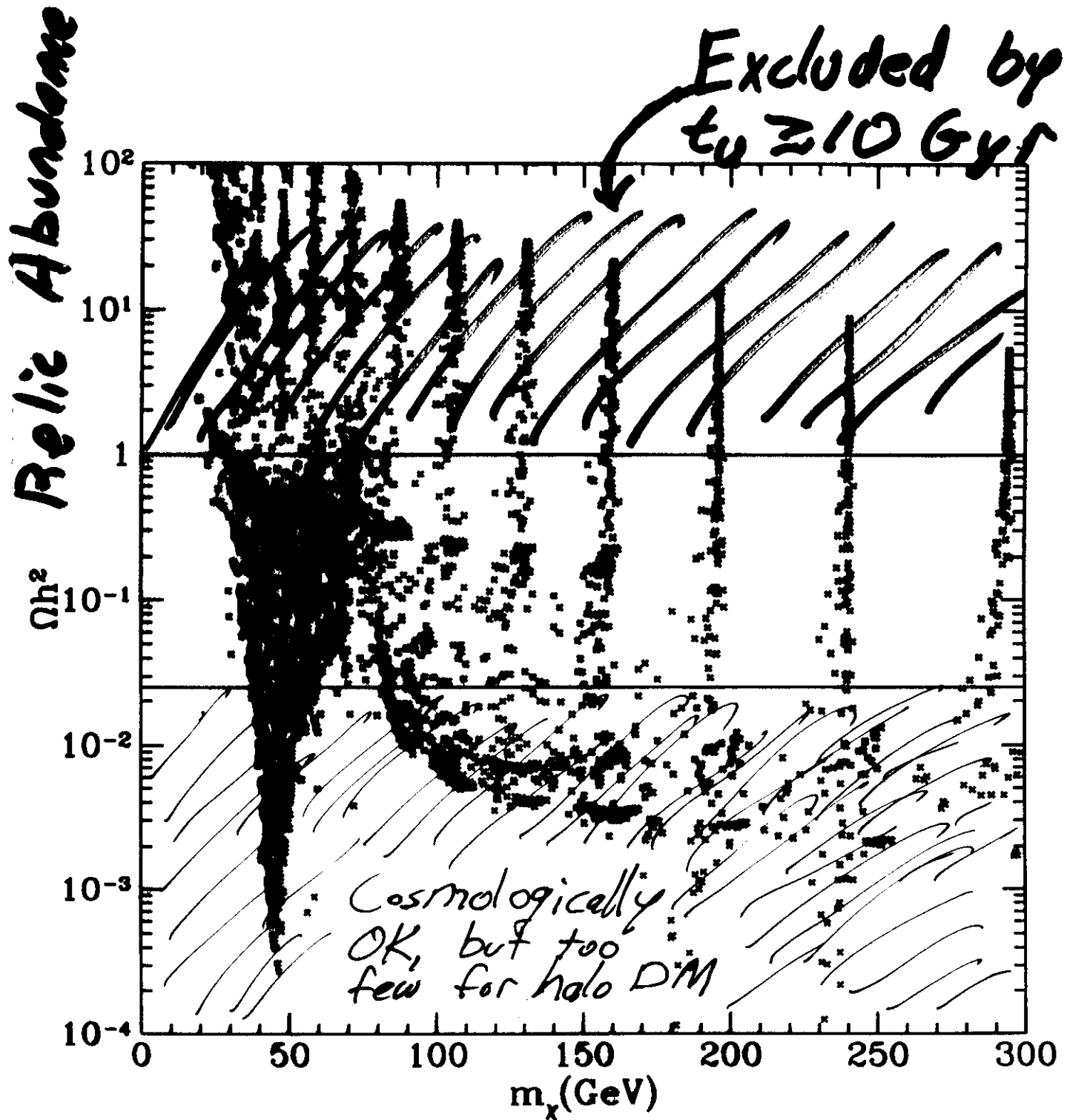
APPENDIX B: CROSS SECTION FOR $\tilde{\chi}\tilde{\chi} \rightarrow Z^0 Z^0$

The matrix element for the process $\tilde{\chi}\tilde{\chi} \rightarrow Z^0 Z^0$ is given by the Feynman diagrams shown in Fig. 3, and the total

- (i) University (5-100) (ii) Dreiss & Nojiri
 (iii) Dreiss & Sheldrick
 (iv) Dreiss & Nojiri



Griest, Kamionkowski, + Turner 1990



WIMP mass
(i.e., neutralino)
mass

Tegmark, MK, + Griest 1996

"The Junk-Bond days of
early-Universe cosmology
are over"

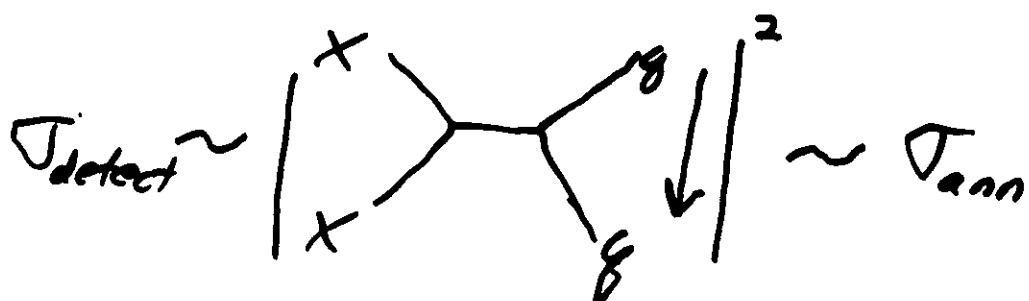
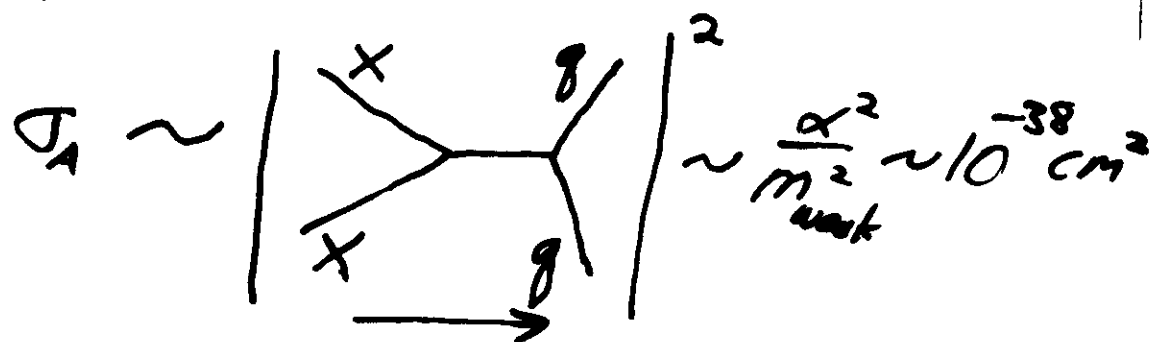
J. Harvey

We've talked the talk.

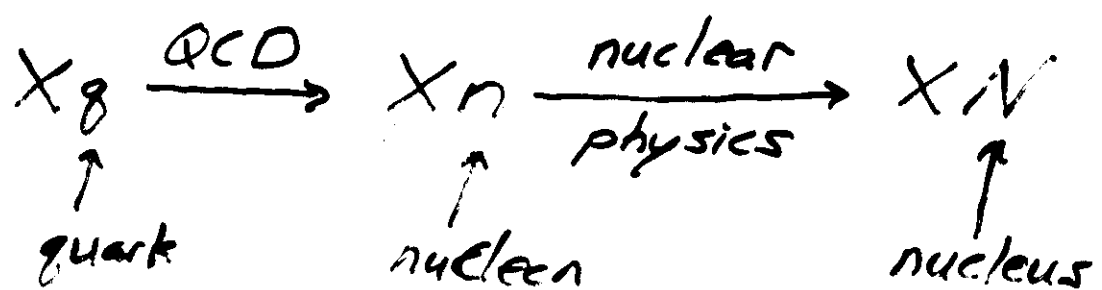
Now it's time
to walk the walk.

WIMP Detection:

$$\sigma_x \sim 1 \implies$$

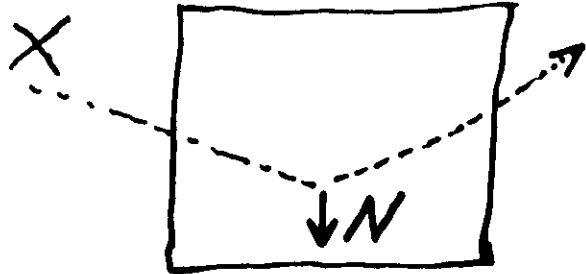


More Carefully:



WIMP DETECTION

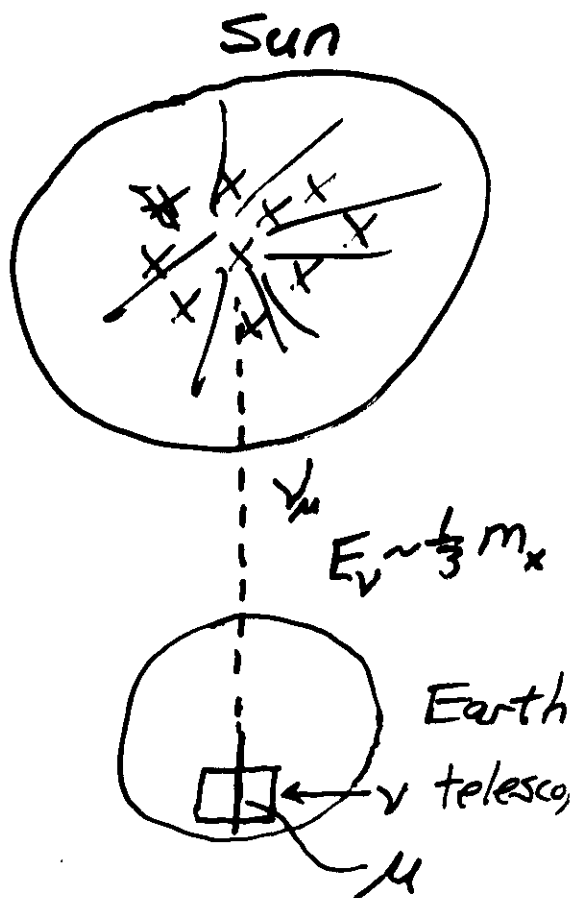
DIRECT



Low-Background
Detector
(e.g., $N = \text{Ge}$)

$\sim 10 \text{ keV}$

INDIRECT



Direct WIMP Detection Experiments

Cryogenic Detectors:

CDMS	Stanford	Ge, Si
CRESST	Gran Sasso	Al_2O_3
EDELWEISS	Frejus	Al_2O_3 , Ge
Tokyo	Tokyo	
Milano/Gran Sasso	Gran Sasso	TeO_2

Semiconductors - Ionization @ 77 K =

Aharonov/Avignone/Drukier	Homestake	Ge
UCSB/UCB/LBL	Oroville Dam	Ge
Caltech/PSI/Neuchatel	St. Gotthard	Ge
Zaragoza/PNL/USC	Canfranc Tunnel	Ge
Heidelberg/Moscow	Gran Sasso	Ge
UCSB/UCB/KSC/Saclay	Oroville	Ge

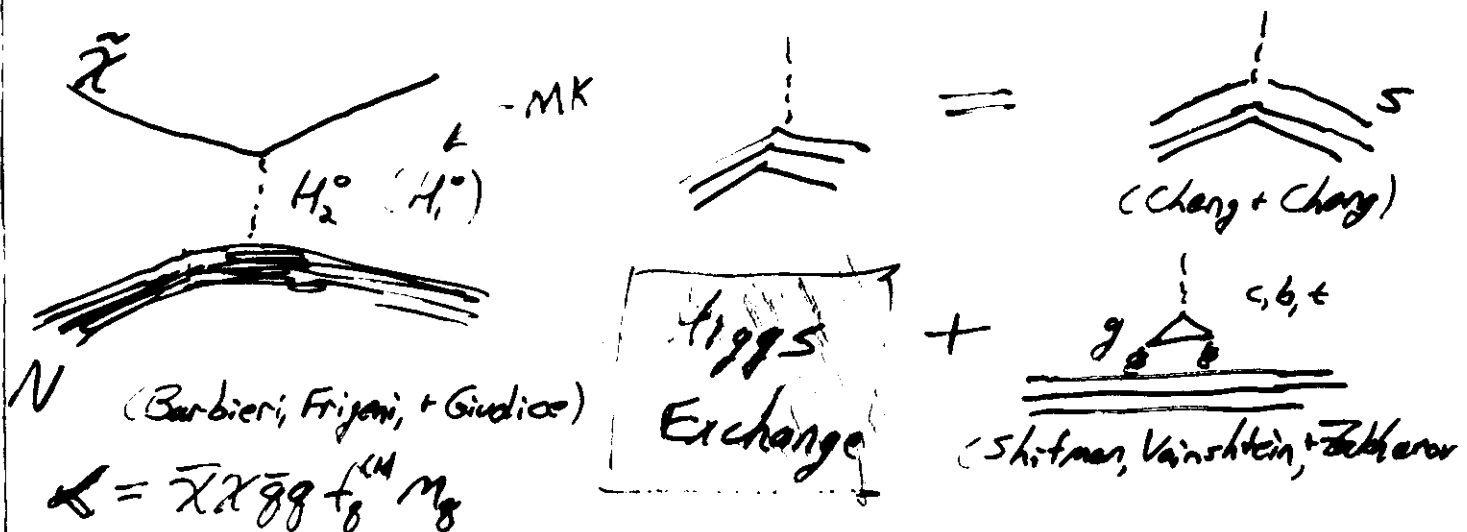
Scintillators:

Beijing/Paris/Rome/Fabris	Gran Sasso	NaI
Zaragoza/PNL/USC	Canfranc	NaI
Osaka	Römioka	NaI, CaF ₂
UKDM	Boulby	NaI
DAMA (Rome)	Gran Sasso	Liq. Xe
ICARUS WIMPs	Mont Blanc	Liq. Xe

Energetic- ν Experiments

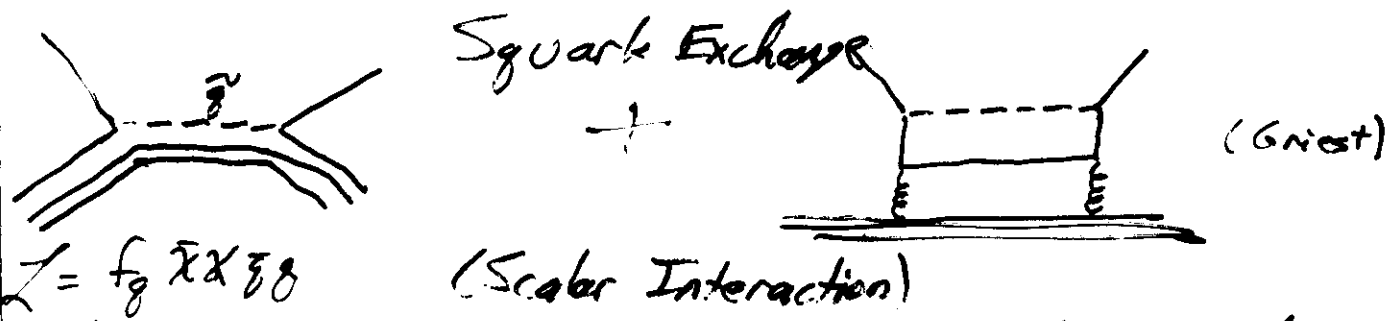
Frejus	Past	Frejus
IMB	Past	Cleveland
Baksan	Current	Baikal, Siberia
Kamikande-II	Past	Japan
MACRO	Current	Gran Sasso
Super-Kamikande	Current	Japan
AMANDA	Current/Future	South Pole
NESTOR	Future	Greece
HANUL	Future (proposed)	Korea

Elastic Scattering of $\tilde{\chi}$ off of N :



Important for mixed-state neutralinos. (+models w. squark mixing)
 H_2^0 is always light so this matrix element is ~~approximately~~ large even for heavy neutralinos.

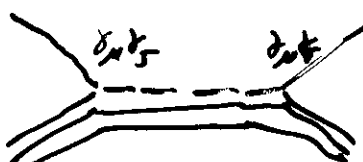
$\tilde{\chi}$ interacts coherently with active N , so $\sigma_{\tilde{\chi}N} \sim m_{\tilde{\chi}}^4 e^{-M_N}$



$$L = f_g \tilde{\chi} \bar{q} q \quad (\text{Scalar Interaction})$$

also important for mixed-states, coherent, and $\sigma_{\tilde{q}} \sim m_{\tilde{q}}^4$
 but generally, $\sigma_{\tilde{q}} < \sigma_{\tilde{\chi}N}$

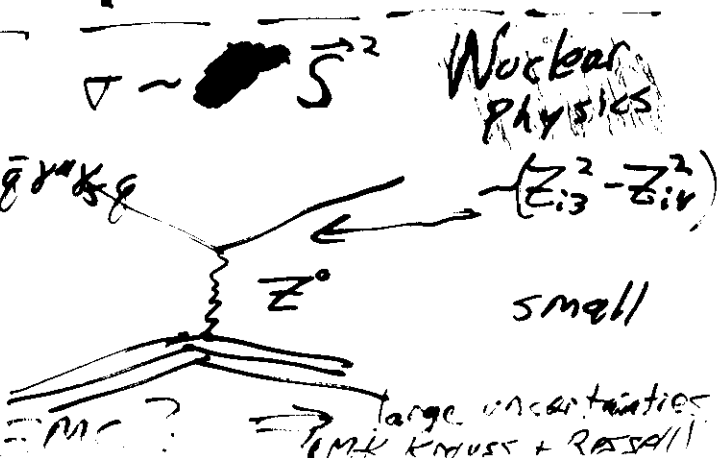
Spin-dependent Interaction
 (Axial)



Important B-ino scattering off H in Sun

$$L = d_g \tilde{\chi} \bar{q} \gamma_5 \chi \bar{g} \gamma^\mu S^2 g$$

+



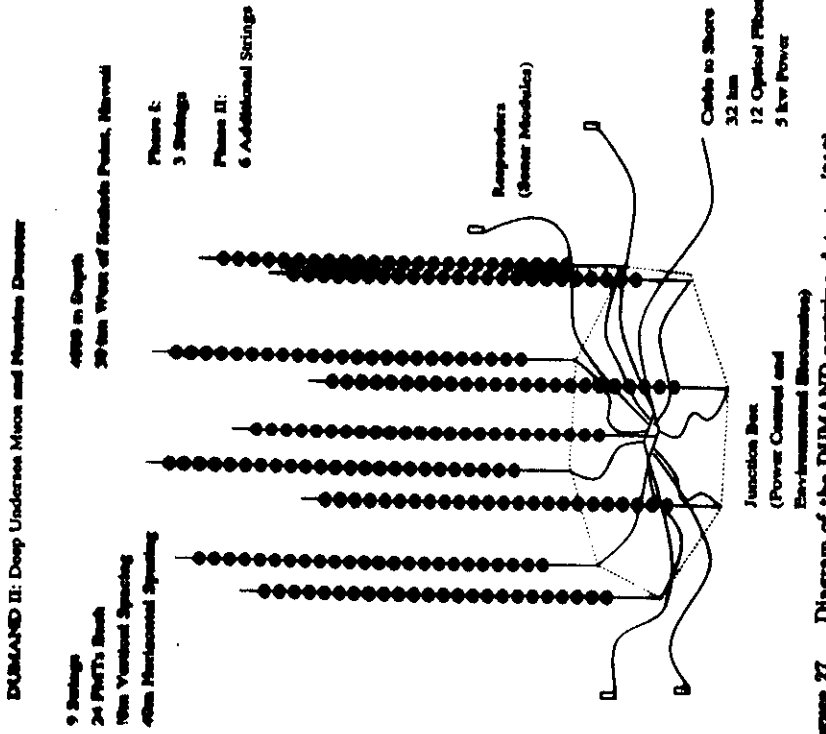


Figure 27. Diagram of the DUMAND neutrino detector [318].

be expanded to 3000 m^2 . The NESTOR (Neutrinos from Supernovae and TeV Sources Ocean Range) experiment is a similar effort located off the coast of Greece. An exposure area of $3 \times 10^4 \text{ m}^2$ is foreseen [320]. The Antarctic Muon and Neutrino Detector Array (AMANDA) is situated at the South Pole [319]. Although ice near the surface is opaque, the ice a km below the surface is relatively clear and has an attenuation length comparable to water. AMANDA is expected to have an exposure of 1000 m^2 .

9.3 Annihilation Rate in the Sun and Earth

The first step in calculating the rate for WIMP-induced neutrino events from the Sun is the determination of the rate at which WIMPs annihilate in

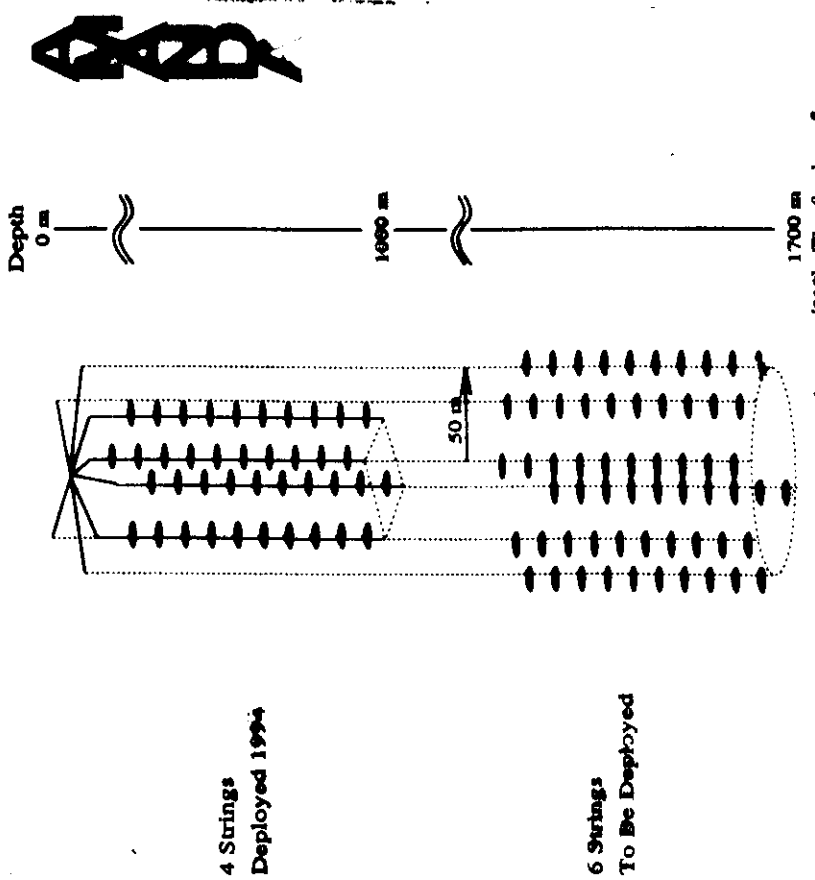
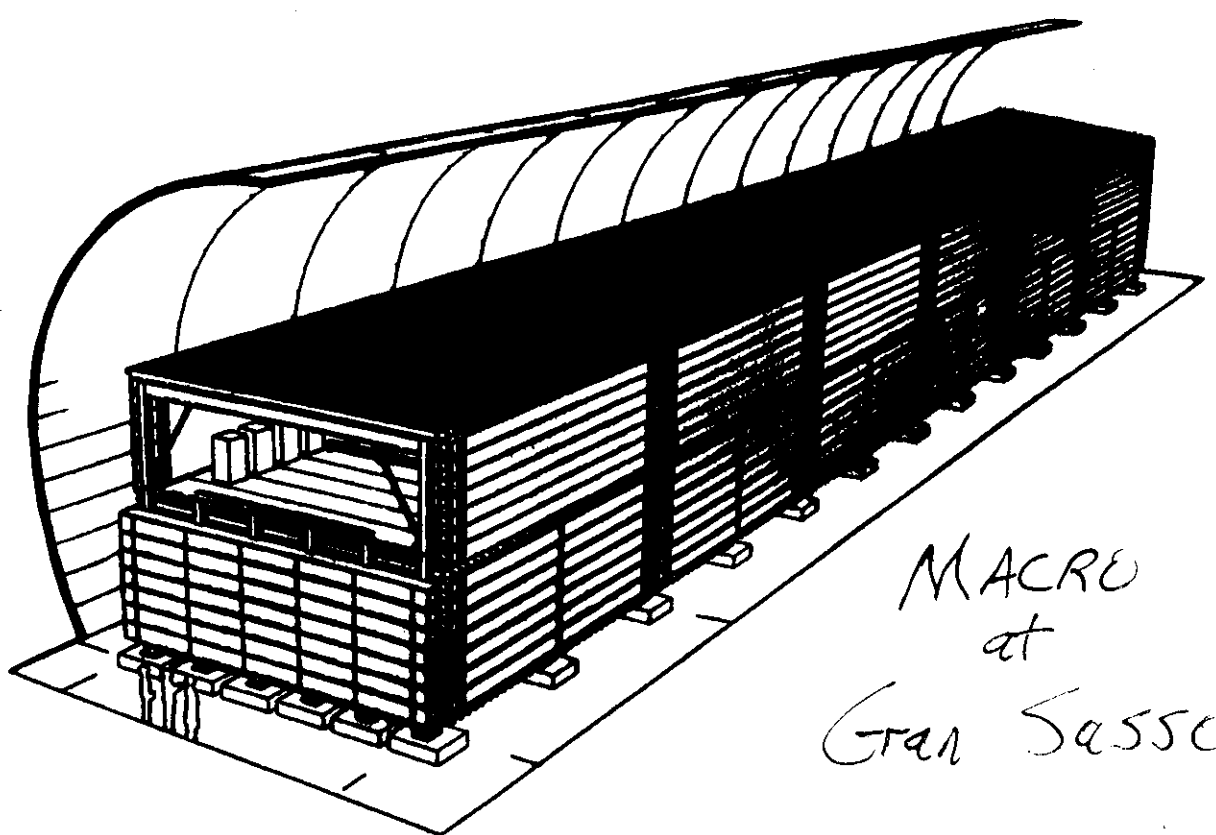


Figure 28. Diagram of the AMANDA neutrino detector [319]. The final configuration may differ slightly from that shown here.

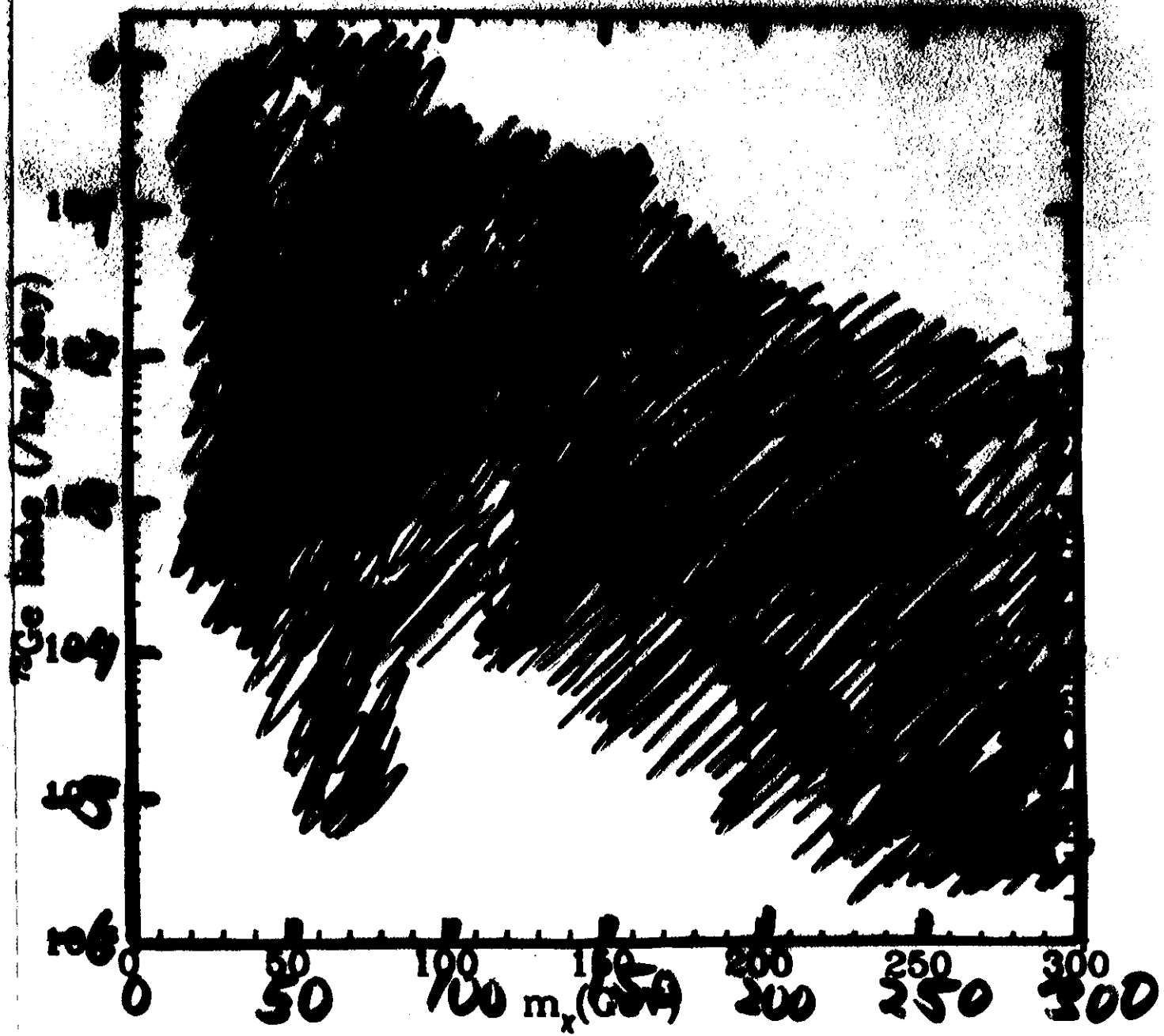
the Sun. WIMPs accumulate in the Sun or Earth by capture from the galactic halo and are depleted by annihilation. If N is the number of WIMPs in the Sun (or Earth), then the differential equation governing the time evolution of N is

$$\dot{N} = C - C_A N^2, \quad (9.4)$$

where the dot denotes differentiation with respect to time. Here, C is the rate of accretion of WIMPs onto the Sun (or Earth). The determination of C is straightforward and will be discussed in detail below, and if the halo density of WIMPs remains constant in time, C is of course time-independent.

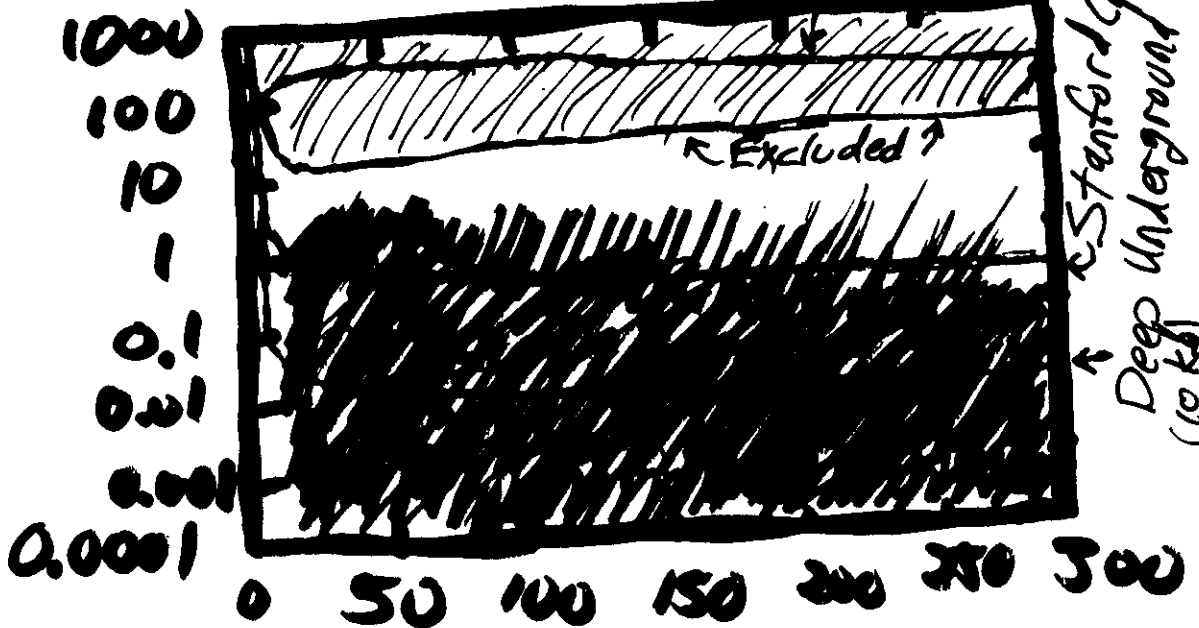


MACRO
at
Gran Sasso



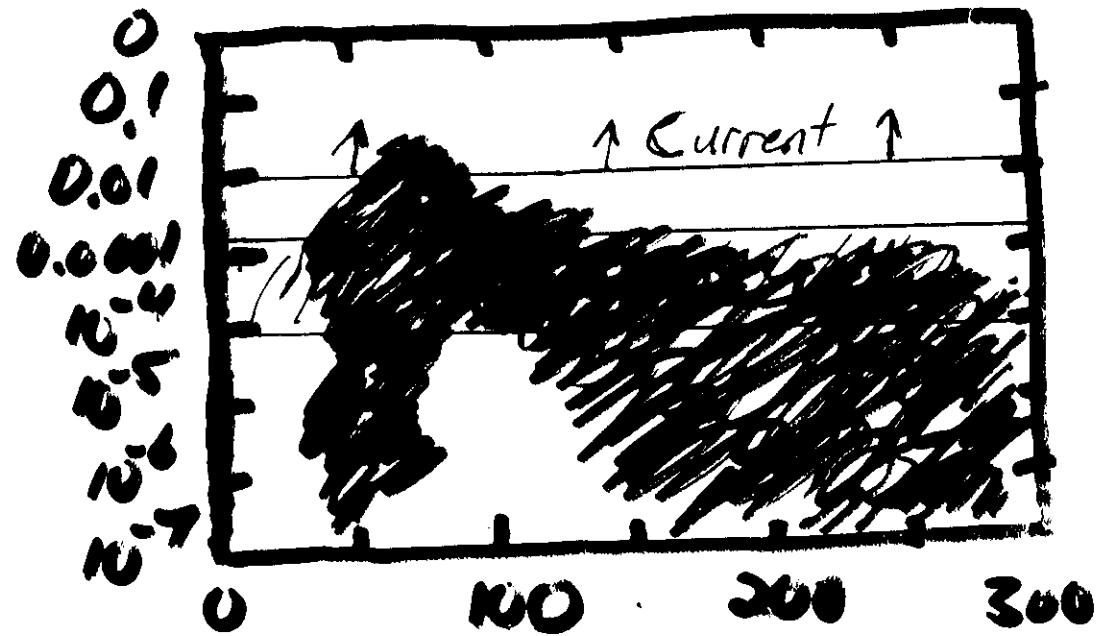
ν_e

Fractions / kg / day



Earth + Sun

M_{WIMPs} / m² / yr



Direct vs Indirect Detection: Which is Better?

MK, Griest, Jungman, Sadaulet 1995
Jungman, MK + Griest 1986 Frazer + MK 1987
Richter + Tao 1994

Two Types WIMP-nucleon interactions:

(i) Scalar

X couples to
mass of nucleus

Direct More Sensitive

(ii) Axial-Vector

X couples to
spin of nucleus

Indirect More Sensitive

Backgrounds:

Sensitivity \propto

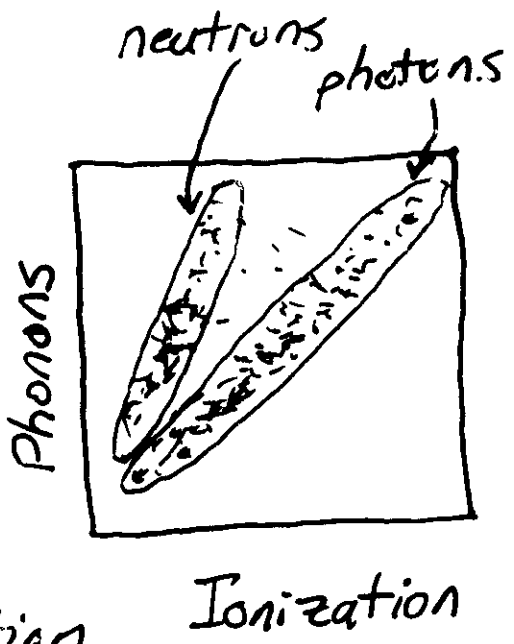
$$\sqrt{\frac{\text{Background flux}}{\text{Exposure}}}$$

e.g., Direct Detection

γ -ray background

Discriminate with
Ionization + Phonons

>99% Background
Rejection



Energetic ν 's:

Atmospheric- ν Background

Reducible with higher threshold
(but bigger at South Pole)

With predicted μ angular and energy
distribution, can improve S/N.
(Bergstrom, Edsjö + Kamionkowski, '96)

Cosmic Rays from WIMP Annihilation in Hb?

$$\chi\chi \rightarrow \text{e}^+ \bar{\nu}_e \rightarrow e^+, \bar{\nu}, \gamma, \dots$$

Signatures:

excess e^+ at high energies

excess: $\bar{\nu}$ at low energies

monochromatic γ ($E_\gamma = m_\chi$)

However:

fluxes appreciable in only
very small fraction of models.

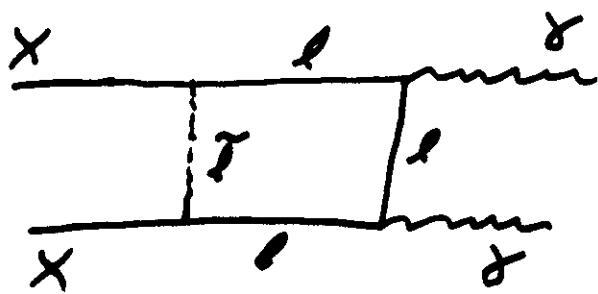
Very difficult to distinguish
from uncertain backgrounds

Will need to be very lucky to
detect WIMPs with CRs.

Null results can not be used to
constrain WIMP models.

Gamma Rays from WIMP Annihilation in the Galactic Halos

Signature #1: Monoenergetic γ Rays



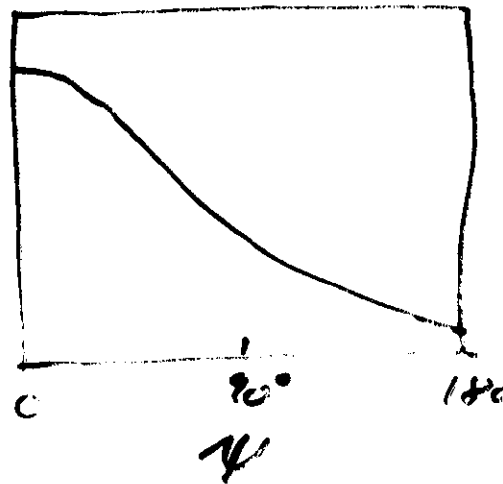
$$E_\gamma = m_\chi (1 \pm 10^{-6}) \sqrt{V_{\text{halo}}^2 / c}$$

(e.g. Jungman + Kamionkowski 1994)

Signature #2: Directional Dependence

ψ = angle between
line of sight
and
Galactic Center $\tilde{J}(\psi)$

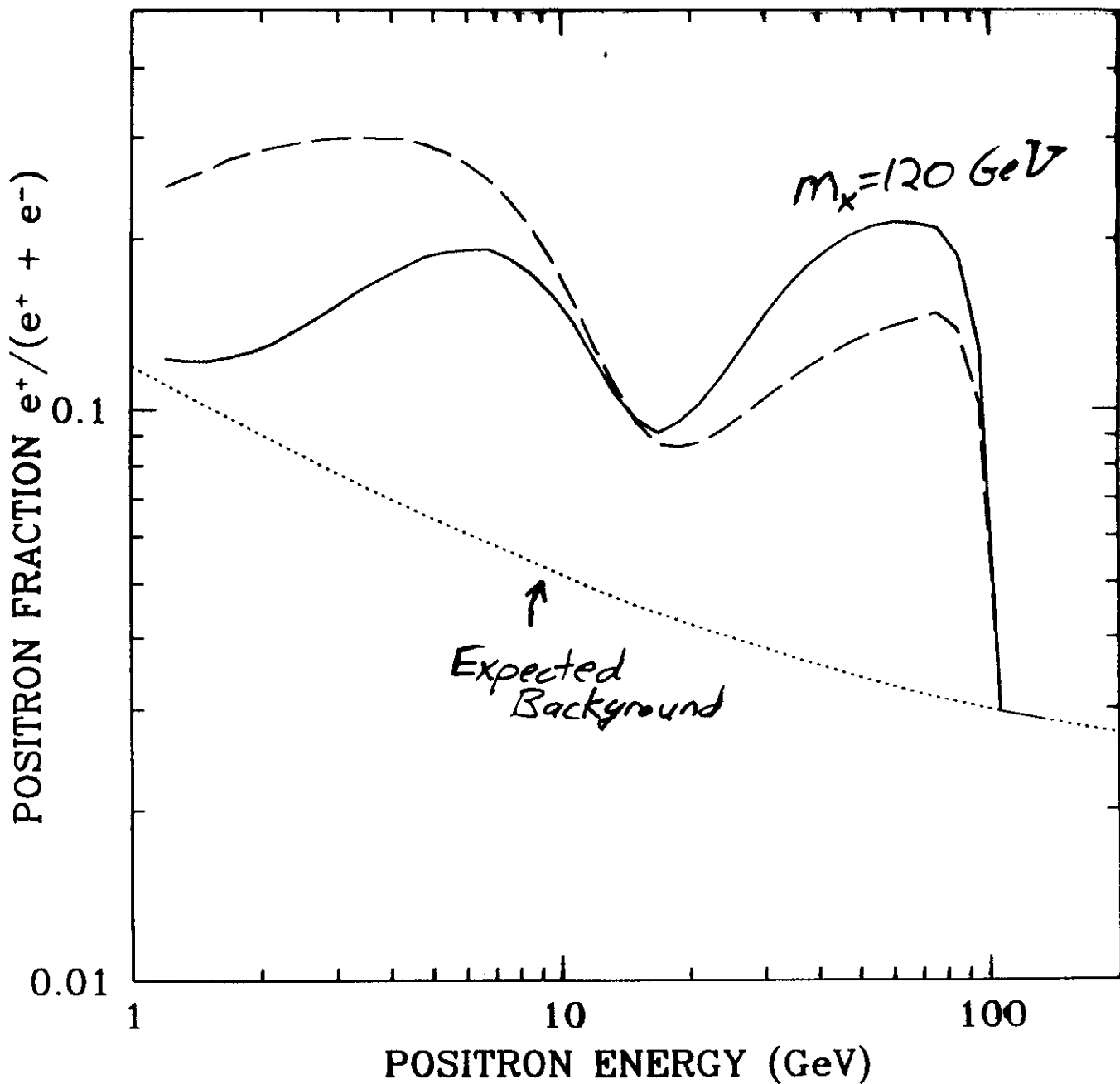
\tilde{J}_ℓ = flux of γ -rays



Gunn et al. 1978
Turner 1986

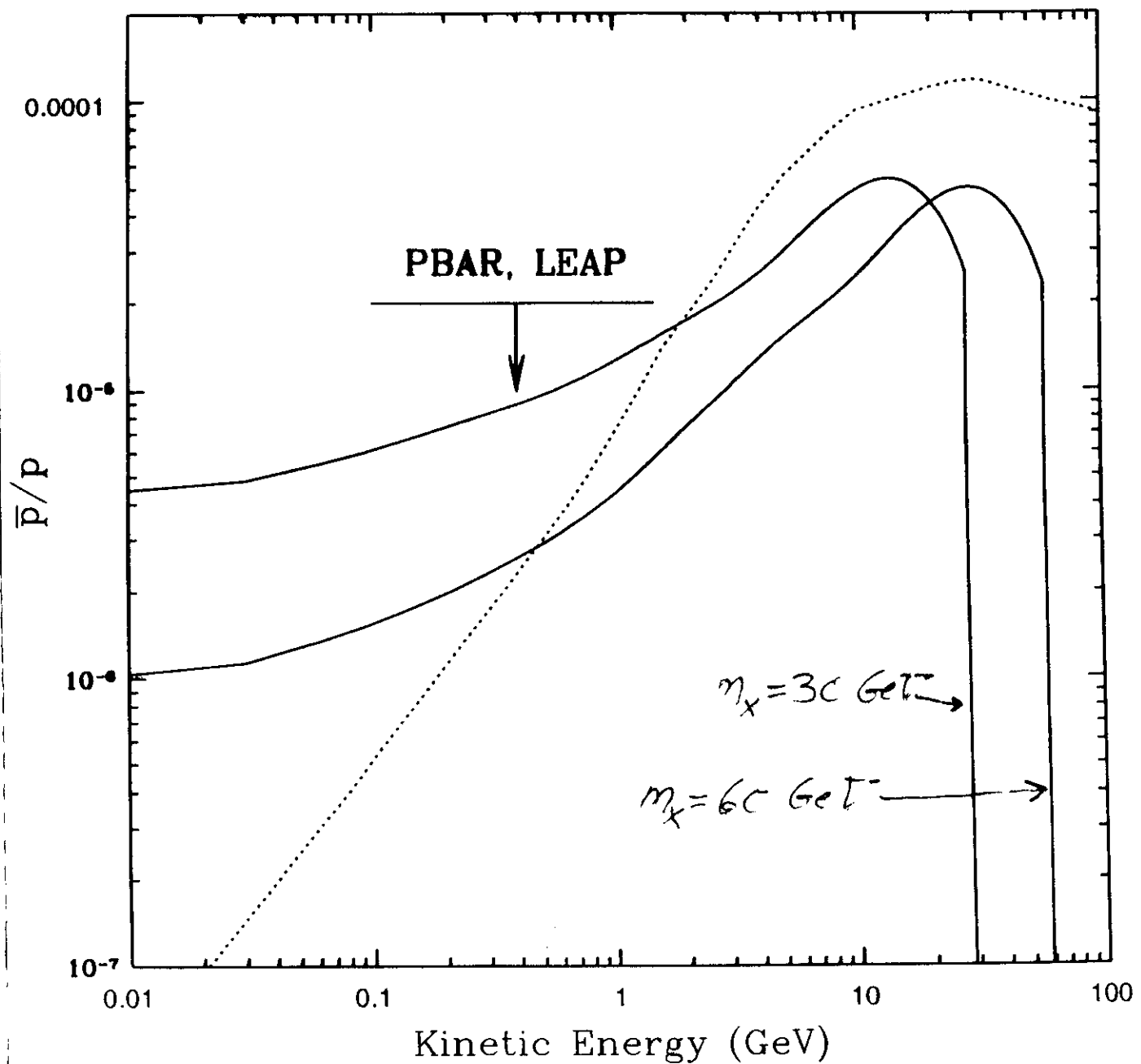
(e.g. Whipple Observatory, GLAST)

Cosmic-Ray Positrons
from $\chi\bar{\chi} \rightarrow W^+W^- \rightarrow e^+e^-\nu_e\bar{\nu}_e$



Kamionkowski + Turner 1991

Cosmic-Ray Antiprotons from WIMP Annihilation in the Halo



Jungman + Kamionkowski 1994

Can a Stable Massive (\gtrsim GeV) ν be Halo DM?

Dirac: (Coherent Vector Interaction),

Heidelberg-Moscow: ~~26 GeV - 44.7 TeV~~

LEP:

~~~ 45 GeV~~

Unitarity:

~~~ 70 TeV~~

(MK, Griest, PRL 64, 615 (1990))

NO!

Majorana: (Axial-Vector)

No constraints from direct detection

Kamiokande:

~~0 (10 GeV) - 0 (500 GeV)~~

LEP:

~~~ 45 GeV~~

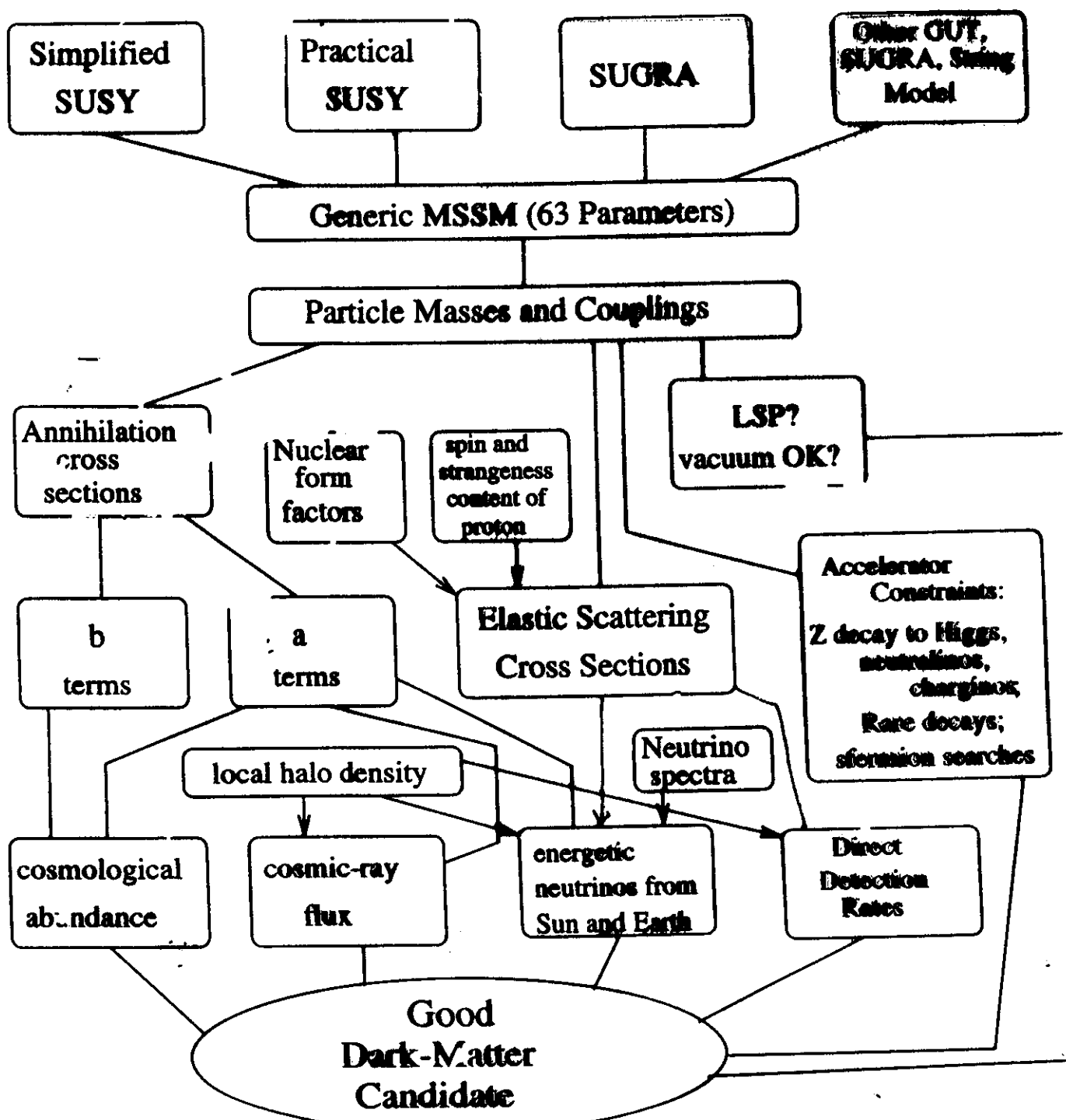
Unitarity:

~~~ 70 TeV~~

OK for $\frac{1}{2}$ TeV $\lesssim m_\nu \lesssim$ TeV

Sneutrinos? \sim Dirac ν

No.



SUSY DM code

contact

kamion@phys.columbia.edu
 jungman@astro.ias.edu
 kniest@ucsd.edu

Summary:

WIMPs, axions arise in leading solutions to fundamental problems in particle physics.

If \exists , have $\Omega_x \sim 1$

\Rightarrow cosmologically relevant

\Rightarrow likely the nonbaryonic DM

Good fraction of viable models will be probed experimentally

If Detected:

Would revolutionize cosmology + physics

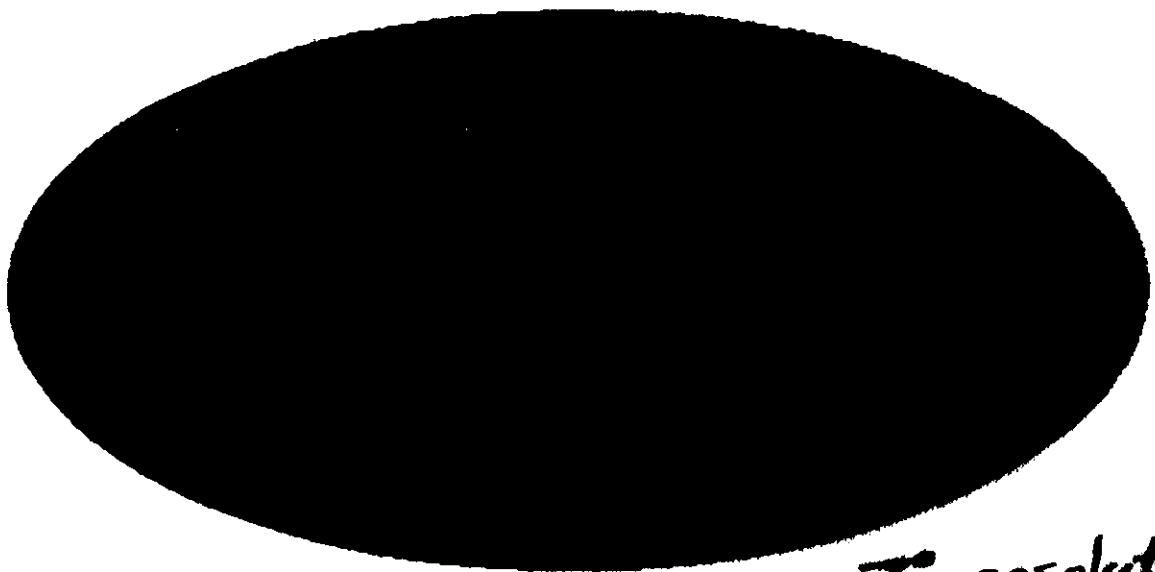
Important for LSS, galaxy formation, galaxy structure.

Could determine phase-space distribution of MW halo

.....

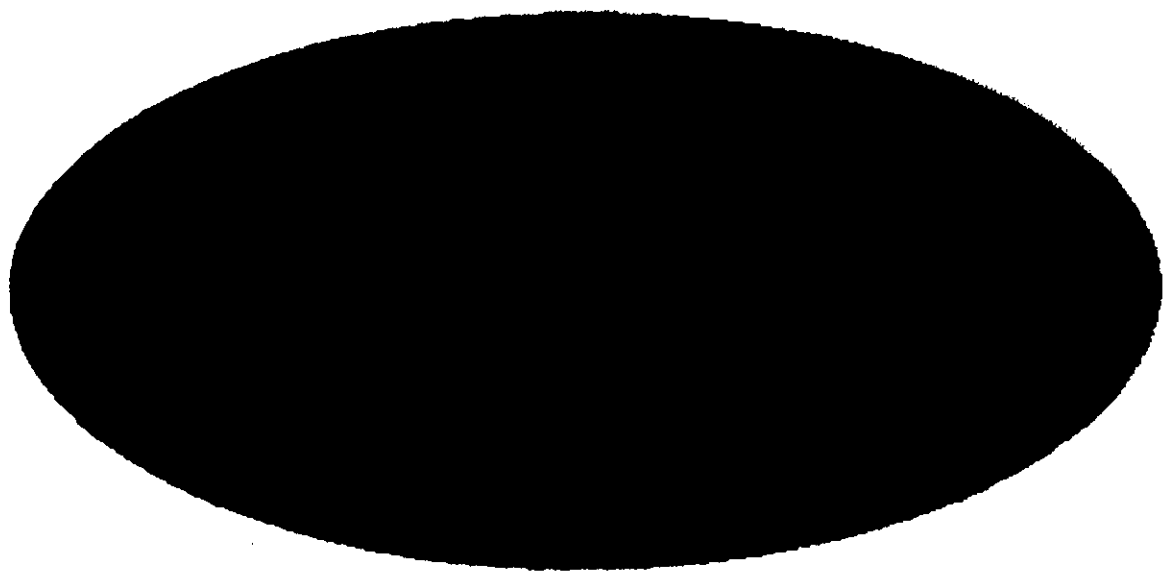
Cosmology \longleftrightarrow Particle Physics

COBE DMR 4-Year Sky Map

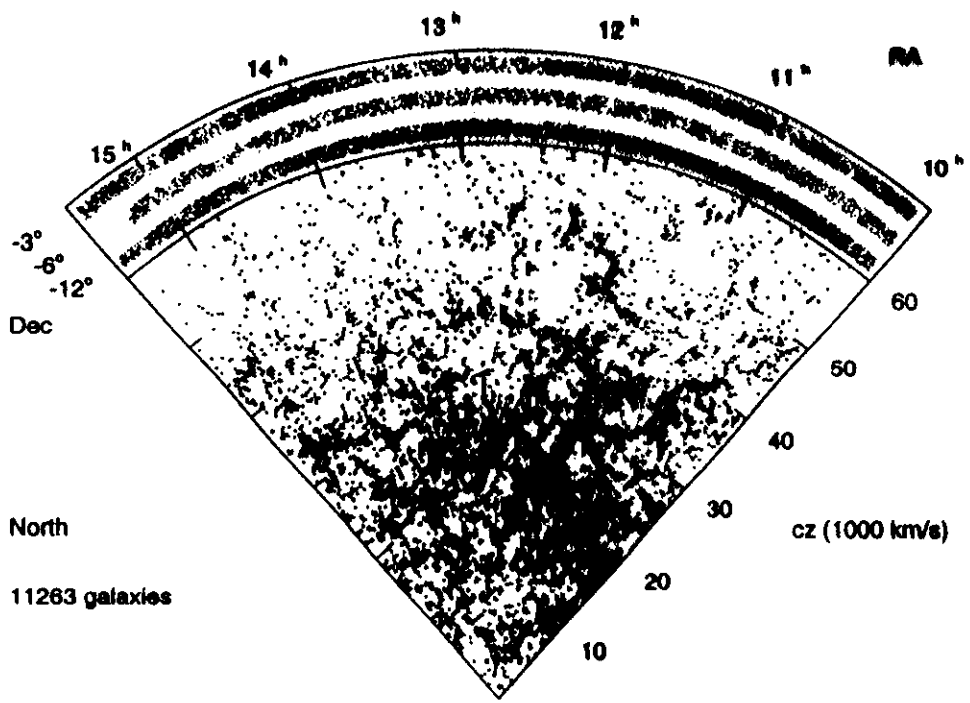


7° resolution

MAP Simulated Sky Map



0.3° resolution



Large-Scale Structures:

$$\delta(\vec{r}) = \frac{\rho(\vec{r}) - \bar{\rho}}{\bar{\rho}}$$

$$\delta_k = \int d^3\vec{x} e^{i\vec{k}\cdot\vec{x}} \delta(\vec{r})$$

Power Spectrum: $P(k) \propto \langle |\delta_k|^2 \rangle$

Leading Paradigm* (Peebles, Harrison-Zeldovich 1970)

(Inflation ~ 1980)
 $P(k)$ from gravitational infall

of $P_{\text{prim}}(k) \propto k^n$ with $n \approx 1$. (Adiabatic)

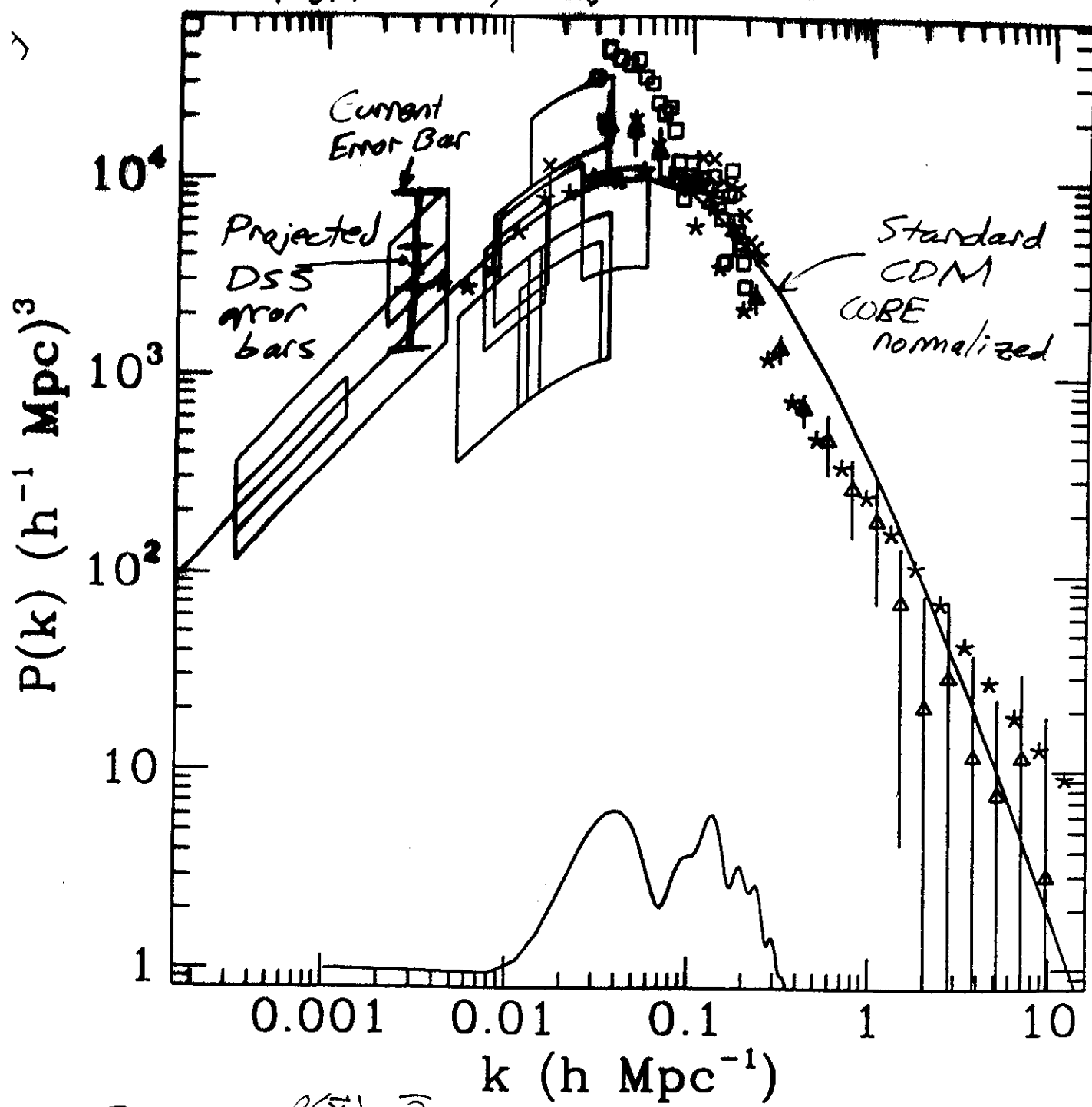
$$\text{Then, } P(k) \propto \begin{cases} k^n & \frac{k}{h \text{Mpc}^{-1}} \lesssim 0.1 \Omega_0 h \\ k^{n-3} & \frac{k}{h \text{Mpc}^{-1}} \gtrsim 0.1 \Omega_0 h \end{cases}$$

For given $\Omega_0, h, A, \Omega_V, \Omega_b, \dots$

get Standard CDM, Λ CDM, open CDM,
 tilted CDM, MDM,

* Runner Up: Topological defects
 (cosmic strings, textures,
 global monopoles....)

from White, Scott & Silk 1994



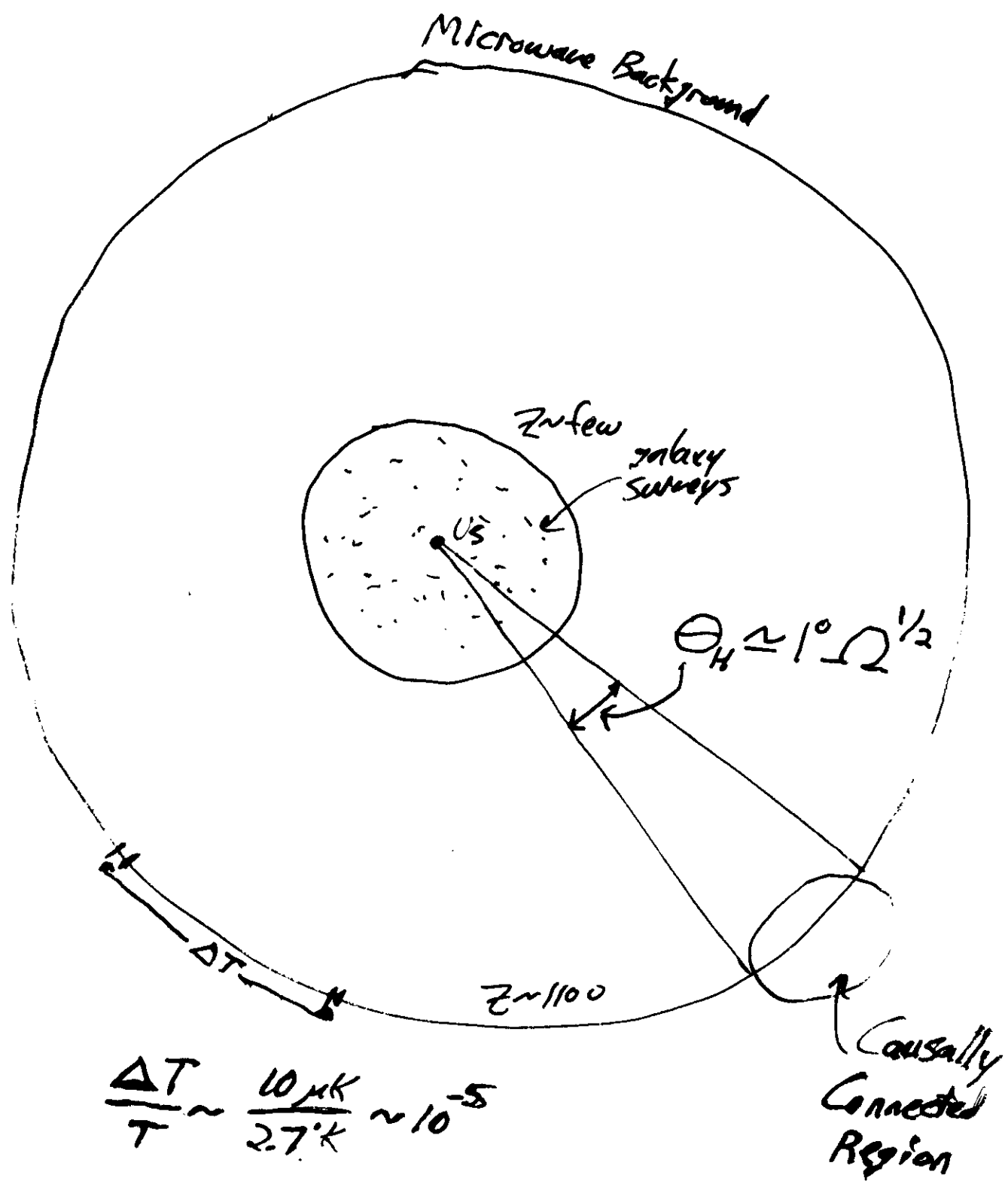
$$\tilde{\zeta}(\vec{x}) = \frac{\rho(\vec{x}) - \bar{\rho}}{\bar{\rho}}$$

$$\tilde{\zeta}_k = \int d^3x e^{i\vec{k} \cdot \vec{x}} \zeta(\vec{x})$$

$$P(k) \propto |\tilde{\zeta}_k|^2$$

$$\frac{\Delta T}{T} \sim \frac{\Delta \phi}{\phi}$$

$$\nabla^2 \phi = 4\pi G \delta \rho$$



$$\frac{\Delta T}{T} \sim \frac{10 \mu K}{27 K} \sim 10^{-5}$$

Cosmic Microwave Background Anisotropies:

Measure $a_{lm} = \int d\Omega Y_{lm}(\Omega) \frac{\Delta T}{T}(\Omega)$

and $C_l = \sum_m \frac{|a_{lm}|^2}{2l+1}$

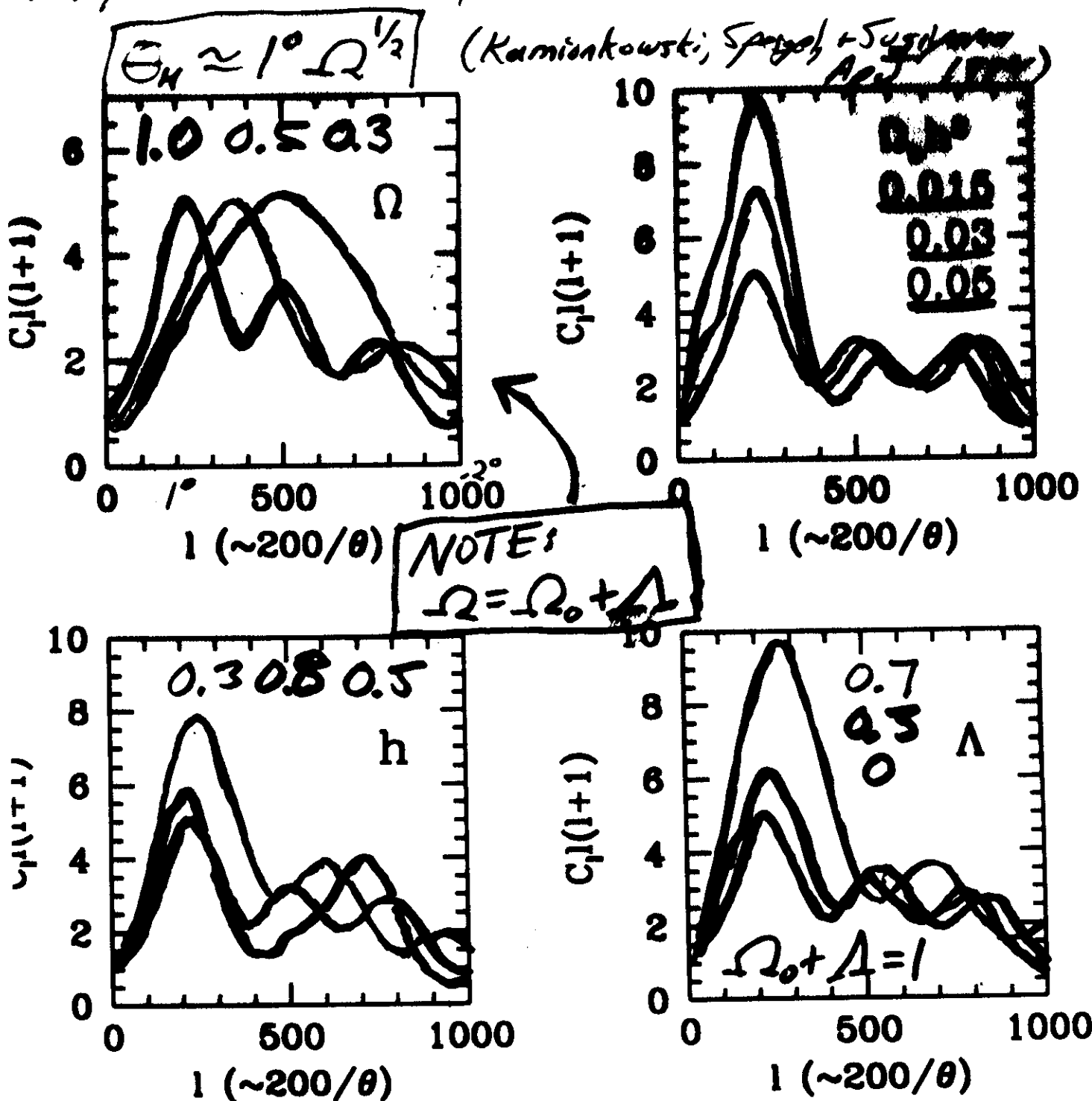
Theory predicts each a_{lm} has to be picked from Gaussian distribution with variance $\langle C_l \rangle$.

Given set of parameters

$\{\Omega_0, h, A, \Omega_b, n, \dots\}$, can calculate the $\langle C_l \rangle$.

Note: $C_l \sim \left(\frac{\Delta T}{T}\right)^2 \left(\frac{\Theta}{\text{deg}} \sim \frac{200}{l}\right)$

Heavy Curves: $\Omega = 1$, $A = 0$, $\Omega_0 h^2 = 0.015$, $h = 0.5$



Similarly, for η , Q , Q_T , η_T , ζ

(Note: $\Omega_0 h^2 \approx 3 \times 10^{-2} \eta$)

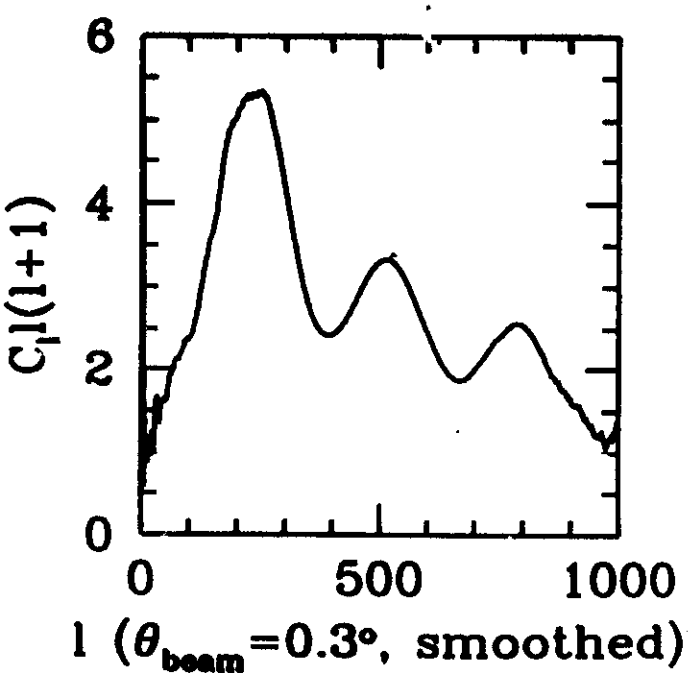
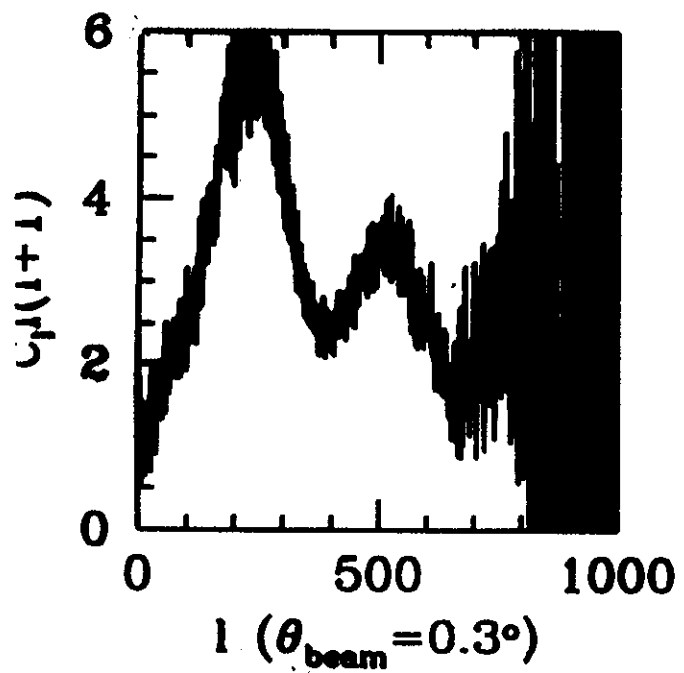
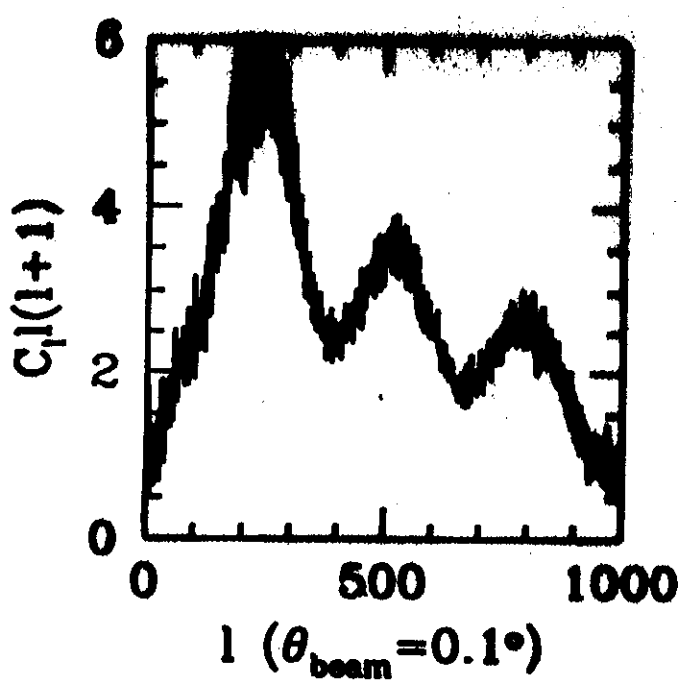
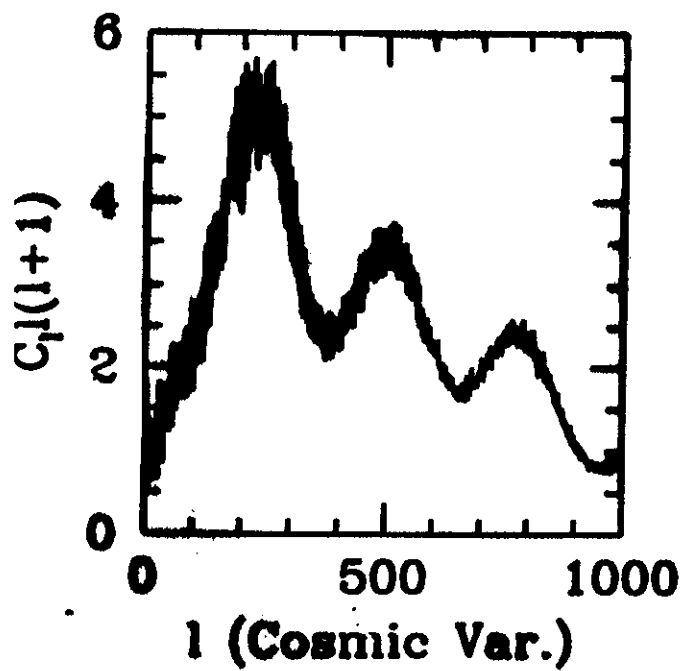
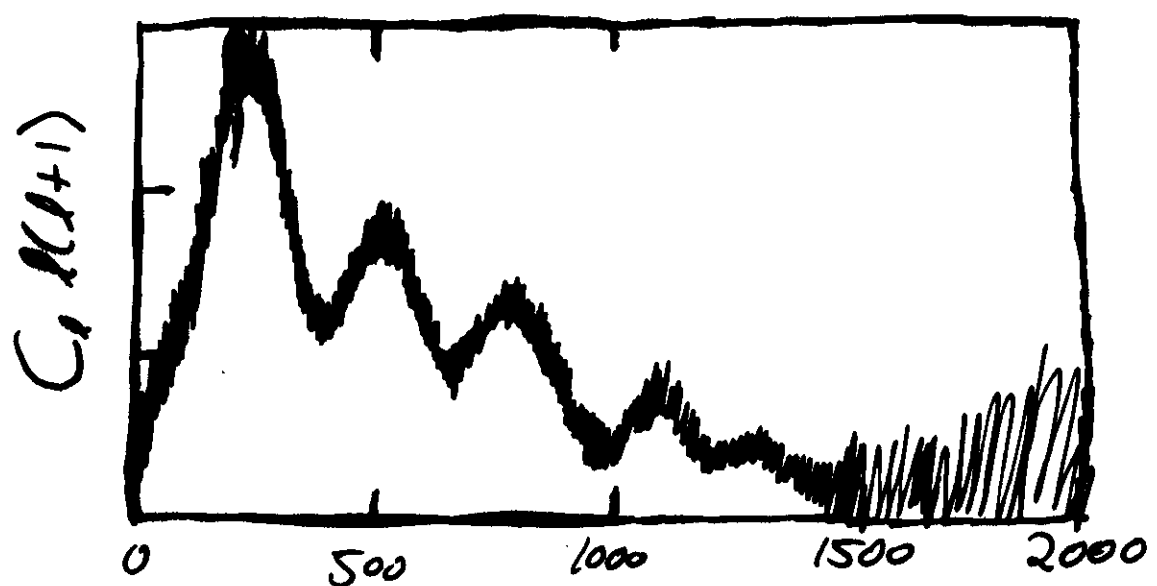
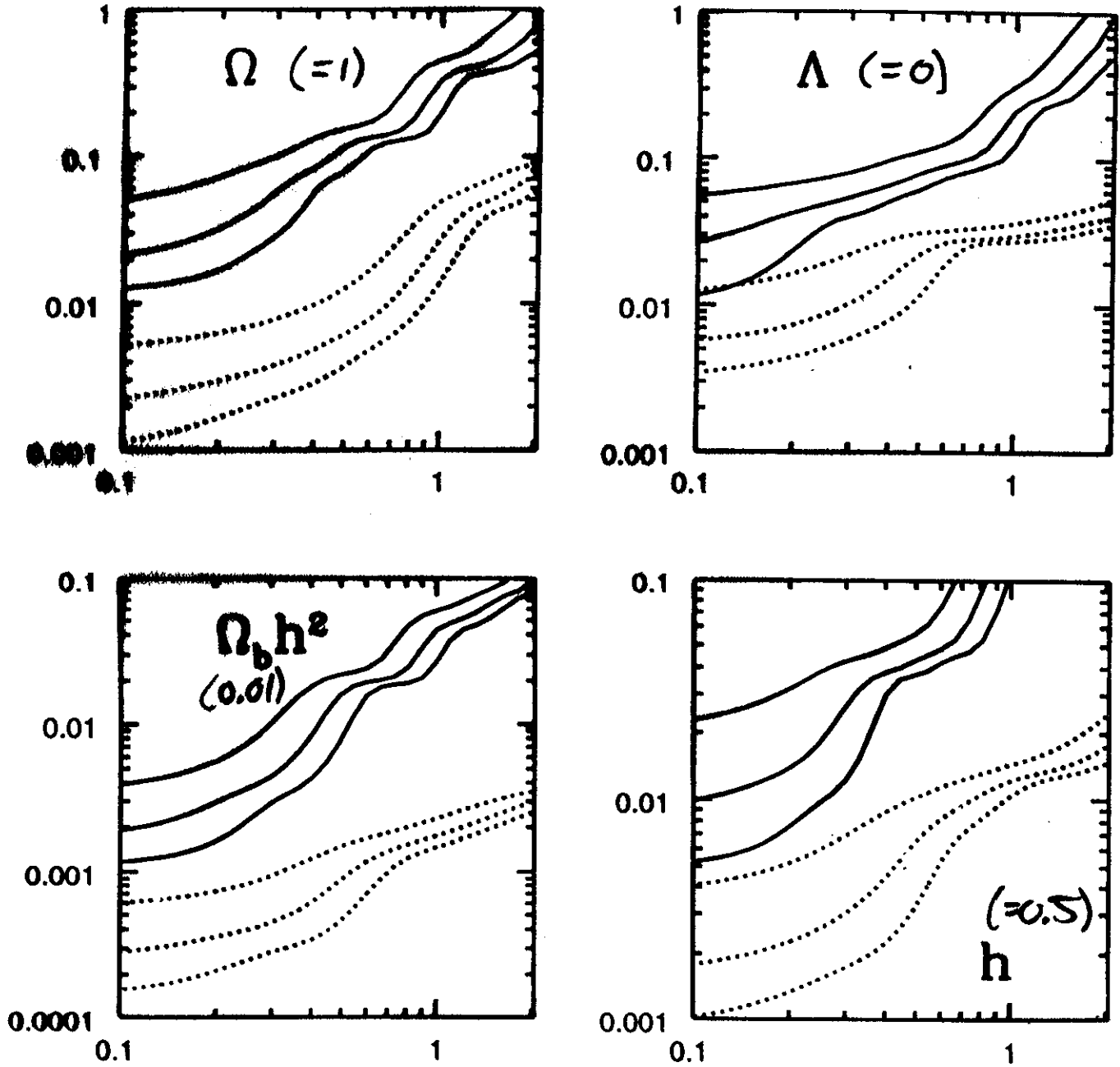


FIG. 2. Simulated data that might be obtained with a CMB mapping experiment, for beam sizes of 0.3° and 0.1° .



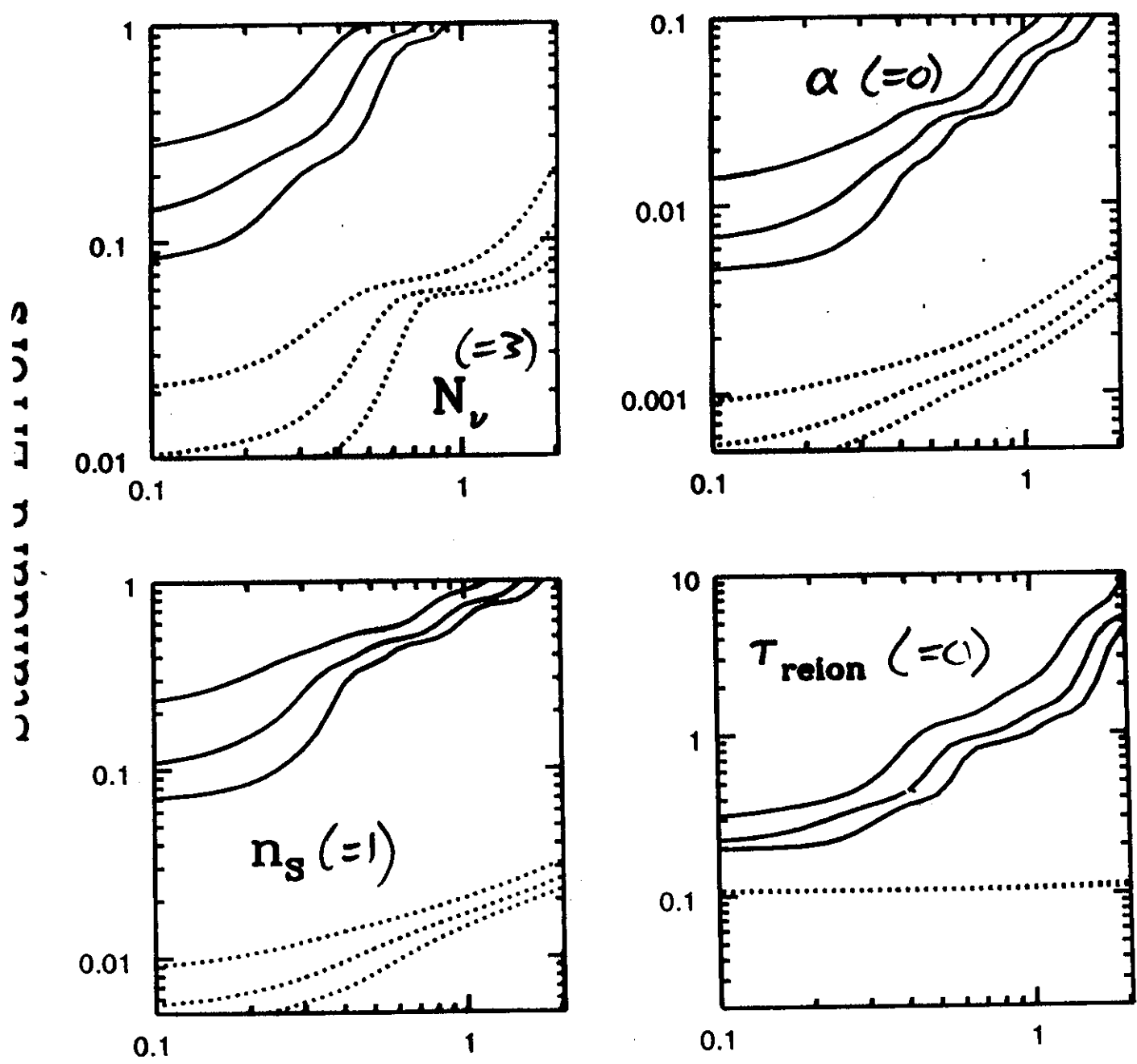
"Simulated" COBRAS/SAMBA
(probably conservative)

Standard errors



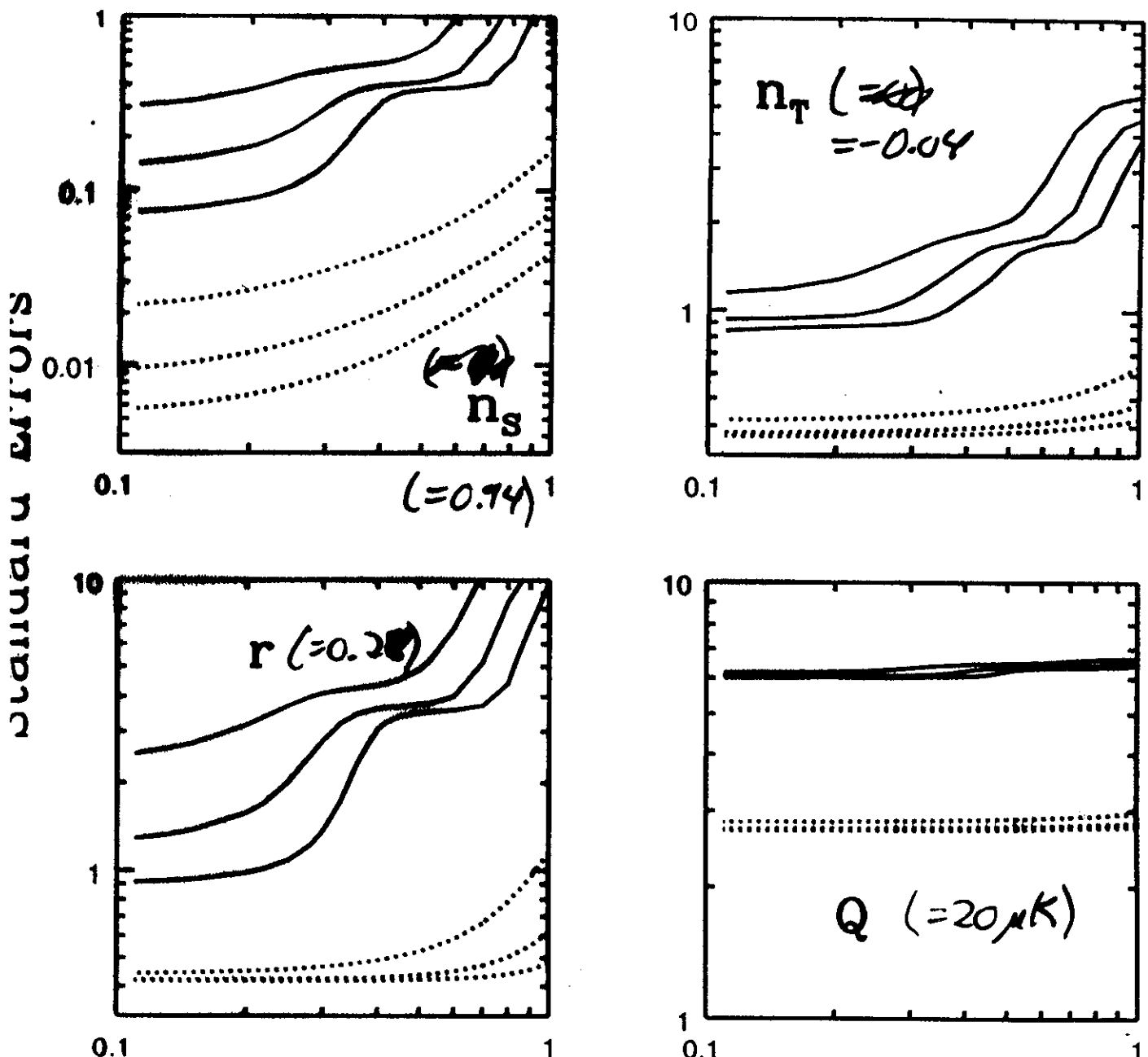
Beamwidth in degrees

FIG. 3. The standard errors for Ω , Λ , $\Omega_b h^2$, and h that can be obtained with a full-sky mapping experiment as a function of the beam width θ_{beam} for noise levels $w^{-1} = 2 \times 10^{-10}$, 9×10^{-10} , and 4×10^{-10} (from lower to upper curves). The underlying model is "standard CDM." The solid curves are the sensitivities attainable with no prior assumptions about the values of any of the other cosmological parameters. The dotted curves are the sensitivities that would be attainable assuming that all other cosmological parameters, except the normalization (Q), were fixed. The results for a mapping experiment which covers only a fraction f_{sky} of the sky can be obtained by scaling by $f_{sky}^{-1/2}$ [c.f., Eq. (20)].



Beamwidth in degrees

FIG. 4. Like Fig. 4, but for α , N_ν , τ_{reion} , and n_s .



Beamwidth in degrees

FIG. 5. The standard errors on the inflationary observables, n_s , n_T , $r = Q_T^2/Q_S^2$, and Q , that can be obtained with a full-sky mapping experiment as a function of the beam width θ_{beam} for noise levels $w^{-1} = 2 \times 10^{-15}$, 9×10^{-15} , and 4×10^{-14} (from lower to upper curves). The parameters of the underlying model are the "standard=CDM" values, except we have set $r = 0.28$, $n_s = 0.94$, and $n_T = -0.04$. The solid curves are the sensitivities attainable with no prior assumptions about the values of any of the other cosmological parameters. The dotted curves are the standard errors that would be attainable by fitting to only these four inflationary observables and assuming all other cosmological parameters are known. (Note that this differs from the dotted curves in Fig. 4.) The results for a mapping experiment which covers only a fraction f_{sky} of the sky can be obtained by scaling by $f_{\text{sky}}^{-1/2}$ [c.f., Eq. (20)].

Polarization and Gravitational Radiation

MK, Kosowsky, and Stebbins, astro-ph/9609132; Seljak and Zaldarriaga, astro-ph/9609169, astro-ph/9609170 **9611/25**

Anisotropic Compton scattering \Rightarrow linear polarization

Temperature: $T(\hat{n})$

Polarization: " \vec{P} " (\hat{n})

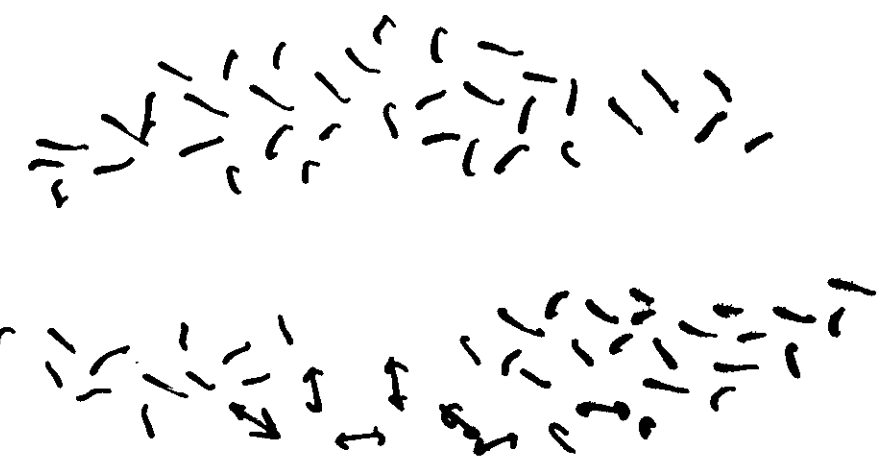
Vector field has curl and curl-free part:

$$\vec{P}(\hat{n}) = \vec{\nabla} A + \vec{\nabla} \times \vec{B}$$

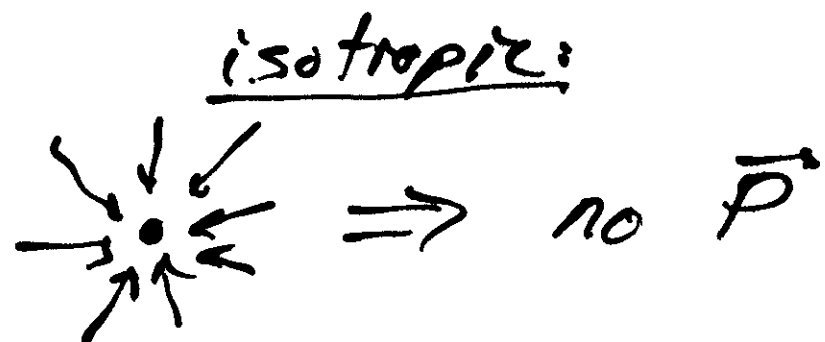
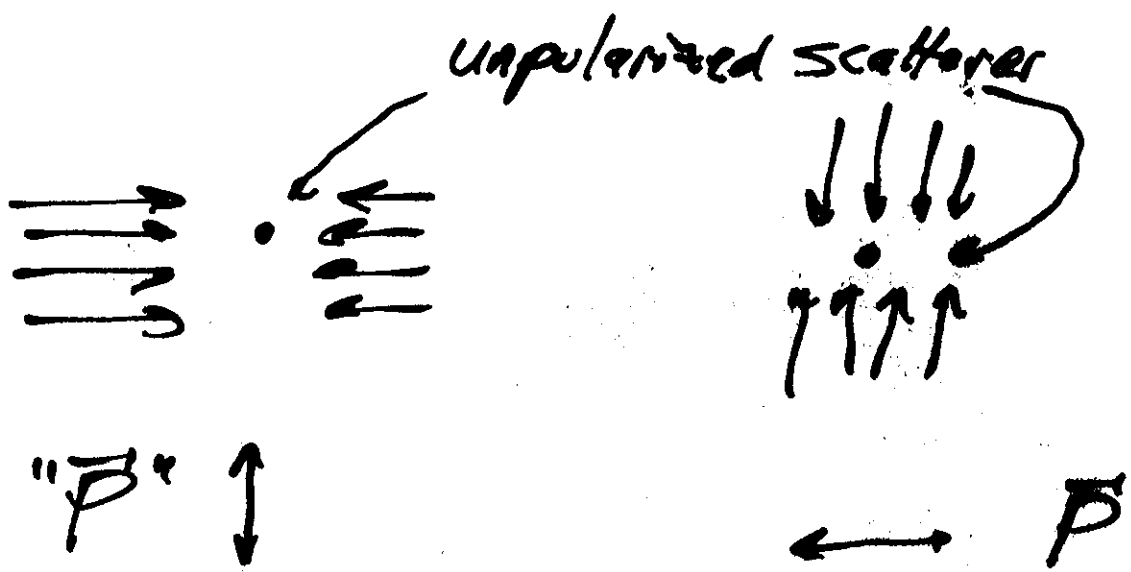
Density perturbations $\Rightarrow \vec{\nabla} \times \vec{P} = 0$ (i.e., scalar perturbations have no "handedness")

Gravitational waves $\Rightarrow \vec{\nabla} \times \vec{P} \neq 0$ (i.e., gravitational waves have "handedness")

Polarization map \Rightarrow model-independent probe of long-wavelength gravitational waves



Polarization:



Tensor Harmonics:

Polarization Tensor: P_{ab}

symmetric: $P_{ab} = P_{ba}$ trace-free $P_{ab}g^{ab} = 0$

e.g., $(\Theta, \phi) \Rightarrow g_{ab} = \begin{pmatrix} 1 & 0 \\ 0 & \sin^2 \Theta \end{pmatrix}$

$$P_{ab}^{(1)} = \frac{1}{2} \begin{pmatrix} Q(\hat{\alpha}) & -U(\hat{\alpha}) \sin \Theta \\ -U(\hat{\alpha}) \sin \Theta & -Q(\hat{\alpha}) \sin^2 \Theta \end{pmatrix}$$

Temperature Map $T(\hat{\alpha})$:

$$\frac{T(\hat{\alpha})}{T_0} = 1 + \sum_{l=1}^{\infty} \sum_{m=-l}^l Q_{(lm)}^T Y_{(lm)}(\hat{\alpha})$$

$$Q_{(lm)}^T = \frac{1}{T_0} \int d\hat{\alpha} T(\hat{\alpha}) Y_{(lm)}^*(\hat{\alpha}) \quad \int Y_{(lm)}^* Y_{(l'm')} d\hat{\alpha} = \delta_{ll'} \cdot \delta_{mm'}$$

Polarization Map:

$$\frac{P_{ab}(\hat{\alpha})}{T_0} = \sum_{l=2}^{\infty} \sum_{m=-l}^l [Q_{(lm)}^G Y_{(lm)ab}^G(\hat{\alpha}) + Q_{(lm)}^C Y_{(lm)ab}^C(\hat{\alpha})]$$

$$Q_{(lm)}^G = \frac{1}{T_0} \int d\hat{\alpha} P_{ab}(\hat{\alpha}) Y_{(lm)}^{G ab*}(\hat{\alpha}) \quad Q_{(lm)}^C = \frac{1}{T_0} \int d\hat{\alpha} P_{ab}(\hat{\alpha}) Y_{(lm)}^{C ab*}(\hat{\alpha})$$

$$\int d\hat{\alpha} Y_{(lm)ab}^{R*} Y_{(l'm')}^{X' ab} = \delta_{ll'} \cdot \delta_{mm'} \cdot \delta_{XX'} \leftarrow \text{orthonormality}$$

$$\{X, X'\} = \{G, C\}$$

Statistics:

$$\langle a_{(lm)}^{\mathbf{Z}} a_{(l'm')}^{\mathbf{Z}'} \rangle = C_{\ell}^{\mathbf{ZZ}'} \delta_{ll'} \delta_{mm'}$$

for $\mathbf{Z} = \{T, G, C\}$

$$Y_{(lm)}, Y_{(lm)ab}^G \text{ parity } (-)^l \\ Y_{(lm)ab}^G \text{ parity } (-)^{l+1} \Rightarrow C_{\ell}^{TC} = C_{\ell}^{GG} = 0$$

\therefore Statistics of Temp/Pol. map
specified (completely for Gaussian theories)
by $C_{\ell}^{TT}, C_{\ell}^{GG}, C_{\ell}^{TG}, C_{\ell}^{GG}$

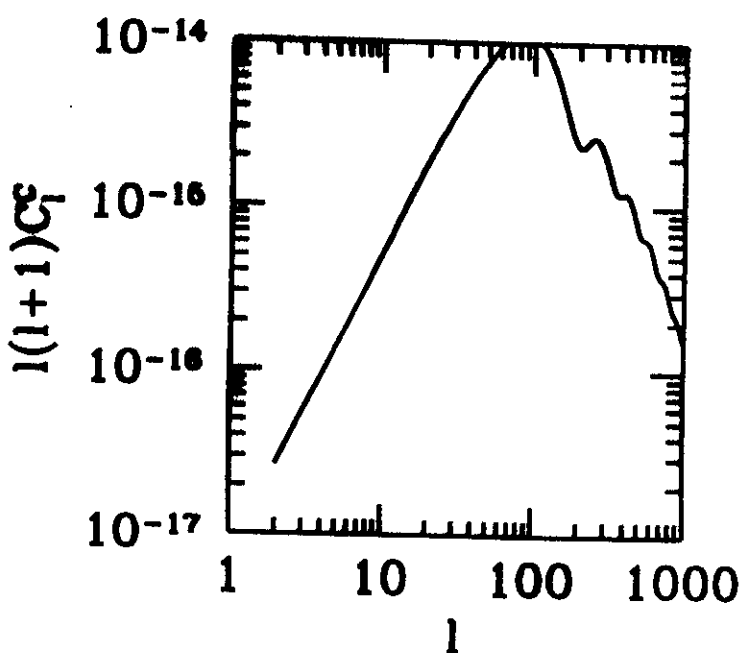
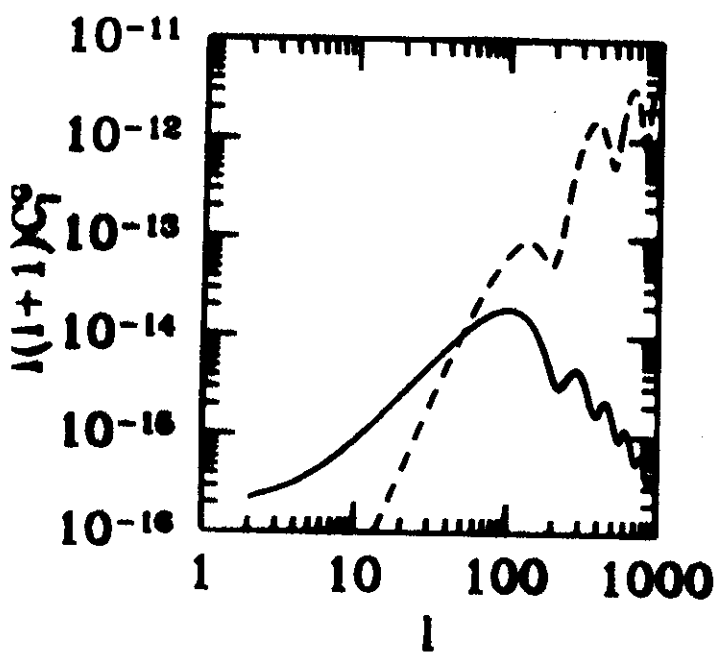
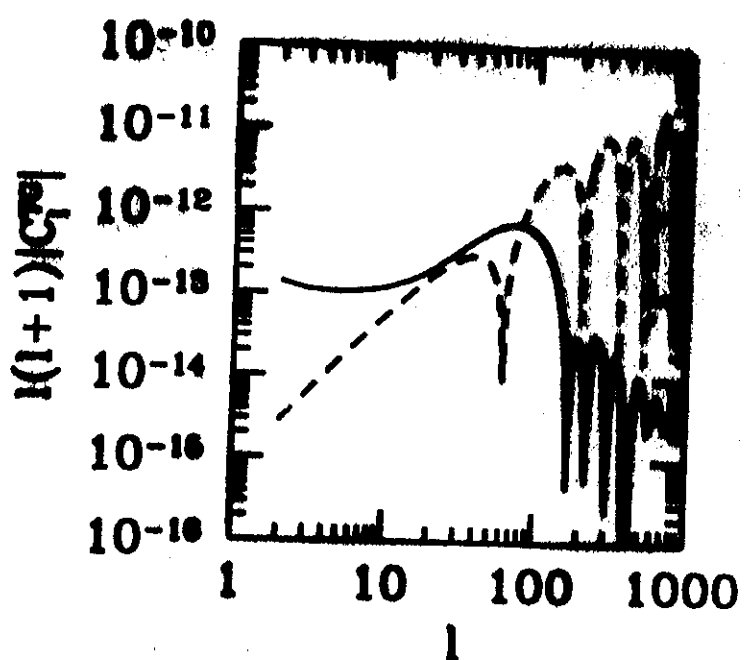
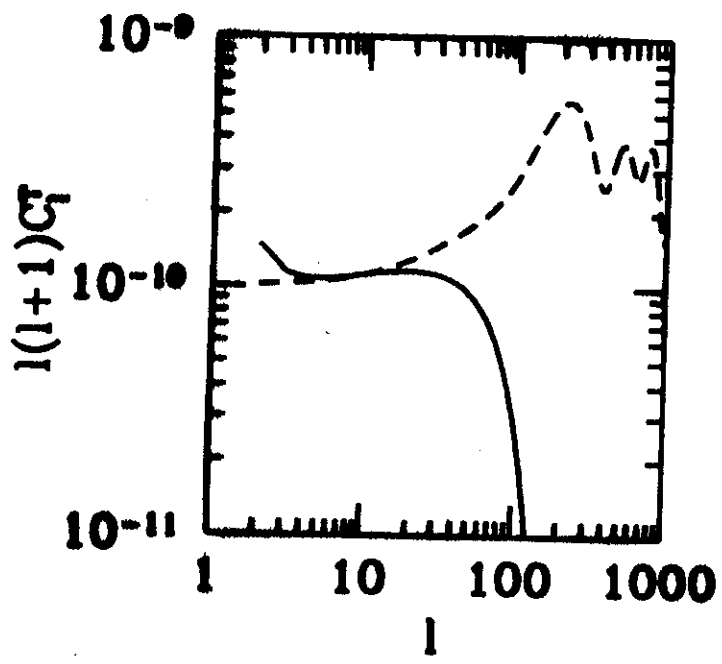
Scalar modes $\Rightarrow C_{\ell}^{GG} = 0$

$$\overline{(\Delta T)^2} = T_0^2 \sum_{\ell=2}^{\infty} \frac{2\ell+1}{8\pi} C_{\ell}^{TT} \quad \begin{matrix} \text{mean square} \\ \Delta T \end{matrix}$$

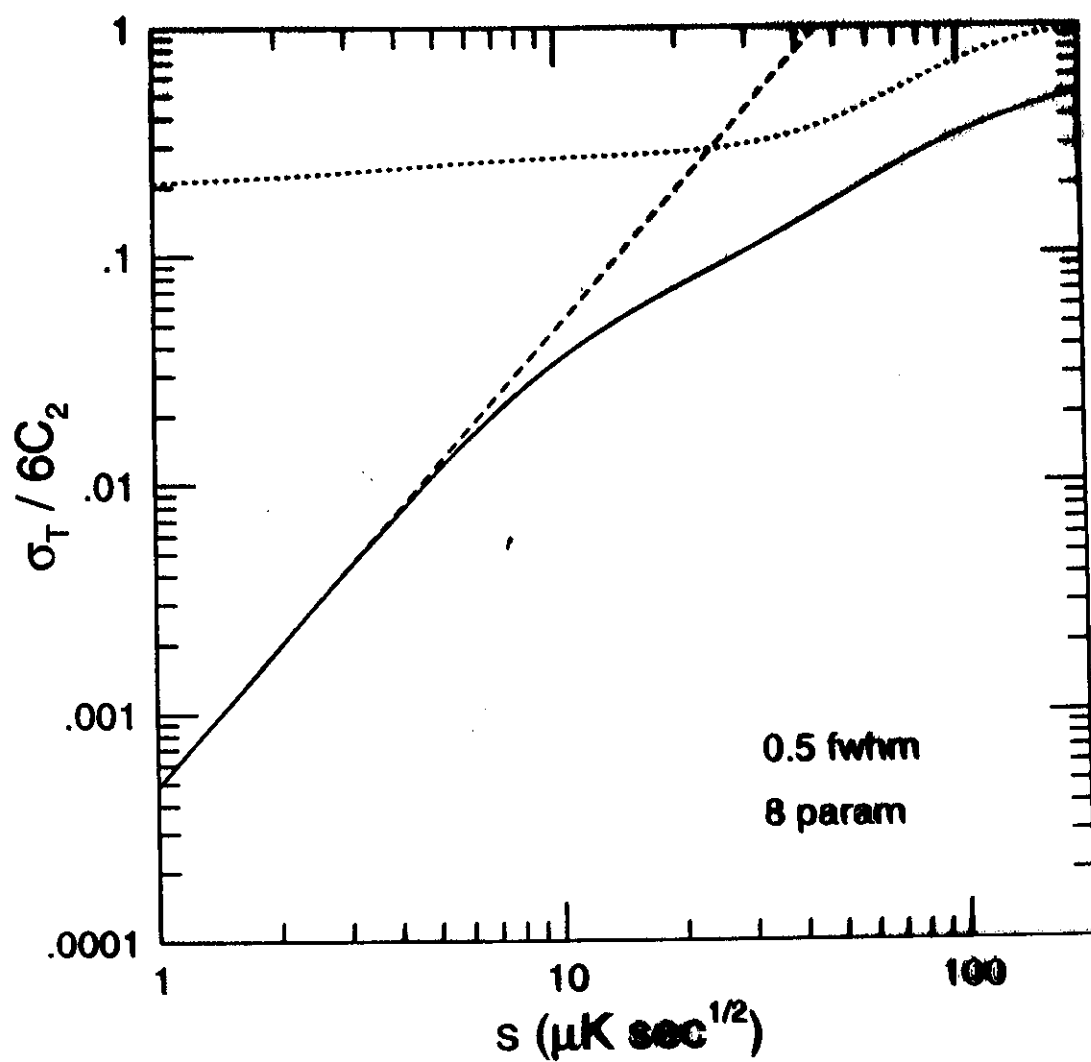
$$\overline{P^2} \equiv \overline{Q^2 + U^2} = \overline{P_G^2} + \overline{P_c^2}$$

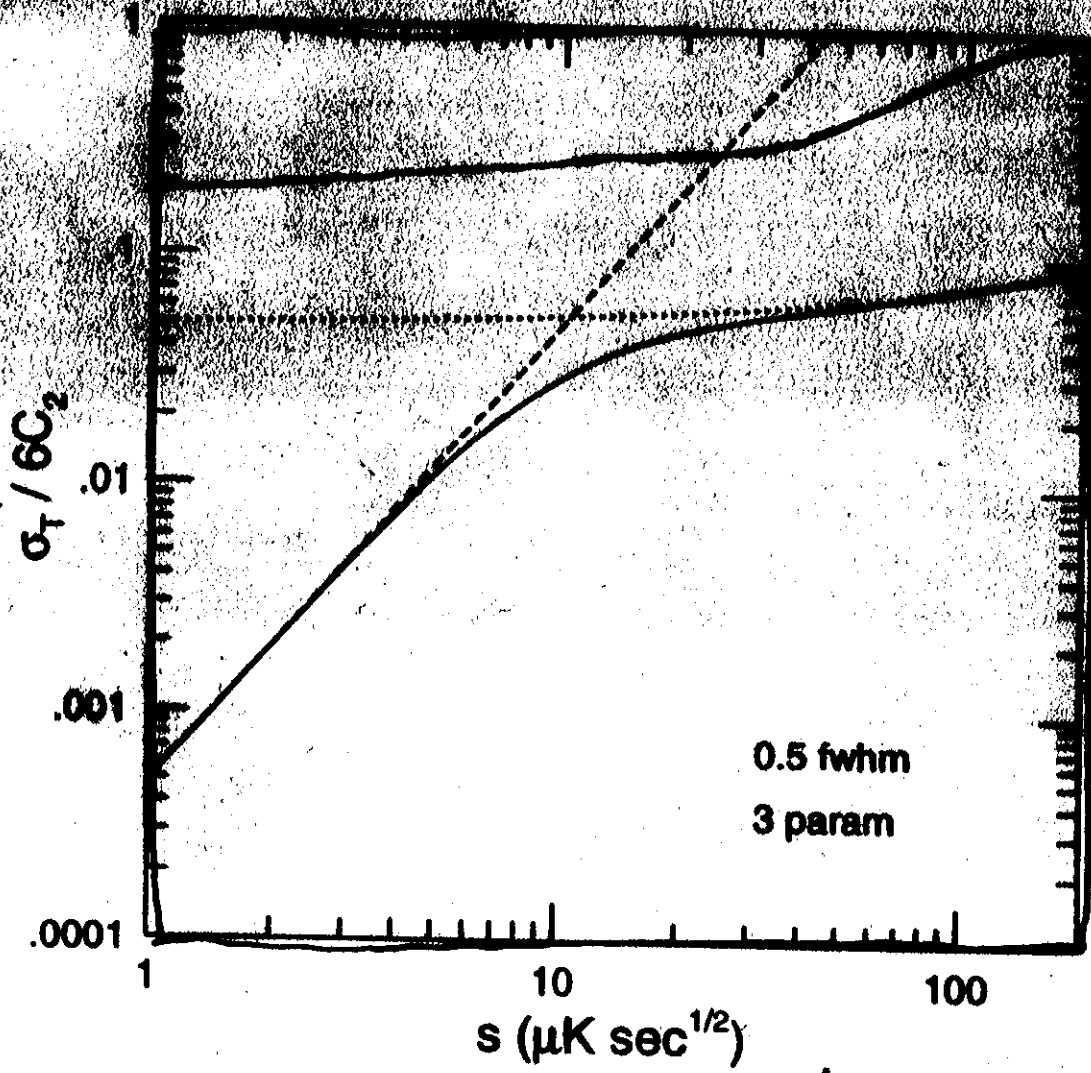
$$\overline{P_G^2} = T_0^2 \sum_{\ell=2}^{\infty} \frac{2\ell+1}{8\pi} C_{\ell}^{GG} \quad \begin{matrix} \text{mean square} \\ \text{polarization} \end{matrix}$$

$$\overline{P_c^2} = T_0^2 \sum_{\ell=2}^{\infty} \frac{2\ell+1}{8\pi} C_{\ell}^{GG}$$

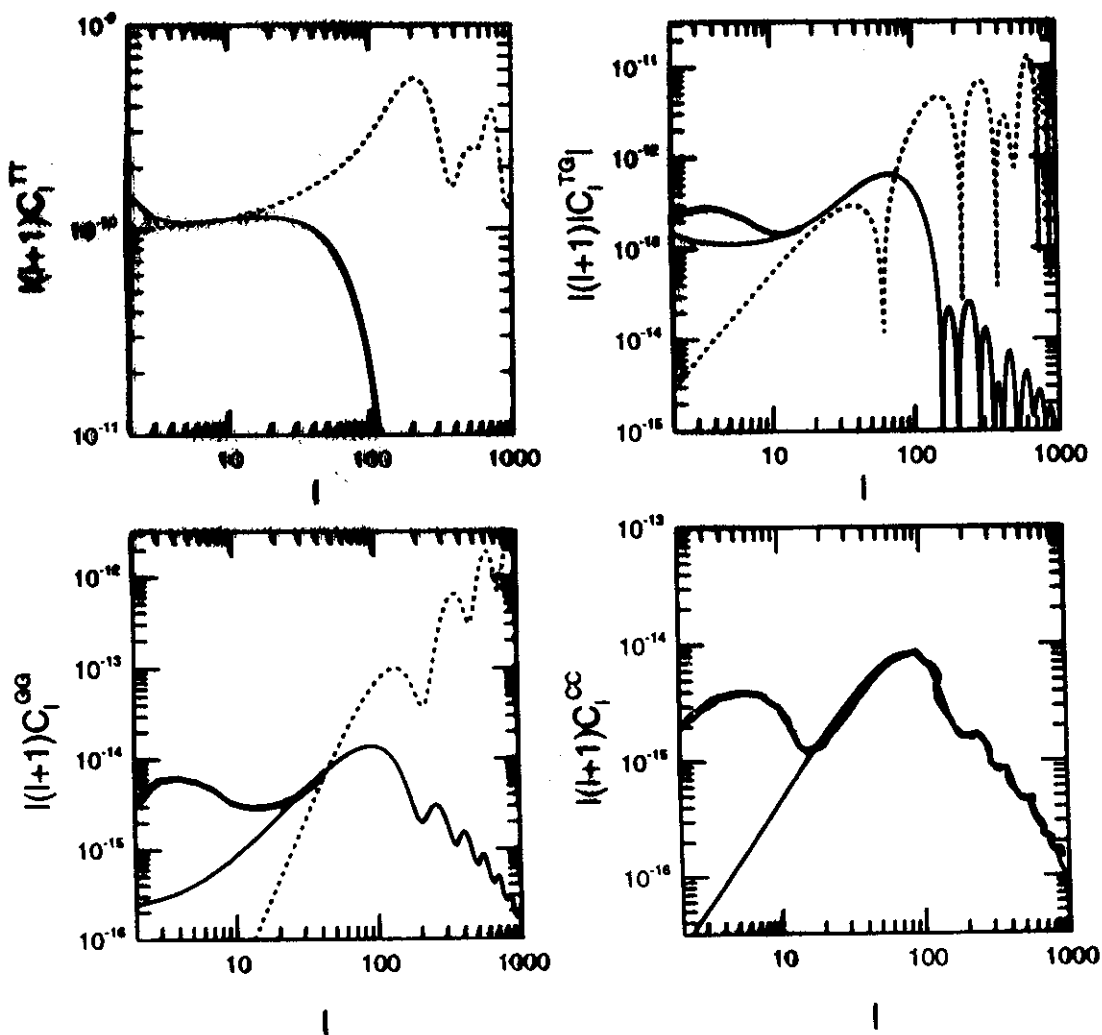


Kamionkowski + Kosowsky
astroph/8705219





Reionization:



49

Conclusions

CMB maps will likely provide information about:

- geometry and cosmological parameters
- structure formation
- ionization history
- long-wavelength gravitational waves
- new tests of inflation

Other uses:

- Matter/CMB correlations $\implies \Omega_0$
- tests for non-Gaussian statistics \implies structure-formation theories
- Sunyaev-Zeldovich effect:
 - H_0
 - learn about clusters
- Blackbody spectrum
 - constrains ionization history
 - constrains exotic phenomena in early Universe

